Aus dem Medizinischen Zentrum für Innere Medizin der Philipps-Universität Marburg
Klinik für Innere Medizin mit dem Schwerpunkt Gastroenterologie, Endokrinologie und Stoffwechsel
Geschäftsführender Direktor: Universitätsprofessor Dr. med. R. Arnold
Leiter der Gastroenterologie: Universitätsprofessor Dr. med. R. Arnold

---

Function of Estrogen on Bone and the Characterization of the Skeletal Phenotype of Steroid Receptor Coactivator (SRC)-1 KO Mice

Inaugural-Dissertation
zur
Erlangung des Doktorgrades der gesamten Medizin
dem Fachbereich Humanmedizin
der Philipps-Universität Marburg

vorgelegt von
Ulrike Mödder
aus Bedburg

Marburg
2005

Angenommen vom Fachbereich Medizin der Philipps-Universität Marburg am 17.03.2005 (Tag der Disputation)

Gedruckt mit Genehmigung des Fachbereich

Dekan: Prof. Dr. B. Maisch

Refferent: Prof. Dr. R. Arnold

Korreferent: PD Dr. H. Westphal

Research is to see what everyone else has seen,
and to think what no one else has thought.

Albert Szent Gyoergi

Table of Contents

1 Introduction

1.1 The Structure of Bone

The skeletal system is assembled of bones. In addition with the cartilage, the bones serve three functions: a) metabolic, as a reserve of ions, especially calcium and phosphate, for the maintenance of serum homeostasis, which is essential to life; b) mechanical, support and site of muscle attachments for locomotion; and c) protective, for vital organs and bone marrow.

Bone consists of two components, the cancellous and the cortical bone. Cancellous and cortical bone is constituted of the same cells and the same matrix elements, but they are structurally and functionally different. Cancellous bone, also named spongy or trabecular bone, is a network of thin, calcified trabeculae. The spaces enclosed by these thin trabeculae are filled with hematopoietic bone marrow. Cancellous bone is relatively prominent in the vertebral column, in the epiphysis, and the metaphysis of the long bones. Cortical bone is a thick and dense calcified tissue, which encloses the medullary cavity where the hematopoietic bone marrow is housed. Cortical bone is the main component in long bone shafts of the appendicular skeleton and fulfils mainly the mechanical and protective function. In the skeleton 80% of the bone is cortical bone, but cancellous bone is metabolically more active per unit volume and so the skeletal metabolism is approximately equally distributed (Eriksen et al., 1994). It is demonstrated that cortical and cancellous bone behave differently and exhibit different responses to metabolic changes and treatments (Riggs et al., 2002) (Parisien et al., 1990) (Daci et al., 2000) (Poli et al., 1994) (Bikle et al., 1990).

Bone is built and resorbed by two different cell types: the osteoblasts and the osteoclasts. Osteoblasts are the bone-forming cells. They build up the bone through the secretion of bone matrix components. Osteoblasts originate from local mesenchymal stem cells. They

are present in the bone marrow and differentiate through the influence of specific factors along the osteoblast differentiation pathway. Two osteoblast-specific transcripts have been identified: one encoding core-binding factor alpha-1 (Cbfa 1), a transcription factor (Ducy et al., 1997), and the other encoding osteocalcin, a secreted molecule that inhibits osteoblast function (Ducy et al., 1996). The osteoblasts are attached to the bone surface and produce type I collagen, are responsive to parathyroid hormone (PTH), and produce osteocalcin when stimulated by 1,25 dihydroxyvitamin D (Williams and Frolik, 1991) (Partridge et al., 1981). Osteoblasts never appear or function individually but are always found in clusters of cuboidal cells along the bone surface. When osteoblasts get trapped in the bone matrix that they produced and which later becomes calcified they are called osteocytes.

On the other hand bone is resorbed by osteoclasts. They derive from hematopoietic cells of the monocyte/macrophage lineage, which fuse to giant multinucleated cells. Osteoclasts are usually found in contact with a calcified bone surface. Characteristic for the osteoclasts is that the zone of contact with the bone has a ruffled border with dense patches on each side (Baron et al., 1993) (Eriksen et al., 1994). The osteoclasts synthesize and secrete lysosomal enzymes such as tartrate resistant acid phosphatase (TRAP), and cathepsin K, and also metalloproteinases such as collagenase and gelatinase. The differentiation of osteoclasts is dependent on the expression of two factors; the macrophage colony-stimulating factor (MCS-F) which is expressed by the macrophages or osteoclasts itself (Udagawa et al., 1990), and receptor for activation of nuclear factor kappa B ligand (RANKL) which is expressed by osteoblastic lineage cells and activated T lymphocytes (Figure 1.1). The signaling receptor (RANK) is located on the surface of osteoclastic lineage cells and their precursors (Lacey et al., 1998), (Kong et al., 1999). Osteoprotegerin (OPG) functions as a secreted inhibitor of the RANK signaling pathway by binding to RANKL and competitively inhibiting the RANKL/RANK interaction on osteoclasts and their precursors (Simonet et al., 1997).

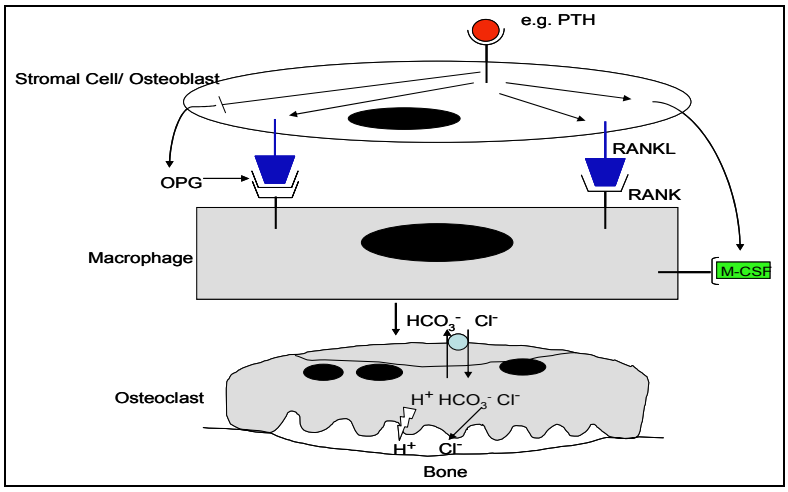

Figure 1.1. Mechanisms of osteoclastogenesis. Osteoclastogenic molecules such as PTH up-regulate the expression of RANKL, M-CSF and OPG of the stromal cells and osteoblasts. The binding of RANKL and M-CSF with their receptors lead to the differentiation of the macrophage (osteoclast precursor) to osteoclast, a process inhibited by OPG. Adapted from Teitelbaum et al.

Targeted deletion of OPG in mice results in an increase of bone resorption and severe, early-onset osteoporosis. The early-onset osteoporosis in the OPG deficient mice is a result of an increased number of osteoclasts and an increased activity (Bucay et al., 1998).

A shift in the balance of the activity of the osteoblasts and osteoclasts leads to an increase (osteopetrosis) or a decrease (osteoporosis) of bone mass. The net loss of bone mass has been causally linked to estrogen loss. It is believed that the main reason for the development of osteoporosis is the declining level of estrogen in postmenopausal women (Albright et al., 1941) and men (Khosla et al., 1998). The decrease of circulating serum estrogen occurs in women in the fifth to sixth decade of life, when the ovaries stop to produce follicles.

1.2 The Synthesis, and Functions of Estrogens

Estrogens belong to the family of steroid hormones. The precursor for the steroid hormone synthesis is cholesterol, which is regulated by the adrenocorticotrophic hormone of the pituitary. Multiple enzymatic steps lead from the cholesterol to the synthesis of the steroid hormones estrogens (Figure 1.2). Estrogens consist of estrone (E_1), estradiol (E_2), and estriol (E_3). The estrogen formation is dependent on A-ring aromatization of its immediate precursor (Cole and Robinson, 1990) (Akhtar et al., 1982). One of the precursors is testosterone which is converted to estradiol, by a particular isoform of the enzyme aromatase (see 1.5), which also catalyses the conversion of the androgen, androstenedione to the weak estrogen, estrone.

Estrogens are the main female hormones and responsible for gender differences and reproduction. In the first decade of life the release of gonadotropin hormones from the pituitary increases and leads to the production of estrogens from the ovaries. During puberty estrogens initiate the development of the secondary sexual characteristics and start and maintain the menstrual cycle. The aim of a menstrual cycle is to produce a mature follicle which is capable of reproduction. From the puberty up to the fifth decade of life 300-400 follicles reach maturity. After that time there are no more follicles in the ovaries and the females stop to have reproductive cycles and to produce estrogen in the ovaries.

In premenopausal women, more than 95% of serum estradiol and most of serum estrone is synthesized in the ovaries.

In the recent years it was demonstrated that also extragonadal sites are capable to synthesize estrogens (Simpson et al., 2000) (Labrie et al., 1997a) (Khosla et al., 1997). These extragonadal sites are the adipose tissue, brain, cardiovascular system, breast, and bone. At the peripheral sites estrogens work in a paracrine or intracrine way (Labrie et al., 1998) (Labrie et al., 1997a). Therefore, estrogens are not released into the blood stream. They

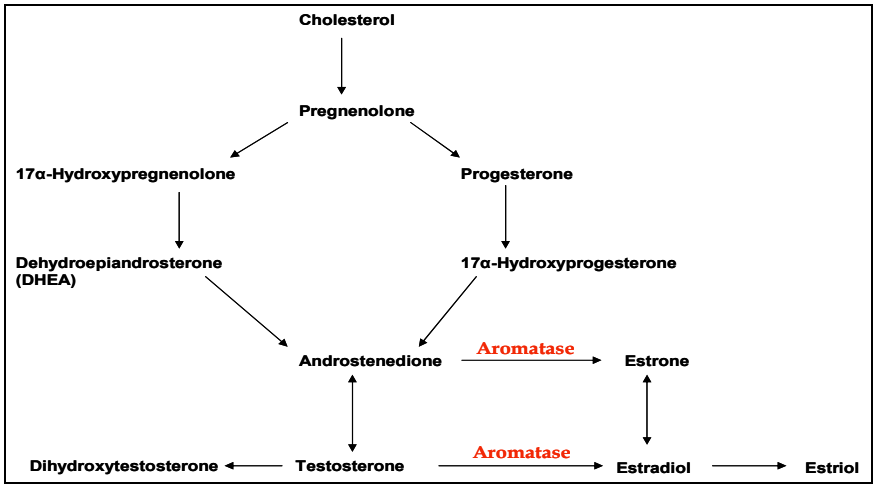

Figure 1.2. Pathway of steroid hormone biosynthesis from cholesterol. Multiple enzymatic steps are necessary to convert cholesterol to androgens and estrogen. The only enzyme which is indicated here is aromatase.

initiate the response in the neighbor cells or in the cell which synthesized the estrogens. One example is the concentration of E_2 present in breast tumors of postmenopausal women which is at least 20-fold greater than that present in the plasma (Pasqualini et al., 1996) (Castagnetta et al., 1996). The paracrine or intracrine biosynthesis of sex steroids is economical because only the concentration required by the cells is synthesized, and the large dilution in the extracellular fluids that occurs after endocrine secretion is avoided. Labrie et al. (Labrie et al., 1997b) estimated that nearly all of the estrogen in postmenopausal women originates from extragonadal syntheses.

The difference between the synthesis of estrogens in the gonads and the extragonadal sites (adipose tissue, brain, cardiovascular system, breast, and bone) is that as mentioned earlier the gonads use cholesterol as a precursor. The cells from the extragonadal sites are dependent on circulating C19 androgenic precursors (androstenedione, testosterone), because they can not convert cholesterol into C19 precursors (Pasqualini et al., 1996) (Castagnetta et al., 1996).

In general the estrogen action in the target tissues is mediated by estrogen receptor-α (ER-α) and the estrogen receptor-β (ER-β) (see 1.3.1). Estrogen receptors (ERs) are members of the nuclear receptor superfamily of transcription factors that can up- or down-regulate the

transcription of certain target genes. The action of the ER occurs through targeting estrogen response element (ERE) on the target genes, by binding to coregulators, which are activators or repressors and recruit other transcription factors (Feng et al., 1998). The coregulators can be broadly defined as cellular factors that are recruited by the nuclear receptors that complement the function of the receptors as mediators of the cellular response to endocrine signals. Both coactivators and corepressors of nuclear receptor function have now been identified [for review see (McKenna et al., 1999)]. Perhaps the most important coactivators are the members of the steroid receptor coactivator (SRC) family (see 1.3.2).

1.3 Estrogen Action on Bone – Role of Estrogen Receptors, and Steroid Receptor Coactivator (SRC) -1

Estrogens play a critical role in regulating bone metabolism in women. Now there is also overwhelming evidence that estrogens are important also in the regulation of bone metabolism in men (Riggs et al., 2002). Estrogens have an essential role in the pubertal growth spurt, skeletal maturation and in the acquisition of normal bone mass in females as well as males. Lack of estrogens lead to a discordance between skeletal growth and skeletal maturation, and the accrual of bone density and mass. Estrogens are known to be the major sex hormones involved in the maintenance of bone mass in the adult (Grumbach and Auchus, 1999) (Bilezikian, 1998) (Rochira et al., 2000). Although knowledge of the action of estrogens on the adult skeleton is incomplete, a few actions have been elucidated. Estrogens suppress cytokine production and action (e.g. interleukin 6 and its receptor) in osteoblasts, decrease the rate of bone remodeling, promote apoptosis of osteoclasts, stimulate OPG by osteoblasts, and decrease apoptosis in osteoblast and osteocytes [see reviews (Karsenty, 1999) (Manolagas, 2000) (Mundy, 1999) (Kameda et al., 1997)]. The anti-apoptotic effect of estrogens on the osteoblast appears to involve the classical, genomic

and also the nongenomic action of estrogens. The nongenomic action of estrogens involve the steroid receptors on the cell surface instead the intracellular nuclear receptors. The nongenomic action is a rapid phosphorylation of extracellular signal-regulated kinases (ERKs), members of the mitogen-activated protein kinase family (Razandi et al., 2000) (Kousteni et al., 2002).

Thus, the decrease of circulating estrogen levels after natural or surgical menopause is perhaps the single most important factor leading to osteoporosis in women and is initially associated with a high level of bone turnover (Turner et al., 1994). Moreover, data from Khosla et al. (Khosla et al., 2002) now indicate that declining biologically available estrogen levels may be a major cause of "age-related" bone loss in men. A commonly used therapy to treat meno- and postmenopausal bone loss and other clinical symptoms like hot flushes, night sweats, and increased risk of cardiovascular disease is the hormone replacement therapy (Lindsay et al., 1976; Lindsay et al., 1978). Clinical and animal studies have demonstrated the beneficial effects of estrogens on bone, the vascular and central nervous system [for review see (Manolagas and Kousteni, 2001)]. However, since the findings of the Women's Health Initiative (Rossouw et al., 2002), which have brought to light clear cardiovascular and breast cancer risks of at least combination therapy with oral conjugated estrogens and medroxyprogesterone a better understanding of estrogen action is clearly important both for defining better the mechanism(s) of bone loss in women and men, as well as for the development of new approaches to prevent or treat osteoporosis in both genders. The cardiovascular and breast cancer risks could perhaps be minimized by the use of selective estrogen receptor modulators (SERMs) which can activate beneficial estrogen signaling pathways in bone and other tissues, without the adverse effects of estrogens on the breast and possibly the coagulation system. The results from the Women's Health Initiative also have led to an interest in lower-than-standard doses for menopausal estrogen therapy.

Of note, in recent years, the mouse is being increasingly used as a model to study mechanisms of bone loss and estrogen action on bone. One reason is the availability of numerous inbred strains with differences in peak bone mass (Klein et al., 1998), (Beamer et al., 1996) and susceptibility to bone loss following ovariectomy (ovx). In addition, a large number of genetically altered mice have been developed with important skeletal phenotypes, some involving defects in estrogen signaling pathways (Sims et al., 2003), (Modder et al., 2004). Most of these mice have been bred into the C57BL/6 background strain.

1.3.1 Effects of Estrogen Receptor-α versus Estrogen Receptor-β on Bone

The biological effects of the steroid hormones are believed to be mediated by specific nuclear hormone receptors that demonstrate great specificity and high affinity for their respective steroid ligands under normal physiological conditions. The following receptors: estrogen receptor-α (ER-α) and estrogen receptor-β (ER-β), androgen receptor (AR), and progesterone receptor (PR) are all members of the nuclear receptor superfamily class I as defined by Mangelsdorf (Mangelsdorf and Evans, 1995). These receptors are characterized as ligand-inducible transcriptional factors composed of a highly conserved modular structure of functional domains termed A-F, with the C domain responsible for binding to specific DNA sequence elements, and the E domain responsible primarily for ligand binding. Also included within the receptor are regions involved in nuclear localization, dimerization, and transcriptional activation (Tora et al., 1989) (Webster et al., 1988) (Tasset et al., 1990). The activation function-1 (AF-1) is located in the amino-terminal A/B domain, and activation function-2 (AF-2) is located within the E domain (Tzukerman et al., 1994) (Pham et al., 1992). The inactive receptor is in form of a large complex made up of loosely bound heat-shock and other accessory proteins. The steroid hormones are lipophilic, enter the plasma

membrane and the nucleus of the cells by diffusion and bind to the nuclear receptor. After the binding of the steroid receptor, the receptor is activated and released from the heat-shock proteins. The receptor-ligand complex interacts with an identical or a related receptor to form a homo- and/or heterodimer (Cowley et al., 1997) (Pace et al., 1997). The homo- or heterodimer binds to specific cis-active elements in the promoter region of the target gene, resulting in transcription of the gene and ultimately leads to a cellular or tissue response.

The two known receptors for estrogen, ER-α and ER-β share a great structural homology and the ligand binding affinity is similar, however, their transactivation domains, tissue distribution, and molecular sizes differ significantly. The levels of the β species are high in prostate, ovary, brain and bladder, but are low or absent in uterus, kidney, pituitary, and epididymis - tissues which contain high levels of the α species (Kuiper et al., 1996) (Kuiper et al., 1997). In certain cell systems, transfection-reporter gene responses indicate that ER-β is a weaker regulator of gene transcription than the extensively studied ER-α (Kuiper et al., 1996) (Kuiper et al., 1997) (Paech et al., 1997) and it has been shown that ER-α activates, whereas ER-β inhibits, AP-1 regulatory elements (Paech et al., 1997).

Osteoblastic cells express both ER-α and -β, but both are differentially expressed during osteoblast differentiation, with ER-α concentrations increasing by almost 10-fold, whereas ER-β concentrations increase only slightly during differentiation of osteoblastic precursor cells into mature osteoblastic cells (Onoe et al., 1997). Immunohistologic studies of developing human bone have demonstrated that whereas ER-α is the predominant species in cortical bone, ER-β is the major receptor present in cancellous bone (Bord et al., 2001). Similarly, ER-β appears to be present primarily in cancellous bone in the rat femoral metaphysis and spine, with much lower levels in the cortical bone of the femur (Onoe et al., 1997).

In humans, the importance of estrogens in bone is clearly demonstrated in the described cases of a defect in the estrogen receptor gene (Smith et al., 1994) and two cases of

aromatase deficiency (Mullis et al., 1997) (Carani et al., 1997) (Morishima et al., 1995), both resulting in a lack of estrogen action. The patients had osteoporosis, unfused epiphyses, increased markers for bone remodeling and continuing linear growth in adulthood. A treatment with estrogens led to a closure of the epiphyses and a dramatic increase of bone density in the patients with the defect of the aromatase gene.

The skeletal phenotypes of the ER-α knock out (ERKO), ER-β knock-out (BERKO) and double ER-α and –β knock-out (DERKO) mice have also been analyzed in some detail. The caveat with the studies on the initial ERKO mouse is that the bones in this mouse expressed a splice variant of ER-α, which allowed partial responsiveness to estrogens (Denger et al., 2001). Using a more complete knock out of ER-α, Sims et al. (Sims et al., 2002) found that the ERKO mice had a decrease (not an increase) in bone turnover and an increase (not a decrease) in trabecular bone volume in both male and female animals. These surprising findings appeared to be due to markedly elevated testosterone and E_2 levels in the male and female mice, respectively. Thus, the elevated testosterone levels likely activated androgen receptor signaling in the male ERKO mice and the elevated E_2 levels likely activated ER-β signaling in the female ERKO mice, demonstrating that these receptors, in the setting of elevated sex steroid levels, could compensate for loss of ER-α. Deletion of ER-β led to different responses in males, where bone was unaffected, and in females, where bone resorption was decreased and trabecular bone volume increased (Sims et al., 2002). This suggested that in females, ER-β may antagonize the action of ER-α in bone, and was consistent with previous data demonstrating that the BERKO females have an increase in cortical bone associated with increased periosteal apposition that develops during growth (age 3-6 months) and is maintained in adults (age 12-13 months) (Ke et al., 2001; Windahl et al., 2001). The adult BERKO females also appear to be protected against the age-related cancellous bone loss that occurs in the wild type (WT) mice (Windahl et al.,

2001) (Ke et al., 2001), suggesting either that ER-β is permissive for age-related bone loss in mice, or that loss of ER-β results in increased sensitivity to estrogens, thus perhaps compensating for the age-related decline in estrogen levels in the BERKO mice. Finally, gene array analysis of bones from either WT, ERKO, or BERKO mice that were ovariectomized (ovx'd) and treated with E_2 has demonstrated that loss of ER-β resulted in an 85% increase in the mRNA levels of genes stimulated by ER-α; in the absence of ER-α, ER-β was effective in stimulating estrogen-responsive genes, albeit to a reduced extent (Lindberg et al., 2003).

Taken together, the collective findings from the ER-α-deficient human male, aromatase-deficient males, and the mouse KO models would indicate that ER-α is likely the dominant ER mediating estrogen action on bone in female and male mice. However, it does appear that, in the absence of ER-α, in female, but not in male mice, ER-β may be able to at least partially compensate for loss of ER-α (Sims et al., 2003). Moreover, the physiological consequences of the higher ER-β levels in cancellous as opposed to cortical bone (Onoe et al., 1997) (Bord et al., 2001) are unclear at present.

1.3.2 Steroid Receptor Coactivator (SCR)-1

SRC-1 is a member of the SRC family. Besides SRC-1, which was the first nuclear receptor coactivator to be cloned (Onate et al., 1995) the SRC family include also SRC-2 (Hong et al., 1996); and SRC-3 (Li et al., 1997). The sequence similarity between SRC-1, -2 and -3 is around 40%. The most highly conserved region in the family is the N-terminal basic helix loop helix (bHLH)-PAS domain. The bHLH region functions as a DNA-binding or dimerization surface, and the PAS domain also plays a role in protein-protein interactions and dimerization (Figure 1.3). The receptor interacting domain (RID) is located following the bHLH-PAS domain. Detailed analysis of the sequence of the RID identified a conserved motif, LXXLL, where L stands for leucine and X stands for any other amino acid. This conserved motif is termed the nuclear receptor (NR) box, which mediates interactions between the SRCs and liganded nuclear receptors. Three such motifs are found in the RID of SRC coactivators. The C-terminus of the SRC proteins contains the activation domain (AD), which interacts with general transcriptional activators, such as CBP/p300. This region also contains a histone acetyltransferase (HAT) activity.

Coactivators mediate the effects of transcriptional activator proteins, presumably by helping to recruit a complex of RNA polymerase II and associated basal transcription factors (a preinitiation complex) to the promoter or by activating a preinitiation complex that has already been assembled on the promoter (Figure 1.4)

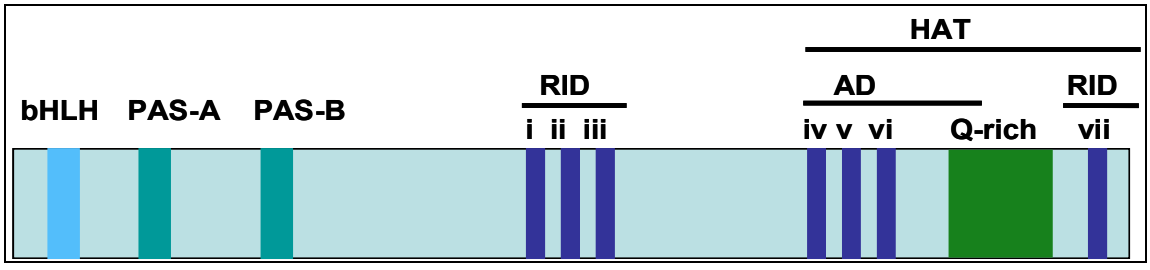

Figure 1.3. Schematic representation of the SRC family domain structure. The N-terminus contains the highly conserved bHLH and PAS A/B domains. The centrally located receptor-interacting (RID) and Activation (AD) domains each contain three LXXLL motifs, while SRC-1 contains an additional, non-conserved motif at the C-terminus. The C-terminus contains a glutamine-rich domain. Also indicated is the domain containing the histone acetyltransferase (HAT) activity. Adapted from Leo et al.

Of the three SRCs, SRC-1 and –2 appear to be the most closely related and able to potentially compensate functionally for each other. SRC-3 appears to have a broader functional role than SRC-1 or –2, since in addition to facilitating the action of nuclear receptors; SRC-3 also enhances the transcriptional activity of a number of different activators, including interferon-α and CREB (Torchia et al., 1997). Thus, for example, while microinjection of anti-SRC-1 antibodies into cells prevented retinoic acid receptor-dependent transactivation of a retinoic acid response element-linked reporter gene, coinjection of a SRC-2 (but not SRC-3) expression vector could rescue transactivation of this reporter gene (Torchia et al., 1997).

It is now appreciated that the relative balance of receptors, coactivator, and corepressor proteins is a critical determinant of the ability to initiate gene transcription. Since the relative concentrations of these molecules are cell specific, sex steroid hormones can have vastly different functions in different tissues of the same organism. Variations in the recruitment of coregulatory molecules also appear to be the mechanism by which selective estrogen receptor modulators (SERMs) produce their tissue-specific effects (Shang and Brown, 2002).

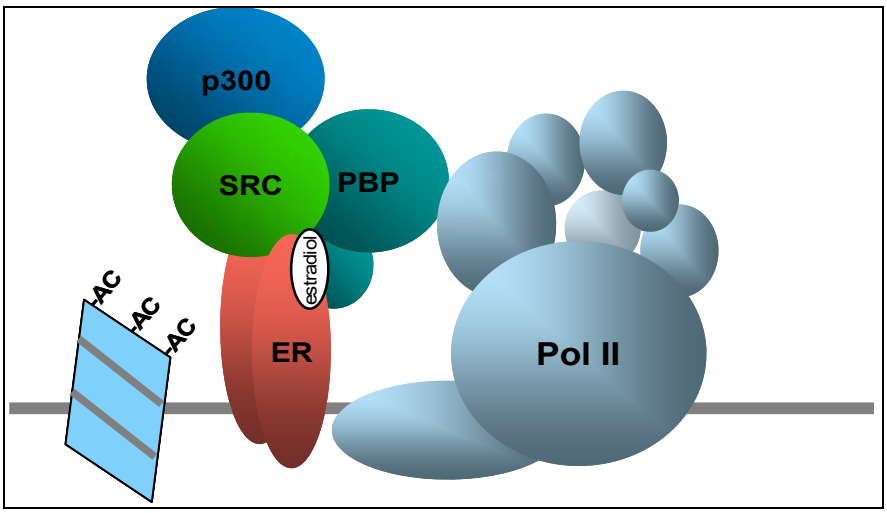

Figure 1.4. Schematic representation of an ER-SRC transcription complex.

AC: acetyl group bound to the histone complex (light blue symbol), ER: estrogen receptor (dimer), p300: transcriptional coactivator (histone acetyltransferase activity), PBP: transcriptional coactivator (PPARgamma-binding protein), Pol II: RNA polymerase II protein complex, SRC: steroid receptor coactivator

The physiological importance of SRC-1 for estrogen action has been demonstrated by the generation of SRC-1 KO mice (Xu et al., 1998). The mice were generated by conventional gene targeting. The targeting event inserted an in-frame stop codon at the Met^{381} in exon 4 causing a downstream deletion of genomic sequence. The SRC-1 functional domains were disrupted.

The homozygous mutants are viable and fertile in both sexes, but exhibit significant resistance to estrogen action in a number of tissues, including the uterus and mammary gland. Xu et al. (Xu et al., 1998) also tested whether the endocrine feedback control systems of the SRC-1 KO mice was affected. Therefore, they measured E_2, and testosterone concentrations in serum from age-matched wild type (WT) and SRC-1 KO mice. The E_2 and testosterone concentration in SRC-1 KO mice were 1.2 and 1.5 times those in WT animals, respectively. Of note, the expression of SRC-2 is increased in several tissues in these mice, suggesting that this related coactivator may be at least partially compensating for loss of SRC-1 function.

In the presented study, I used SRC-1 KO female and male mice to characterize in detail the consequence of SRC-1 deficiency for E_2 action on bone *in vivo*. Recognizing that these mice have compensated estrogen resistance (Xu et al., 1998), I not only characterized their skeletal phenotype under basal conditions but also after gonadectomy and replacement with a physiological dose of E_2.

1.4 Function of Androgen in Bone

Like estrogens, androgens play an important role in skeletal metabolism, too. Androgen deficiency results in a number of abnormalities of bone metabolism, such as lower peak bone mass and accelerated bone loss due to increased bone resorption, resulting in higher fracture risk, and a tall eunuchoid stature due to unfused growth plates (Orwoll and Klein, 1995).

In men, androgens are produced by both the testes and the adrenal glands. In women, the ovaries are the major source for androgens. Androgens belong to the steroid hormones and are also synthesized from cholesterol (see Figure 1.2.). Androstenedione is the precursor for the synthesis of testosterone, which is the major circulating adrenal androgen in both women and men (Orwoll, 1996). Testosterone is bound to albumin and sex-hormone binding globulin and circulates through the bloodstream to the peripheral tissues, where it is converted by the enzyme, 5α-reductase, to the more potent 5α-dihydrotestosterone (5α-DHT). In addition, testosterone, but not 5α-DHT, can be metabolized to estradiol by the enzyme aromatase (see 1.5).

Androgen action is mediated by androgen receptors (ARs) which have been identified and cloned. During development, ARs are expressed in different reproductive and non-reproductive tissues, including external and internal genitalia, mammary gland, adrenal glands, kidneys, muscles, pituitary gland, hypothalamus, and larynx. The ARs were also detected in various bone cell types, including osteoblasts (Colvard et al., 1989), osteoclasts (Mizuno et al., 1994), osteocytes, and heterotrophic chondrocytes (Abu et al., 1997).

Besides the important control of bone turnover in older man by estrogens, a minor role is attributed to androgens (Falahati-Nini et al., 2000). However, it was demonstrated that androgens influence the bone size and result in an increase of bone mass. In male rats, furthermore, it has been shown that after castration, nonaromatizable androgen (5α-DHT) can prevent bone loss (Vanderschueren et al., 1992) (Wakley et al., 1991). In the counterpart syndrome, testicular feminization syndrome, in which the androgen receptor in humans is

defect, bone density in these males is reduced (Marcus et al., 2000). Affected rodents with these conditions have a cancellous bone volume and density similar to those in normal littermates; a finding attributed to high serum estrogen and estrogen precursor concentrations (Vanderschueren et al., 1994; Vanderschueren et al., 1993).

In vitro, it was demonstrated that SRC-1 interacts with the ligand-activated AR (Bevan et al., 1999). Here as well, one of the main functions of the SRC-1 protein is to recruit additional general transcription factors and to facilitate access of the basal transcription machinery to the promoter. The transcription complex is able to initiate mRNA transcription of the target gene. It seems that in the AR the N-terminal activation function-1 (AF-1) domain is the most critical for transcriptional activation (Alen et al., 1999; Bevan et al., 1999).

In vivo, the necessity of SRC-1 in mediating the function of androgens in bone is not clear yet. Therefore, SRC-1 KO male mice were treated with testosterone or the nonaromatizable androgen, 5α-DHT, and changes of bone mass were determined by dual energy x-ray absorptiometry (DXA) and peripheral quantitative computed tomography (pQCT) measurements.

1.5 Aromatase

As mentioned before the conversion from androstenedione to estrone and testosterone to E_2 in the ovaries and also in the peripheral tissues is mediated by the enzyme aromatase. This enzyme is complex and consists of two components: aromatase cytochrome P450 and, coupled to it, an ubiquitous flavoprotein, NADPH-cytochrome P450 reductase. The heme protein is responsible for binding of the C19 androgenic steroid substrate and catalyzing the series of reactions leading to the formation of the phenolic A ring characteristic of estrogens. The aromatase complex is highly conserved among mammals and all vertebrates (Simpson et al., 2002).

Aromatase cytochrome P450 is encoded by the single copy of the human CYP19 gene (Means et al., 1989) (Harada et al., 1990) (Toda et al., 1990). CYP 19 consists of 10 exons with the coding region including only exon 2 through 10. Untranslated exon 1 is a habitat of the promoter. At least eight different exons 1 have been identified. However, the protein expressed in various tissue sites is always the same. For example placental transcripts contain at their 5′-end a distal exon, I.1 (Means et al., 1991). By contrast, transcripts in cells of mesenchymal origin such as adipose stromal cells and osteoblasts contain the exon I.4 (Mahendroo et al., 1993). Transcriptional regulation of CYP 19 is the major mechanism controlling the expression of aromatase, which is archived by tissue-specific alternative splicing of the various exon 1.

In humans, aromatase is expressed in a variety of tissues including the brain, placenta, adipose tissue, breast, ovaries and bone. In bone the aromatase is expressed in osteoblasts, chondrocytes and osteoclasts (Purohit et al., 1992) (Sasano et al., 1997) (Jakob et al., 1997) (Nawata et al., 1995) (Schweikert et al., 1995). So far in rodents the aromatase was just demonstrated in the ovaries, testis, and brain.

Recently, Eyre et al. (Eyre et al., 1998) were able to demonstrate the expression and activity of aromatase in rat osteosarcoma cells (ROS 17/2.8). The mechanism responsible for regulation of aromatase expression in bone remains unclear. In the presented experiments, the potential role of estrogens in aromatase regulation in bone tissue was investigated using bone cell cultures from human and rodents and bone tissue from rodents.

1.6 Aims of the Study

Decades ago, Albright F. (Albright et al., 1941) related postmenopausal osteoporosis to estrogen deficiency and found that estrogens can improve the calcium balance of postmenopausal women. Still pieces to complete the picture how estrogens regulate the development and maintenance of bone are missing.

One aim of the present study is to systematically define the dose response of estradiol (E_2) on bone and also to monitor the E_2 effects on the uterus in C57BL/6 mice. The effects of E_2 on different tissues are of great interest due to recent concerns about the treatment of postmenopausal women with estrogen replacement therapy. A further aim is to define whether the E_2 dose response in these tissues differs, depending on the particular experimental paradigm used.

After defining the effect of different doses of E_2 on bone and the uterus in general the next aim is to test the hypothesis that due to the presence of both estrogen receptor (ER) -α and –β in cancellous bone versus the predominant expression of ER-α in cortical bone and a preferred interaction of steroid receptor coactivator (SRC)-1 with ER-α/β or ER-β alone the SRC-1 KO female mice have a defect in estrogen action in cancellous bone.

Moreover, as a recent report found that ER-β plays no role in estrogen action on bone in male mice, I seek to demonstrate that there is a gender-related difference in estrogen action in cancellous bone. Therefore, SRC-1 KO male mice are treated with E_2 in the same way as the female SRC-1 KO and WT mice. In addition I seek to establish the response of the cancellous and cortical bone to administrated androgen in SRC-1 KO male mice.

In the last part of the presented work I test the hypothesis that aromatase, the enzyme that converts C19 precursors to estrogens, is expressed and active in human and rodent bone cell lines and rodent bone tissue and that the regulation of the enzyme is mediated by E_2 itself.

2 Material and Methods

All cell culture media, supplements and additional reagents were either purchased from Sigma Chemical Co. (St. Louis, MO) or GIBCO BRL (Grand Island, NY). The tissue culture plastic ware was purchased from Corning (Corning, NY). Molecular biology reagents and enzymes were purchased from Boehringer Mannheim (Indianapolis, IN) unless otherwise indicated.

2.1 Cell Culture

All human cell lines (hMS, SaOS2, hFOB-ER9, MG-63) were cultured in a humidified atmosphere of 5% CO_2 in a phenol-free α modified essential medium (αMEM) supplemented with 10% heat inactivated fetal bovine serum (HI-FBS) and 1% Penicillin/Streptomycin (standard growth medium).

After the experiments the RNA was isolated (see 2.2.1.1) from the differently treated cells and the expression of aromatase was examined by RT-PCR (see 2.3.2).

The hMS cells are conditionally immortalized marrow stromal cells. This cell line was established and characterized by Dr. Gori (Gori et al., 1999). The hMS cell express an immortalized state at 33,5°C and a nonimmortalized state at 39°C, because of the transfection with a gene coding for a temperature-sensitive mutant of the SV-40 large T-antigen. These cells can simulate the complete developmental sequence from undifferentiated precursors to cells with the complete osteoblast phenotype that are capable of forming mineralized nodules.

First I differentiated the hMS cells for 0, 3, 7, 14 or 21 days at 39,5°C. Therefore, the standard growth medium was supplemented with 10^{-8} M dexamethasone (Dex), 10^{-8} M 1α,25

dihydroxyvitamin D_3 ($1,25(OH)_2D_3$), 10mM β-glycerolphosphate (βGP), and 100µM ascorbic-phosphate (Asc-P) (standard differentiation medium).

To test if E_2 regulates the expression of the aromatase, I cultured undifferentiated hMS cells with standard growth medium supplemented with 10% charcoal stripped serum (CSS) instead of HI-FBS for 24h. This CSS is derived from plasma processed with charcoal to remove hormone proteins, to ensure that the measured effects result from the experimental treatment. For another 24 h I cultured the hMS cells with 1% CSS together with ICI 182,780 (10^{-7}M). ICI 182,780 (ICI, estrogen antagonist) is an analogue of E_2 and acts by competing with E_2 for binding to the ER. Following the time of incubation I added vehicle, E_2 (10^{-8}M), IL-1β (10ng/ml), or ICI (10^{-7}M) to the medium and incubated the hMS cell for another 24 h.

The conditionally immortalized human fetal osteoblastic hFOB-ER9 cell line (this cell line was established earlier in cooperation with Dr. Spelsberg's and Dr. Khosla's laboratory and is now maintained in Dr. Khosla's laboratory) containing physiological concentration of functional estrogen receptors were maintained at a temperature of 33,5°C. To examine if these cells express estrogen receptor-α (ER-α) and if the deficiency or presents of E_2 will change the expression of aromatase, I cultured the cells with standard growth medium supplemented with 10% CSS instead of HI-FBS for 24 h, in medium supplemented with 1% CSS plus ICI (10^{-7}M) for another 24 h and were then treated with E_2 (10^{-8}M), or IL-1β (10ng/ml) for again 24 h.

The human osteoblastic osteosarcoma cell line SaOS2 was maintained in standard growth medium at a temperature of 37°C. During the experiment the standard growth medium was supplemented with 10^{-6} M Dex for 72 h and 10 ng/ml IL-1ß for the last 24 hours. For the dose response experiment the cells were again grown in the standard growth medium supplemented with 10^{-6} M Dex for 72 h and 10 ng/ml IL-1ß for the last 24 hours and than treated with different doses of E_2 (10^{-10}- 10^{-7} M).

The rat osteosarcoma cell line ROS 17/2.8 has a more osteoblastic phenotype. The rat osteosarcoma cell line UMR106 has a premature phenotype. Both cell lines (ROS 17/2.8, and UMR106) were maintained in Ham's F-12 medium (GIBCO BRL, Life Technologies, Grand Island, NY) supplemented with 10% HI-FBS and 1% Penicillin/Streptomycin. All subsequent experiments were performed using this medium with or without additional reagents at doses and time indicated for each experiment.

All the cell experiments were performed in 6-well plates in triplicate.

Mr. Lamsam, a technician of Dr. Khosla's laboratory, introduced me to the different cell lines which were used and stored in the laboratory. In the past I had already worked with plant cell culture, hence, I was able to learn the handling of the human bone cells in a short period of time. After the training time I was able to maintain the cell lines and perform the described experiments myself.

2.2 Molecular Biologic Methods

2.2.1 Isolation of Total RNA

2.2.1.1 Cells *in vitro*

I isolated total RNA from cells in cell culture using the RNeasy Mini Kit (Qiagen, Inc Valencia, CA) following the manufacturer's protocol.

2.2.1.2 Rodent Bones

Dr. Sanyal introduced me to the RNA isolation protocol and the freezer mill (SPEX CertiPrep, Metuchen, NY), so that I was able to perform the here described experiments myself afterwards.

Total RNA from the rodent bones was isolated from the lumbar vertebrae (L1-L4) and the mid-shaft of the femur. The metal tubes from the freezer mill (SPEX CertiPrep, Metuchen, NY) were cooled down in liquid nitrogen or on dry ice. The frozen bones were placed into the metal tubes and ground in the freezer mill for 1 minute together with 1 ml Trizol (Invitrogen™ life technologies, Carlsbad, CA**)**. After the grinding the pulverized bone was transferred into a 50 ml sample tube (Corning, Corning, NY) and 4 ml Trizol was added. The frozen Trizol and the pulverized bone thaw in the additional Trizol and were incubated for 1.5 h in a water bath at 37°C under permanent shaking. Every 15 minutes the samples were vortexed and at the end of the incubation time centrifuged for 5 minutes at 3000 rpm. The supernatant was transferred into a 2.0 ml vial (Corning, Corning, NY) and per 1 ml of Trizol supernatant 0,2 ml of chloroform (24:1 chloroform/isoamyl alcohol) was added. The samples were shook vigorously by hand for 15 seconds, incubated for 5 minutes at room temperature, and than centrifuged for 15 minutes at 12500 rpm at 4°C. The upper colorless aqueous phase was transferred into a new 2.0 ml vial and 300 µl isopropylalcohol (2-propanol)/500µl aqueous phase was added. The samples were mixed well, incubated for 5-

10 minutes at room temperature and centrifuged for 15 minutes at 14000 rpm at 4°C. The supernatant was removed and the pellet was air dried for 3 minutes. The RNA pellet was dissolved in 30 µl of RNase-free sterile water by incubation for at least 15 minutes at 58-60°C. All vials from one sample were pooled, brought up to a total volume of 200 µl, and 400 µl equal volumes of phenol and chloroform (24:1 chloroform/isoamylalcohol) were added. The samples were centrifuged briefly. The aqueous phase was used and the phenol/chloroform step was repeated two more times. At the end the aqueous phase was mixed with chloroform (24:1 chloroform/isoamylalcohol). For the RNA precipitation 1/10 of 3 M sodium acetate (RNase free) and two volumes of cold 100 % ethanol was added to the aqueous phase and mixed well. For one hour or over night the samples were kept at -70°C. The samples were heated up to room temperature and centrifuged for 15 minutes at 14000 rpm. The pellet was washed with 70 % ethanol (~400 µl/vial) and dissolved in 30 µl of RNase-free sterile water by incubation for at least 15 minutes at 58-60°C. After quantitation by UV absorption at 260 nm, 1 µg of the total RNA was used for the cDNA synthesis.

2.2.2 cDNA Syntheses

I completed 1 µg of total RNA and 2 µl of Random Primer p(dN)6 (0.25 units) with sterile water to a volume of 12 µl. After incubation at 65° C for 5 minutes, I mixed the RNA with a cocktail containing 5x RT AMV buffer, RNase inhibitor (20 U), dNTPs (2 mM) and reverse transcriptase RT AMV (25 Units, Roche Diagnostics GmbH, Mannheim, Germany). The final volume was 20 µl. The samples were incubated at 42° C for 2 hours. The RT AMV was inactivated at 95°C for 5 minutes. Thus, I diluted the cDNA mix 5-fold and used the cDNA for the PCR analysis (see 2.3.2 and 2.3.3).

I also used the iScript^{TM} cDNA Synthesis Kit (Bio-Rad Laboratories, Hercules, CA) to synthesize cDNA; iScript is a modified MMLV-derived reverse transcriptase, optimized for reliable cDNA synthesis over a wide dynamic range of input RNA. The enzyme is provided pre-blended with RNase inhibitor. The unique blend of oligo (dT) and random hexamer primers in the iScript Reaction Mix works exceptionally well with a wide variety of targets. This bled is optimized for the production of targets < 1 kb in length.

I used a total volume of 20 µl for this reaction. 1µg of total RNA was mixed with 4 µl of 5x iScript Reaction Mix, 1 µl iScript Reverse Transcriptase, and nuclease-free water. First the reaction was incubated at 25°C for 5 minutes, than at 42°C for 30 minutes. The iScript Reverse Transcriptase was inactivated through an incubation at 85°C for 5 minutes. Thus, the cDNA mix was then diluted 5-fold and used as a source of template for the PCR analysis (see 2.3.2 and 2.3.3).

2.3 PCR-Reactions

2.3.1 Used Oligonucleotides

I selected and ordered the necessary oligonucleotides for the PCR reactions. The synthesis of the oligonucleotides was carried out by the Mayo Syntheses Group. The oligonucleotides are dissolved in autoclaved, bidestillated water and stored at -20°C.

Oligonucleotides for the cDNA amplification are:

mSRC-1: A) 309 bp B) 687 bp

A) 5'-CAACCAGCAAAGGCTGAGTCCA-3' and 5'-AGTACCTCCTGAGGGGTTAGAG-3'

B) 5'-TGCCGACGCGCTAGACGATTTC-3' and 5'-ACACAGCAAAGAACTGGAGGTG-3'

mSRC-2: 338 bp

5'-CTACCAGCAGCCATGAGCAATC-3' and 5'-CATCGACACACTGATGTTCATGTTG-3'

mER-α: 306 bp

5'-GGCAAAGAGAGTGCCAGGCTTTG-3' and 5'-CAGAAACGTGTACACTCCGGAATT-3'

mER-β: 300 bp

5'-GCAGCACAAAGAATATCTGTGTGTG-3' and 5'-AGCGTGTGAGCATTCAGCATCTC-3'

GAPDH

Mouse and Rat: 239 bp

5'-CATCACCATCTTCCAGGAGCGAG-3' and 5'-GTGCAGGATGCATTGCTGACAATC-3'

Aromatase:

Human: 542 bp

5'-GAGAAGTCTGTCAAGGATTTGAA-3' and 5'-CCTATAAGGAACATTCTTTG CAA-3'

Mouse: 247 bp

5'-GAGTATCCAGAGGTCGAAGCAGCAA-3' and 5'-TACTCGAGCCTGTGCATTCTTCCGA-3'

Rat: 339 bp

5'-AGGAGAACGTGAATCAGTGTATA-3' and 5'-TACTCGAGCCTGTGCATTCTTCCGA-3'

2.3.2 Conventional Polymerase Chain Reaction

For conventional PCR a total volume of 50 µl consists of:

5 µl	10x PCR Buffer
1 µl	10 mM dNTPs
1 µl	(10 pmol/µl) forward primer
1 µl	(10 pmol/µl) reverse primer
1-2 units	DNA Polymerase (Roche Diagnostics Corporation, Indianapolis, IN)
5 µl	cDNA (see 2.2.2) or genomic DNA
x µl	bidestillated water

The amplification was performed in a Perkin Elmar Gene Amp PCR System 9600 with the following incubation times and temperatures:

	94°C	5 min initial denaturation step
(30 -35 x)	94°C	5 min denaturation of double strain DNA
	60-62°C	1 min hybridization of the primers with the template DNA
	70°C	1 min elongation
	70°C	5 min

The hybridization temperature was dependent on the primer pair which was used in the reactions. The time of the elongation and the cycle number was dependent on the length of the PCR product.

After the reaction 1/10 of stopping buffer was added to the PCR product and was analyzed on an ethidiumbromid-agarose gel. For the documentation the gel was monitored on an UV light table.

I performed all conventional PCR reactions of the different cell lines and bone tissues myself.

2.3.3 Real Time Polymerase Chain Reaction

Unlike with conventional PCR the real time PCR offers the possibility to quantify starting amounts of nucleic acid in individual reactions quickly and accurately. The real time PCR machine is designed to detect fluorescent reporter molecules that increase in signal with each successive round of amplification. A visual representation of the increase of fluorescent signal allows to determine starting amounts of nucleic acid in each sample, as well as to monitor real-time kinetics of each amplification.

The real-time PCR was performed in an I-Cycler (Bio-Rad, Hercules, CA).

Dr. Sanyal introduced me to the handling of the I-Cycler. The determination of the expression level of SRC-2 (see 3.2.1.7) was performed by Dr. Sanyal.

A 50 µl PCR mix, contained

25 µl	iQ SYBR Green Supermix	100 mM KCl,
		40 mM Tris-HCl, pH 8.4,
		0.4 mM of each dNTP,
		iTap DNA polymerase,
		6 mM $MgCl_2$,
		SYBR Green 1,
		20 nM fluorescein,
		stabilizers

7.5 pmol forward primer (see 2.3.1)

7.5 pmol reverse primer (see 2.3.1)

5.0 µl cDNA (see 2.2.2)

2.4 Activity Test to Determine Aromatase Activity

2.4.1 Preparation of the Mouse Bones

Three-month old C57BL/6 female mice were sham-operated or ovariectomized by the supplier (Charles River Laboratories, Wilmington, MA). Fourteen days after the surgery I harvested the femur and the tibia with assistance by one of our technicians (Mr. Fraser).

Six-month old SW female mice (Charles River Laboratories, Wilmington, MA) were used for an initial experiment (without surgery). In these mice the femur and the tibia were harvested, too. After resection, I flushed out the bone marrow with ice-cold isotonic saline and the bones were stored on ice until all bones were flushed out. After the flush out I ground the bones in a liquid N_2 cold mortar with 2.5ml of Krebs-Ringer phosphate buffer, pH7.4 (with a final androstenedione concentration of 100nM, NADPH 1mM, glucose 1mM). The tissue was ground until fine ivory-colored bone spicules remained.

2.4.2 Incubation with ^{3}H-Androstenedione

I placed the ground bones in six-well plates. The plates were incubated for 3h at 37°C in a humidified atmosphere of 5% CO_2 in the presence of 1 µl of [1β-^{3}H] androstenedione (^{3}H-1βA; specific activity 25,9 Ci/mmol; Perkin Elmer, Life Sciences Inc.,Bosten, MA) and stirred every 30 minutes. I terminated the reaction by transferring the plates into an ice bath (4° C) for 15 minutes. The blank samples contained the medium without bone.

To demonstrate the specificity of the aromatase activity assay one sample of ground bones were treated with 4-hydroxyandrostenedione [4-OHA], an aromatase inhibitor. This aromatase inhibitor down-regulated the expected activity of the aromatase.

2.4.3 Determination of Tritiated Water

The standard assay of aromatase activity in mouse bone measures the release of $^{3}H\text{-}H_2O$ from ^{3}H-1βAndrostenedione during estrogen synthesis.

All procedures were done on ice. I transferred the supernatant and the bone spicules into 50 ml tubes (Corning, Corning, NY) and centrifuged for 5 minutes at 1300 rpm. The supernatant was stirred with 3 ml Chloroform and centrifuged for 5 minutes at 1300 rpm. 800 µl of the aqueous phase were mixed well and incubated with 2 ml of 2.5% activated charcoal in 1 x PBS. To allow sufficient adsorption of free steroids, the samples were mixed again after 15 minutes. After centrifugation at 1000 rpm for 15 minutes, 800µl of the supernatant was mixed with 10ml Ultimate Gold (Packard, Meriden, CT). The radioactivity was counted in a LS 6000 IC scintillation counter (Beckman-Coulter, Fullerton, CA).

I adapted the here described activity test for the determination of aromatase activity as published by Ackerman et al. (Ackerman et al., 1981) earlier. I performed all the experiments using this method myself.

2.5 Maintenance and Care for Mice

2.5.1 Housing

Two female and one male SRC-1 KO mice were provided from Dr. J. Xu from Dr. B. O'Malley's Laboratory at the Baylor College of Medicine, Houston, Texas USA to establish a breeding colony. The generation of the SRC-1 KO mice has been described (Xu et al., 1998), and the mice used in this study have been extensively back-crossed (for 7 or more generations) into the C57BL/6 background. The generation and back-crossing of the SRC-1 mice was already done in Dr. B. O'Malley's laboratory.

The mice for my dose response study (C57BL/6 mice) were purchased from an animal supplying company (Charles River Laboratories, Wilmington, MA). They were ten-weeks of age and housed in our animal unit until they were old enough for the experiment and had time to adjust to the new environment.

The animals were housed in a temperature-controlled room (22±2° C) with a daily light/dark schedule of 12 h. During the experiment the animals had free access to water and were pair fed (approximately 28 gram per mouse per week) standard laboratory chow (Laboratory Rodent Diet 5001, PMI Feeds, Richmond, VA) containing 0.95% calcium. The Institutional Animal Care and Use Committee approved all animal procedures.

The general maintenance, care and cleaning of the mice and mice cages was performed by the animal care personal of the Mayo Clinic. Especially Mr. Fraser, one of the technicians in Dr. Khosla's laboratory, took care of the breeding of the SRC-1 KO mice and helped me organizing all mice for the different experiments; food control and pair feeding was done by me.

2.5.2 Genotyping of the SRC-1 KO Mice

Pups from the SRC-1 KO mice were genotyped at 4-5 weeks of age by polymerase chain reaction (PCR) (see 2.3.2) as described previously (Xu et al., 1998). For the genotyping, genomic DNA was isolated from tail biopsies, respectively, after overnight proteinase K treatment and ethanol precipitation (Qiu et al., 1997). The genomic DNA was used for PCR to distinguish between wild-type (+/+), homozygous mutant (-/-), or heterozygous (+/-) mice. For the analyses four specific primers were used (Xu et al., 1998). The paired primers P1 (5'-caaccagcaaaggctgagtcca) and P2 (5'-agtacctcctgaggggttagag) detected a 309-base pair exon region that represents wild-type SRC-1. Primers P3 (5'-tgccgacgcgctagacgatttc) and P4 (5'-acacagcaaagaactggaggtg) detected a 687-base pair fragment which represents homozygous mutant SRC-1.

The breeding and genotyping of the SRC-1 KO mice were carried out by Mr. Fraser, who works as a technician in Dr. Khosla`s laboratory.

2.6 Determination of Bone Mineral Density

2.6.1 Dual Energy X-ray Absorptiometry

Dual energy x-ray absorptiometry (DXA) allows accurate and precise measurements of soft tissue and bone. The instrument provides an excellent correlation to total ash weight ($r = 0.99$), which is commonly used as a standard. The source for the x-ray is a cone beam with stationary area detectors. An advantage of the DXA is that low doses of x-ray energy are used for the examinations and also a fast measurement of BMD at multiple sites is possible. The results are reported in mg/cm^2 for bone mineral density (BMD), and in mg for bone mineral content (BMC).

It is to keep in mind that DXA is a projectional (two-dimensional) rather than a cross-sectional method, it includes both cortical and trabecular components into the measurement.

For an adequate evaluation of the overall BMD status, both cortical and trabecular sites should be examined.

In the presented study the Lunar PIXImus densitometer (DXA, software version 1.44.005, Lunar Corp, Madison, WI) was used. A calibration of the machine was performed daily using the hydroxyl apatite phantom provided by the manufacturer. To determine the BMD in the mice *in vivo*, they were first anesthetized with Avertin (2,2,2 tribromoethanol, 720 mg/kg, ip). They were than placed on the animal tray in a prone position. In this position, the whole body of the mouse can be scanned at the same time, only the head is partially outside the area scanned by the machine. However, in all analyses, the bones of the skull were excluded. After scanning, regions of interest were identified for more specific analyses. In this study I always evaluated the BMD of the lumbar spine and the whole femur. In repeatedly scanned mice (with repositioning between scans), the coefficients of variation (CVs) for total body; lumbar, and femoral BMD were 4,9%, 2,7%, and 4,3%, respectively.

After an introduction of the handling of the Lunar PIXImus densitometer, I performed all BMD measurements and subsequent data analysis myself. I also anesthetized and positioned the mice for the scans.

2.6.2 Peripheral Quantitative Computed Tomography (pQCT)

Computed tomography (CT) was introduced by Hounsfield (Hounsfield, 1973, 1976) at the beginning of the 70s for medical imaging. The absorption of x-ray by an object yields an absorption profile. The raw data are corrected for dead time and beam hardening. By mathematical folding of many absorptions profiles from different angular positions a cross sectional image can be calculated which represents the original object. Each point of the image (voxel) corresponds to an attenuation coefficient with the dimension 1/cm. By calibration with phantoms of a specified hydroxyl apatite concentration the attenuation coefficients can be transformed to density values.

The pQCT bone scanner is a fully automated measuring system for the determination of bone density. The detector-system consists of a series of miniature-semiconductor-crystals. The scan is divided into two steps: scout view and CT-scan. During the scout view the object is scanned in steps along the longitudinal axis. The beam moves perpendicular to this axis. The computer screen shows a color-coded digital image similar to a x-ray image with bright areas for bone and dark areas for soft tissue. The scout scan is used to determine the desired position of the measurement.

During the CT-scan the x-ray beam passes the object perpendicular to the axis of the arm. After each transverse scan the gantry is rotated 12° which is the angular distance from the first to the last of the detectors for the CT-scan. 15 rotations of the gantry therefore cover the necessary angular range of 180°.

The pQCT measures cortical and trabecular combined, but also distinguish between these two bone compartments. It defines the volume rather than its two-dimensional projection. The results which are reported for BMD are true volume (mg/cm^3) and are less influenced by bone size.

For the pQCT measurements the mice were first anesthetized with Avertin (2,2,2 tribromoethanol, 720 mg/kg, ip) and than placed in a supine position on the gantry of the Stratec XCT Research SA Plus using software version 5.40 (Nordland Medical Systems, INC., Fort Atkinson, WI). The calibration of the machine was performed daily with the hydroxyl apatite phantom provided by the manufacturer. The mice were positioned so that the total length of the femur and tibia were visible on the scout view. The scout view speed was set at 15.0 mm/sec with a slide distance of 0.5 mm. Once the scout view was completed, the reference line for the CT scans was set at the most proximal point of the tibia. Slice images were set at 1.9 mm (proximal metaphysis of the tibia) and for the dose response study cortical bone was measured at the tibia-fibula junction. The CT speed was set at 3 mm/sec, pixel size was 100 μm x 100 μm and slice thickness was 0.5 mm. After scanning, the CT

slices were analyzed using peel mode 2, cortmode 1 and contour mode 1 to evaluate trabecular and cortical parameters. To determine the cancellous bone the threshold was set at 214 mg/cm^3 and for cortical bone at 710 mg/cm^3. CV was 4.4% for the total tibial volumetric BMD.

A technician of the Stratec Company explained the handling, functions and options of the pQCT. He monitored some of the practice scans and help with the analysis. Later, I performed all the scans described in this study myself, including intra-abdominal anesthesia and positioning of the mice.

2.7 Micro computerized tomography (µCT) scanning

In addition to pQCT scanning µCT scanning was used which provides a much higher spatial resolution and therefore reduces the volume render effect. The µCT made it possible to analyze the bone specimens in more detail. The specimen is placed on a sample table and is rotated in 721 equiangular steps around 360° between an exposure with X-ray and the recording by a charge-coupled device (CCD) detector. It allows non-invasive imaging and analysis of the three-dimensional bone structure.

The whole tibia was scanned using a µCT system (Physiological Imaging Research Laboratory, Mayo Clinic, Rochester, MN, Principal Investigator: Dr. Ritman) as described by Jorgensen et al. (Jorgensen et al., 1998) with a resolution of 20 µm in all three dimensions. The raw data were reconstructed and the resulting 3-D images were displayed using image analysis software (Analyze® 4.0; Biomedical Imaging Resource, Mayo Clinic, Rochester, MN). The volume of interest was 30 slices below the growth plate and covered 0.6 mm of the proximal metaphysis of the tibia. This region was chosen because it allowed for measurements of cortical and cancellous bone and it represents the comparable region that was measured by pQCT. Cortical thickness was measured at nine equally distributed sites at every second cross-section within the volume of interest. The full width half max function

was used for this measurement. The trabecular bone volume was also measured in the same volume of interest. To determine trabecular bone a threshold was chosen which represented bone in all samples. Thus, every voxel with a grey scale above the threshold was trabecular bone and every voxel with a grey scale below the threshold was determined as marrow within the cortical shell.

The positioning and scanning of the isolated tibias was done by technicians of Dr. Ritman's laboratory (Physiological Imaging Research Laboratory, Mayo Clinic, Rochester, MN). The 3-D-reconstruction of the raw data was performed by a technician who is specialized for this work. I analyzed the resulting 3-D data sets for cancellous and cortical bone volume and thickness using Analyze® 4.0 (Biomedical Imaging Resource, Mayo Clinic, Rochester, MN).

2.8 Gonadectomies

Before naturally occurring menopause 95% of serum estradiol (E_2) and most of estrone (E_1) is derived from ovarian secretion. The remaining 5% come from peripheral conversion of steroid precursors. In men 95% of circulating androgen is derived from testicular secretion. To create comparable steroid hormone levels in mice, the gonads which produce the majority of the sex steroids were removed, and resulted in estrogen or androgen deficiency. Slow steroid release pellets (Innovative Research of America, Toledo, OH) were used to replace a defined concentration of steroid hormone levels in the mice.

2.8.1 Ovariectomy

For the ovariectomy the mice were anesthetized and prepared for the surgery, and a dorsal midline skin incision was made caudal to the posterior border of the ribs. Using blunt dissection to tunnel subcutaneously, lateral to the skin incision, the muscles of the posterior abdominal wall were separated in order to enter the abdominal cavity. The ovary was located in a fat pad just beneath the muscles. Using forceps, the periovarian fat was gently grasped to lift and exteriorize the ovary. Mosquito forceps were used to crush the fallopian tube and cranial-most part of the uterine horn distal to the ovary, being careful not to crush or contact the ovary. The ovary was removed by cutting above the clamped area. The uterine horn was returned into the abdomen, and the process was repeated on the other side. The skin incision was closed using wound clips. Following the surgery, the mice were inspected every day for the first week. The wound clips were removed 7-10 days after the surgery.

Because of the large number of animals and the time consuming nature of the procedure Mr. Fraser assisted me with all the ovariectomies; post-surgical animal care and the removel of the wound clips was done by me.

2.8.2 Orchidectomy

For orchidectomy (orc) the mice were anesthetized and then placed in a supine position on a sterile working area. A small 1.0 cm median incision was made through the skin at the tip of the scrotum. The cremaster muscles were opened with a small 7 mm incision. The testicular fat pad on the left side was localized and pulled it through the incision using a blunt forceps. The caudal epididymidis was pulled out together with the testis, followed by the caput epidpidymidis, the vas deferens and the testicular blood vessels. A single ligature was placed around the vas deferens and the blood vessels. The testis was removed and the procedure was repeated for the other testis. After both testes were removed, the remaining pieces of the vas deferens, the fat and the blood vessels were replaced back in the scrotal sac. The muscle layer was closed by using a resorbable 6-0 suture and the skin with non-resorbable 4-0 suture material. Following the surgery, the mice were inspected every day for the first week. The non-absorbable suture material was removed 7-10 days post-operative.

Similar to the earlier described ovariectomies Mr. Fraser also assisted me with all the orchidectomies because of the large number of animals and the time consuming nature of the procedure; again post-surgical animal care and the removel of the non-absorbable suture material was done by me.

2.9 Pellet Implantation

For the implantation of the slow steroid release pellet (Innovative Research of America, Toledo, OH), the anesthetized mice were laid out on a sterile work area. The animal was shaved between the shoulder blades and betadine applied to the shaved area. A small incision was made with a surgical scissors, at which time a hemostat was inserted into the incision to create a small pocket under the skin. The pellet was placed in the incision and sutured with 4-0 silk. Also an additional skin clip was used to close the incision. The skin clip was removed 7-10 days after the pellet implantation. Following pellet implantation, the mice were inspected every day for the first week. If the pellet was coming out, it was noticed and that mouse was eliminated from the study. Also, at the termination of the study after the mice have been euthanized, the skin between the shoulder blades was laid open and the remains of the pellet were identified. The pellets were manufactured to last 60 days.
After the surgery Mr. Fraser and I performed the pellet implantation together.

2.10 Bone Histomorphometry

At the end of the SRC-1 female study the lumbar spines (L1-L4) were collected and the dorsal side was marked to ensure the correct orientation of the samples at the time of embedding. The lumbar spines were fixed in 70% ethanol for at least 72. Subsequently, the specimens were dehydrated in 95% ethanol for 1 day and in 100% ethanol for 6 days. The adjusting muscles were carefully removed from the spine so that the vertebral bodies are visible. In the bone histomorphometry laboratory (Mayo Clinic, Rochester, MN, manager of the Mayo Bone Histomorphometry Lab: Dr. Sibonga) the lumbar spines were then embedded without demineralization in a mixture of methylmethacrylate-2-hydroxyethyl and methylacrylate 12.5:1 and sectioned at a thickness of 5 μm on a Reichert-Jung Supercut 2050 microtome using tungsten-carbide tipped steel knives. Dorsal spine sections were collected from the middle of the lumbar spine. After clearing in xylene the sections were mounted in

Eukitt (ProSciTech, Thuringowa Central Qld, Australia) for microscopic examination. All static cancellous measurements were performed on unstained sections under UV and normal light with the use of the Osteomeasure software, image analysis software programmed for measurements made specifically in bone (Osteometrics Inc., Atlanta, GA). Cancellous bone was measured in secondary spongiosa in the spine. The site did not include trabecular profiles immediately adjacent to cortical bone (to exclude peripheral modeling bone). The measurements were performed in multiple frames, the sum of which totaled approximately 1 mm^2. Histomorphometric measurements were obtained at the spine in order to correlate with the spine DXA measurements. The measurements for cancellous bone included Bone Volume (Bone Volume/Measured Tissue Volume, BV/TV; %), Trabecular thickness (TbTh; μm), Trabecular separation (Tb.Sp.; μm), and Trabecular number (Tb.N,; mm^{-1}). The measured and calculated values for cancellous bone histomorphometry are measured, derived and expressed in standardized units and nomenclature for bone histomorphometry (Parfitt et al., 1987).

However, since bone turnover in the vertebra is slower relative to the long bones. Bone formation rates (BFR) were determined in the various groups in the femoral metaphysis. To determine dynamic parameters like BFR the mice received the fluorochromes calcein (10 mg/kg dissolved in 1% sodium bicarbonate) and tetracycline (10 mg/kg dissolved in water) twelve and four days, respectively, before the end of the study. The fluorochromes were injected into the tail vein of the mice, which were positioned in a mouse holder. The fluorochromes incorporate at the calcification front of new forming bone. When administered over a distinct labeling period, measurements of fluorochrome labels and the interlabel bone growth can be used to estimate bone turnover.

The left femurs were processed in the same way as the lumbar spine with sections collected from the middle of the long bone. After sectioned and mounted, the samples slides were examined under UV light. The BFR (BFR/BS; mm^2/mm/day) was measured in cancellous

bone at the proximal femoral metaphysis at a standard sampling site in secondary spongiosa. Only distinct, double fluorochrome labels were used for calculation of formation rates.

I was trained in the different steps of bone histomorphometry sample preparation. During the study I received additional help with the embedding and sectioning of the bone samples by technicians of the histomorphometry laboratory (Mayo Clinic, Rochester, MN, manager of the Mayo Bone Histomorphometry Lab: Dr. Sibonga). After I was trained in the handling of the microscopes and the image analysis program by Dr. Sibonga, I performed all histomorphometric measurements and calculations myself.

2.10.1 Goldner's Masson Trichome Stain

To assess whether a normal skeletal phenotype exists in the SRC-1 KO mice, longitudinal sections of the vertebral spine were stained with Goldner's Masson Trichrome stain. Evidence of osteomalacia in the SRC-1 KO mouse bones was carefully examined since SRC-1 may also modulate 1,25-dihydroxyvitamin D action.

Weigerts A:

2.5 gm ferric chloride

1.0 ml HCL

Total volume of 100 ml with distilled water

Weigerts B:

1.25 gm hematoxylin

Total volume of 100 ml with 95% ETOH

Ponceau de Xylidene-Acid Fuschin Stock Solution:

0.6 gm ponceau de xylidene G,R,2R (Acid Red 26)

0.3 gm acid fuschin

0.9 ml glacial acetic acid

Total volume of 90 ml with distilled water

Orange G Stock Solution:

1 gm	orange G

Total volume of 100 ml with distilled water.

Ponceau de Xylidene-Acid Fuschin-Orange G Staining Solution:

10 ml	ponceau-acid fuschin stock soln.
10 ml	orange G Stock soln.
80 ml	distilled water

1% Phosphomolybdic Acid:

1 gm	phosphomolybdic acid

Total volume of 100 ml with distilled water.

Light Green:

0.1 to 0.2gm	light green SF yellowish
0.2 ml	glacial acetic acid

Total volume of 100 ml with distilled water.

First, the 5 μm sections were flattened with 50 % ethanol. For the Goldner's stain equal volumes of Weigerts A and Weigerts B solution were mixed and the sections were incubated in the Weigert Hematoxylin solution for 5 minutes. The sections were rinsed in water until they were clear. In the next step the sections were incubated for 3 minutes in the Ponceau de Xylidene-Acid fuschin-Orange G Staining solution and rinsed now with 1 % acetic acid until they were clear. For 3 minutes the sections were stained in 1 % Phosphomolybdic Acid and than again rinsed in 1 % acetic acid. In the last staining step the sections were incubated for 3 minutes in Light Green. Briefly, the sections for slide preparation were rinsed in 1 % acetic acid and subsequently rinsed in water and than dehydrated in increasing concentrations

of ethanol (70, 95, 100, and 100 %). The sections were immersed in 50/50 % Xylene/Methanol and cleared in 100 % Xylene. After clearing in Xylene the sections were mounted in Eukitt and were examined under the microscope.

After training in Dr. Sibonga`s laboratory I was able to do all the stains, analyses and photographs described in this study myself.

2.11 Uterus Histology

At the end of the experiments the mice were sacrificed and the uteri were excised. The tissue samples were fixed overnight in 10 % paraformaldehyde at 4°C, rinsed, and stored in 70 % ethanol before routine processing into paraffin wax. The sections of the uteri were prepared and stained with hematoxylin-eosin.

The uterus histology was performed by Dr. Frisk (Mayo Clinic).

2.12 Estradiol Measurement

Serum estradiol was measured by radioimmunoassay (RIA) (Diagnostic Products Corporation, Los Angeles, CA). The DPC's Double Antibody Estradiol procedure is a sequential radioimmunoassay in which the serum sample is preincubated with anti-estradiol antiserum. ^{125}I-labelded estradiol then competes with E_2 in the sample for antibody sites. After incubation for a fixed time, separation of bound from free ^{125}I-labelded estradiol is achieved by the PEG-accelerated double-antibody method. Finally, the antibody-bound fraction is precipitated and counted. The estrogen concentrations are read from a calibration curve. The antiserum is highly specific for E_2, with an extremely low crossreactivity to other naturally occurring steroids or therapeutic drugs that may be present in serum samples.

The blood collection was performed by orbital sinus venipuncture in anesthetized mice. After the blood was coagulated it was centrifuged for eight minutes at 8000 rpm to separate the serum from the cells. The serum was stored at -20°C. Before the radioimmunoassay procedure all components except the Precipitating Solution must be at room temperature (15-28°C). As

controls some tubes were labeled with T (total counts), NSB (non-specific binding), A (maximal binding), and B through G to calculated the calibration curve. 100 µl of the zero calibrator A was pipetted into the NSB and A tubes, and 100 µl of each of the remaining calibrators B through G into correspondingly labeled tubes. Also, 100 µl of each serum sample was pipetted into the prepared tubes. 50 µl of E_2 Antiserum was added to all tubes expect NSB and T tubes. After vortexing everything well it was incubated for 2 hours at room temperature. 50 µl of ^{125}I-labelded E_2 was added to all tubes and vortexed again. The T tube was removed for the counting at the end, it requires no further processing. The remaining tubes were incubated for one hour at room temperature. Finally, 500 µl of cold Precipitating Solution was added to all tubes and vortexed. An additional incubation for 10 minutes at room temperature was performed. The samples were centrifuged for 15 minutes at 3000 x g. The supernatant was decanted and all the residual droplets were removed. Each tube was counted for one minute in the gamma counter. All samples were prepared in duplicates. The interassay CV is < 16%.

The estrogen measurements were performed by Mrs. Hoey, a technician of Dr. Khosla's laboratory.

2.13 Experimental Design

2.13.1 Estrogen Dose Response Study

Experiment 1. The first experiment was been done in 6 month old female C57BL/6 mice (average body weight 0.028 kg). The mice were assigned to seven groups (n= 6-12 per group) as follows: sham operated, ovx'd and implanted a vehicle pellet (0 μg/kg/day E_2), or ovx'd and implanted with 60 day slow release pellets delivering 5, 10, 20, 40, or 500 μg/kg/day E_2 (Innovative Research of America, Toledo, OH) (see 2.8.1 and 2.9). Following 56 days of treatment, bone mineral density (BMD) was measured at the spine and femur using dual energy X-ray absorptiometry (DXA, see 2.6.1) and at the proximal tibial metaphysis and the tibia-fibula junction using peripheral quantitative computed tomography (pQCT, see 2.6.2). After appropriate anesthesia, blood was drawn by cardiac puncture and the animals were sacrificed by inhalation of CO_2. The uterus was excised and weighed.

Experiment 2. In the second experiment, 3 month old C57BL/6 mice were used and the duration of the experiment was reduced to 1 month (average body weight 0.025 kg). The rationale for this was that if similar results were observed in younger mice treated for a shorter period of time that would be preferable for future studies, given the cost of animal care and maintenance. These mice were assigned to six groups (n= 4-7 per group) and were either sham operated, ovx'd and implanted a vehicle pellet (0 μg/kg/day E_2), or ovx'd and implanted with 60 day pellets delivering 5, 10, 20, or 40 μg/kg/day of E_2 (Innovative Research of America, Toledo, OH) (see 2.8.1 and 2.9). BMD was measured by DXA and pQCT (see 2.6.1, 2.6.2) after 30 days of treatment, the animals were sacrificed by inhalation of CO_2, and the uteri were excised and weighed.

2.13.2 Effects of Ovariectomy and Estradiol Treatment on the Skeletal Phenotype of SRC-1 KO Female Mice

In order to compare the skeletal response to estrogens in WT versus the SRC-1 KO mice, three month old female SRC-1 KO and WT littermates had baseline measurements of BMD performed by DXA (lumbar spine and femur) and pQCT (proximal tibia) (see 2.6.1 and 2.6.2) and were then divided into three groups (n = 8-11 mice per group). Mice were assigned to the three groups based on the cancellous BMD measured by pQCT to assure comparable tibial BMD among groups at baseline. Subsequently, the mice were either sham operated, ovx'd and implanted with a vehicle pellet (0 μg/kg/day E_2), or ovx'd and implanted a 10 μg/kg/day E_2 pellet (0.015 mg/60 d pellets) (see 2.8.1 and 2.9). On day 48 after the pellet implantation, the mice received the fluorochrome tetracycline (10 mg/kg) by tail vein injection followed by a calcein (10 mg/kg) injection on day 56 (see 2.10). BMD was again measured by DXA and pQCT 60 days post-surgery. Following this, the animals were sacrificed by inhalation of CO_2 and various tissues harvested. The uterus was excised and weighed, and the lumbar spine (L_1-L_4), tibias, and femurs were excised for histomorphometry (see 2.10) and μCT measurements (see 2.7).

Subsequent to this initial experiment, a fourth group was added to both the WT and SRC-1 KO mice (n = 9-11 for each) in order to test whether the defects in estrogen action noted in the SRC-1 KO mice using an E_2 dose of 10 μg/kg/day could be overcome using a high dose of E_2. These mice were ovx'd and received pellets delivering 40 μg/kg/day of E_2 (see 2.8.1 and 2.9). In our preliminary dose finding study, this relatively high dose of E_2 was clearly supraphysiological (see 3.1.1 and 3.1.2), but did not induce a sclerotic response in the tibial metaphysis, as has been seen with very high doses of E_2 (Edwards et al., 1992). All procedures in these mice were identical to those noted for the mice treated with the E_2 dose of 10 μg/kg/day.

2.13.3 Effects of Orchidectomy and Estradiol Treatment on the Skeletal Phenotype of the SRC-1 KO Male Mice

This experiment was performed parallel to the experiment with the female SRC-1 KO mice. BMD was also measured at the beginning and at the end of the experiment by DXA and pQCT (see 2.6.1 and 2.6.2). After the baseline measurement the three month old male SRC-1 KO mice and the WT littermates were assigned to three groups based on the cancellous BMD measured by pQCT to assure comparable tibial BMD among groups at baseline. Subsequently, the mice were either sham operated, orchidectomized (orc'd) and implanted with a vehicle pellet (0 μg/kg/day E_2), or orc'd and implanted a 10 μg/kg/day E_2 pellet (0.015 mg/60 d pellets) (see 2.8.2 and 2.9). On day 48 after the pellet implantation, the mice received the fluorochrome tetracycline (10 mg/kg) by tail vein injection followed by a calcein (10 mg/kg) injection on day 56 (see 2.10). BMD was again measured by DXA and pQCT 60 days post-surgery. Following this, the animals were sacrificed by inhalation of CO_2 and various tissues harvested. The seminal vesicles was excised and weighed. The lumbar spine (L_1-L_4), tibias, and femurs were excised but because of the clear results of the DXA and pQCT measurements the histomorphometry was not performed.

2.13.4 Effect of Orchidectomy and Treatment with Androgens on the Skeletal Phenotype of the SRC-1 KO Male Mice

To clarify if loss of SRC-1 in male mice has an impact of the action of androgens on bone, three month old orc'd WT and SRC-1 KO mice were treated with approximately 7 mg/kg/day of testosterone, another group of orc'd mice were treated with 5,5 mg/kg/day of 5α-DHT for 60 days. Sham operated, and orc'd age-matched SRC-1 KO and WT littermates receiving a vehicle pellet (0 μg/kg/day) were used as controls (see 2.8.2 and 2.9). The BMD was measured at the beginning and at the end of the experiment by DXA and pQCT (see 2.6.1 and 2.6.2).

2.14 Statistical Analyses

All data are presented as mean ± SEM. The primary comparison in the SRC-1 KO experiments was between the WT, ovx'd plus E_2, versus the SRC-1 KO, ovx'd plus E_2, mice since the key question was the skeletal response to estrogen in the two groups of mice. The sham and ovx'd plus vehicle groups were included in all cases to demonstrate that changes in the WT and SRC-1 KO mice were comparable under these conditions. Overall comparisons within groups were made using ANOVA, and individual comparisons between groups were made using non-paired t-tests. A P-value of < 0.05 was considered significant.

I did all statistical analyses of the SRC-1 KO mice experiments which were double-checked by Mr. Peterson (mathematical assistant, Division of Endocrinology).

For the dose response experiments all data are presented as means ± SEM. The overall dose effect was tested by ANOVA. Pair wise comparisons between the 0 dose versus the other doses were made using the Dunnett method, which adjusts for multiple comparisons. The sham and ovx'd groups were compared using t-tests. A P-value of < 0.05 was considered significant. I calculated all means and standard errors, all subsequent analyses using the Dunnett method was done by Ms. Atkinson (Division of Biostatistics, Mayo Clinic).

3 Results

3.1 Estradiol Dose Response in Mice

3.1.1 Effects of Increasing Doses of E_2 on Bone and Uterus in 6 Month Old C57BL/6 Female Mice Treated for 2 Months

I initially compared the effects of increasing doses of E_2 on bone and the uterus using ovx'd mice treated with 0, 5, 10, 20, 40, and 500 µg/kg/day of E_2 for 2 months (see 2.13.1). Estrogen deficiency caused by ovx significantly decreased spine and femur BMD (Figure 3.1) measured by DXA (see 2.6.1). However, treatment with an E_2 dose of as little as 5 µg/kg/day was effective in preventing bone loss at both the spine and the femur in these mice (Figure 3.1). Moreover, there was a dose-dependent increase in spine and femur BMD with higher doses (20 and 40 µg/kg/day) and even more so at a pharmacological E_2 dose of 500 µg/kg/day.

Table 3.1 shows the values for volumetric BMD at the proximal tibial metaphysis (total, cancellous, and cortical) and the cortical volumetric BMD at the tibia-fibula junction as measured by pQCT (see 2.6.2) in the various groups. In contrast to the spine (which also contains predominantly cancellous bone), cancellous BMD at the tibial metaphysis was not significantly lower in the ovx'd mice treated with vehicle as compared to the sham operated mice.

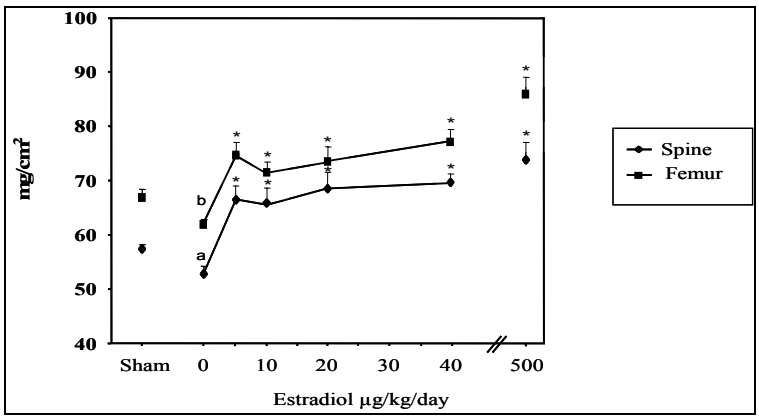

Figure 3.1. BMD of the spine and the femur (measured by DXA) in 6 month old female C57BL/6 mice following 56 days of either sham surgery or ovx plus pellets delivering 0, 5, 10, 20, 40, or 500 µg/kg/day of E_2. Data are means ± S.E.M. *, $P < 0.05$ versus 0 µg/kg/day, adjusted for multiple comparisons by the Dunnett method; a, $P < 0.05$, b, $P < 0.01$ versus sham.

However, similar to the DXA measurements at the spine and femur, the 5 μg/kg/day dose was sufficient to increase (above the level of the sham mice) BMD at the tibial metaphysis. In fact, the overall dose response relationship at the tibia using pQCT was similar to that seen at the femur using DXA. The high dose of E_2 (500 μg/kg/day) clearly resulted in a sclerotic response at the tibial metaphysis, with a marked increase in bone mass (approximately 200% increase in cancellous BMD). As expected, the high dose stimulated endosteal bone formation and increased cortical thickness (data not shown). Cortical volumetric BMD was maintained at the level of the sham mice by an E_2 dose of 5 μg/kg/day at the proximal site and the tibia-fibula junction of the tibia, with a further increase at higher doses (Table 3.1). Figure 3.2 shows the changes in uterine wet weight in these mice. As expected, uterine weight decreased following ovx. In contrast to the protective effects of very low doses of E_2 on cancellous and cortical bone, however, an E_2 dose of 40 μg/kg/day was necessary to fully restore uterine weight in the ovx'd mice to the level of the sham mice (Figure 3.2). Figure 3.3 shows changes in uterine histology with the various doses of E_2 in these mice (see 2.11).

Table 3.1. Volumetric BMD at the proximal tibial metaphysis (total vBMD, cancellous vBMD, and cortical vBMD) and at the tibia-fibula junction (cortical vBMD[§]) in 6 month old female C57BL/6 mice following 56 days of either sham surgery or ovx plus pellets delivering 0, 5, 10, 20, 40, or 500 μg/kg/day of E_2 measured by pQCT. Data are means ± S.E.M. *, $P < 0.05$ versus 0 μg/kg/d, adjusted for multiple comparisons by the Dunnett method; c, $P < 0.001$ versus sham.

	Total vBMD (mg/cm^3)	Cancellous vBMD (mg/cm^3)	Cortical vBMD (mg/cm^3)	Cortical vBMD[§] (mg/cm^3)
Sham	434.67 ± 6.26	172.8 ± 3.52	887.71 ± 7.65	1139.46 ± 7.94
Ovx + 0 μg/kg/day	386.39 ± 5.64[c]	173.18 ± 5.76	851.48 ± 4.86[c]	1091.62 ± 6.94[c]
Ovx + 5 μg/kg/day	518.63 ± 32.21*	280.11 ± 29.62	881.87 ± 14.32	1173.81 ± 17.90*
Ovx + 10 μg/kg/day	492.70 ± 28.88	246.01 ± 16.34	899.11 ± 10.13*	1152.57 ± 15.36*
Ovx + 20 μg/kg/day	517.85 ± 42.45*	266.82 ± 34.35	888.71 ± 12.74*	1159.06 ± 20.84*
Ovx + 40 μg/kg/day	607.76 ± 44.92*	352.76 ± 48.38*	902.79 ± 9.03*	1177.86 ± 10.94*
Ovx + 500 μg/kg/day	744.13 ± 53.68*	586.25 ± 59.46*	881.72 ± 8.61	1212.68 ± 185.89*

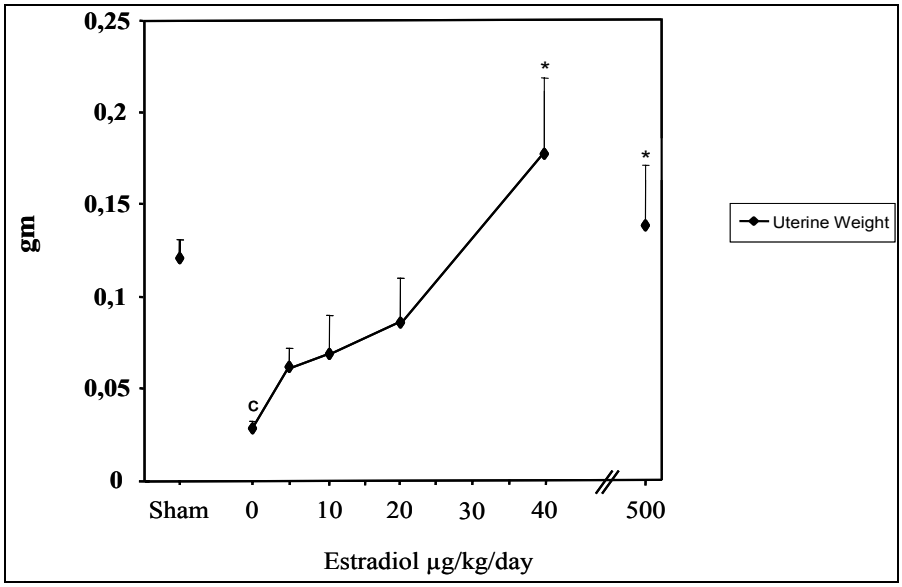

Figure 3.2. Uterine wet weights in 6 month old female C57BL/6 mice following 56 days of either sham surgery or ovx plus pellets delivering 0, 5, 10, 20, 40, or 500 µg/kg/day of E_2. Data are means ± S.E.M. *, $P < 0.05$ versus 0 µg/kg/d, adjusted for multiple comparisons by the Dunnett method; c, $P < 0.001$ versus sham.

The uteri of sham operated mice show tortuous endometrium with tall columnar epithelium, large endometrial glands and the stroma had a significant infiltration with polymorphonuclear (PMN) cells (Figure 3.3.A). By contrast the endometrium from the ovx'd mice had cuboidal epithelium, the endometrial glands were small, and the stroma contained closely packed hyperchromatic cells with no cytoplasm (Figure 3.3.B). At a dose of 10 µg/kg/day, there was a shift from cuboidal to columnar epithelium. Endometrial glands were getting larger again and contained a large amount of eosinophilic cytoplasm (Figure 3.3.C). However, a dose of 40 µg/kg/day was necessary to see tall columnar endometrial epithelium and stromal cells with abundant eosinophilic cytoplasm (Figure 3.3.D).

Serum estradiol levels (see 2.12) decreased significantly after ovx (Table 3.2). E_2 treatment at doses of 5 to 20 µg/kg/day resulted in serum E_2 concentrations similar to the level in the sham mice (with differences between these doses being hard to see due to the variability of even this sensitive assay at these low levels). However, the 40 µg/kg/day dose did result in serum E_2 levels that were approximately 4 times above the physiological level and even higher at the pharmacological E_2 dose of 500 µg/kg/day (Table 3.2).

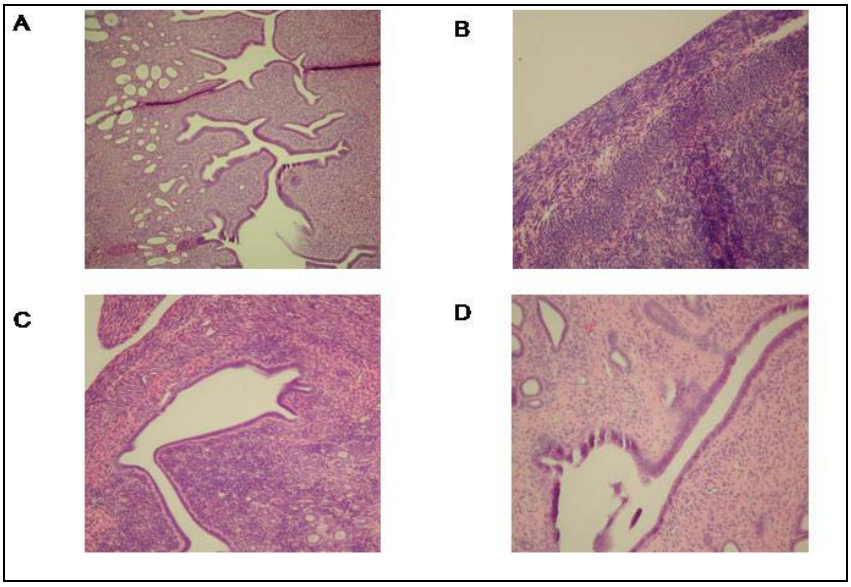

Figure 3.3. Uterine Histology. At the end of the experiment the uterus from the mice was isolated and fixed in paraformaldehyde. **(A)** Uterus from a sham mouse showing tortuous endometrium with tall columnar epithelium. **(B)** Uterus of an ovx'd mouse showing densely packed hyperchromatic cells within the stroma. **(C)** Uterus of a mouse treated with 10µg/kg/day E_2 showing columnar endometrial epithelium and hyperchromatic cells within the stroma. **(D)** Uterus of a mouse treated with 40µg/kg/day E_2 showing tall columnar epithelium and stromal cells with abundant eosinophilic cytoplasm. The sections were stained with hematoxylin-eosin. Magnification x100. Histology was performed by Dr. Frisk. Photographs were taken by Mr. Fraser.

Table 3.2. Serum estradiol concentration of 6 month old female C57BL/6 mice following 56 days of either sham surgery or ovx plus pellets delivering 0, 5, 10, 20, 40, or 500 µg/kg/day of E_2. Data are means ± S.E.M. *, $P < 0.05$ versus 0 µg/kg/day, adjusted for multiple comparisons by the Dunnett method; c, $P < 0.001$ versus sham. Estrogen concentrations were measured by Mrs Hoey.

	Serum E_2 (pmol/L)
Sham	19.86 ± 1.98
Ovx + 0 µg/kg/day	11.71 ± 0.48[c]
Ovx + 5 µg/kg/day	18.13 ± 2.64
Ovx + 10 µg/kg/day	18.65 ± 3.45
Ovx + 20 µg/kg/day	14.61 ± 1.28
Ovx +40 µg/kg/day	71.25 ± 28.49
Ovx + 500 µg/kg/day	184.39 ± 88.43*

3.1.2 Effects of Increasing Doses of E_2 on Bone and Uterus of 3 Month Old Mice Treated for 1 Month

In the second experiment, I used a different experimental paradigm. Three months old mice were treated for only 1 month (see 2.13.1). As in experiment 1, the 5 μg/kg/day dose was effective at preventing bone loss at the femur (which contains predominantly cortical bone) in the younger mice in experiment 2 (Figure 3.4.). Although the changes in cortical volumetric BMD at the tibia (proximal site and at the tibia-fibula junction) did not achieve statistical significance, the overall pattern was similar to that noted for the femur by DXA (Table 3.3). By contrast to cortical bone, however, a higher dose (10 μg/kg/day) was necessary to prevent bone loss in these mice at the spine, which contains predominantly cancellous bone (Figure 3.4). Similar to the findings at the spine, the 10 μg/kg/day dose was also necessary in the 3 months old mice in order to prevent loss of cancellous bone at the tibial metaphysis, although again, the individual changes in cancellous bone by pQCT were not significant (Table 3.3). However, in contrast to the 6 months old mice treated for 2 months, uterine weight was restored to the level of the sham mice even by the 5 μg/kg/day dose in the 3 months old mice treated for 1 month (Figure 3.5.).

Table 3.3. Volumetric BMD at the proximal tibial metaphysis (total vBMD, cancellous vBMD, and cortical vBMD) and tibia-fibula junction (cortical vBMD[§]) in 3 months old female C57BL/6 mice following 30 days of either sham surgery or ovx plus pellets delivering 0, 5, 10, 20, or 40 μg/kg/day of E_2 measured by pQCT. *, $P < 0.05$ versus 0 μg/kg/day, adjusted for multiple comparisons by the Dunnett method; c, $P < 0.001$ versus sham.

	Total vBMD (mg/cm^3)	Cancellous vBMD (mg/cm^3)	Cortical vBMD (mg/cm^3)	Cortical vBMD[§] (mg/cm^3)
Sham	430.23 ± 4.85	216.26 ± 8.14	863.21 ± 8.15	1069.19 ± 8.10
Ovx + 0 μg/kg/day	375.08 ± 13.09 [c]	203.85 ± 5.06	836.65 ± 10.05	1050.10 ± 13.47
Ovx + 5 μg/kg/day	420.36 ± 23.35	201.20 ± 7.30	867.60 ± 15.02	1074.40 ± 13.10
Ovx + 10 μg/kg/day	464.16 ± 21.94	217.58 ± 9.17	868.54 ± 14.83	1077.60 ± 8.37
Ovx + 20 μg/kg/day	479.80 ± 34.46	233.88 ± 14.93	889.62 ± 18.01	1104.00 ± 14.60*
Ovx + 40 μg/kg/day	529.43 ± 80.67	276.27 ± 60.90*	882.03 ± 19.03	1096.78 ± 19.62

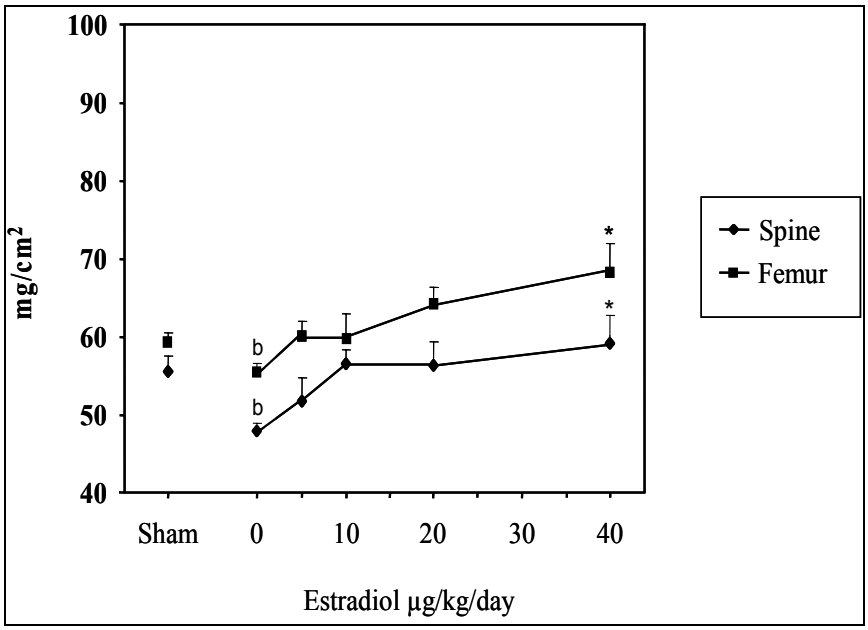

Figure 3.4. BMD of the spine and the femur (measured by DXA) in 3 months old female C57BL/6 mice following 30 days of either sham surgery or ovx plus pellets delivering 0, 5, 10, 20, or 40 µg/kg/day of E_2. Data are means ± S.E.M. *, $P < 0.05$ versus 0 µg/kg/day, adjusted for multiple comparisons by the Dunnett method; a, $P < 0.05$ versus sham.
Note the scale of the y-axis is the same as in Figure 3.1.

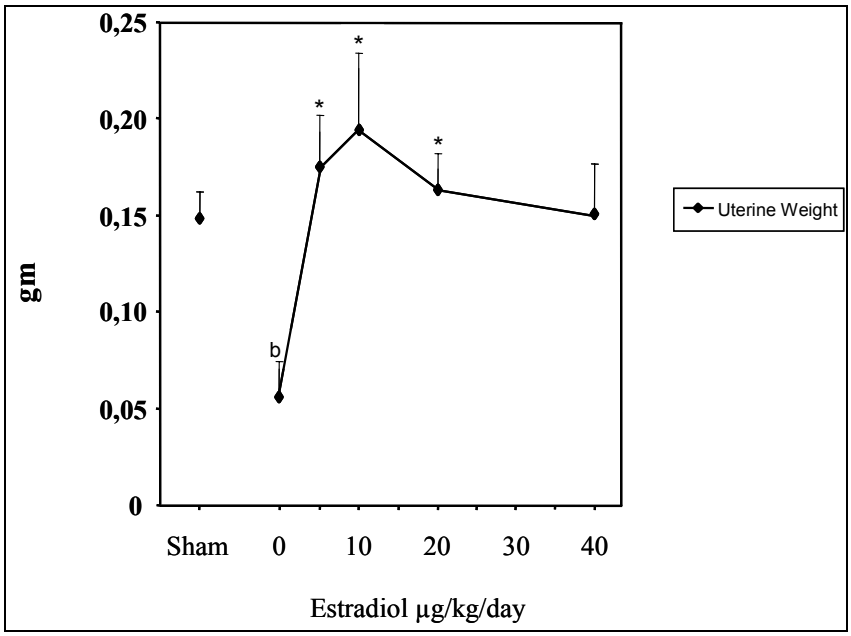

Figure 3.5. Uterine wet weights in 3 months old female C57BL/6 mice following 30 days of either sham surgery or ovx plus pellets delivering 0, 5, 10, 20, or 40 µg/kg/day of E_2. Data are means ± S.E.M. *, $P < 0.05$ versus 0 µg/kg/day, adjusted for multiple comparisons by the Dunnett method; b, $P < 0.01$ versus sham.

3.2 Characterization of the Skeletal Phenotype of the SRC-1 KO Mice

The SRC-1 KO mice have been made available to Dr. Khosla's laboratory by Dr. B. O'Malley to study the possible role of the SRC-1 coactivator in the skeletal response to E_2 and androgens. Both male and female homozygote SRC-1 KO mice were fertile and showed growth rates similar to WT animals, with virtually identical body weights, bone dimensions, and BMD at various sites at 3 and 5 months of age (Figure 3.6).

Moreover, as shown in Figure 3.7, the bones in the SRC-1 KO mice were histologically normal (see 2.10.1). Importantly, there was no evidence in the SRC-1 KO mouse bones of osteomalacia or impaired mineralization, which is a significant point, since SRC-1 may also modulate 1,25-dihydroxyvitamin D action (Herdick and Carlberg, 2000) (Gill and Bell, 2000). In addition, Xu et al. (Xu et al., 1998) have noted that SRC-1 KO mice have modest elevations in serum E_2 (~20%) and testosterone (~50%) levels as compared to WT mice. These findings were confirmed in this study for serum E_2 levels and, by measuring serum E_2 levels through various phases of the estrous cycle in pooled serum from 4-8 female SRC-1 KO and WT mice. Also it was demonstrated that during diestrus, the SRC-1 KO mice had ~60% higher serum E_2 levels as compared to the WT mice (see 2.12). These data provided further support to the hypothesis that the SRC-1 KO mice have compensated estrogen resistance in a number of tissues (Xu et al., 1998), including bone; the latter was studied in detail in the experiments described below.

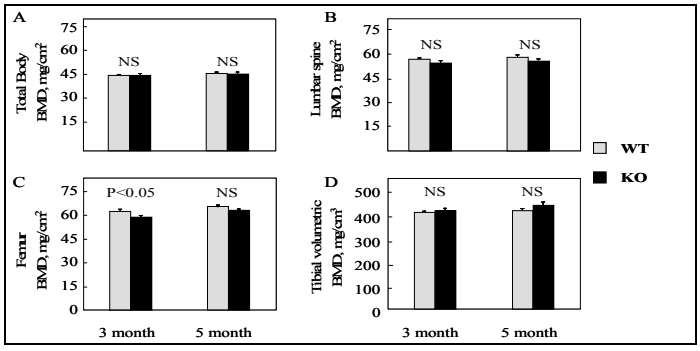

Figure 3.6. (**A**) Whole body BMD, (**B**) lumbar spine BMD, and (**C**) femur BMD (all measured by DXA) and (**D**) volumetric BMD at the proximal tibia (measured by pQCT) in WT and SRC-1 KO female mice at 3 and 5 months of age. n = 8-11 mice per group.

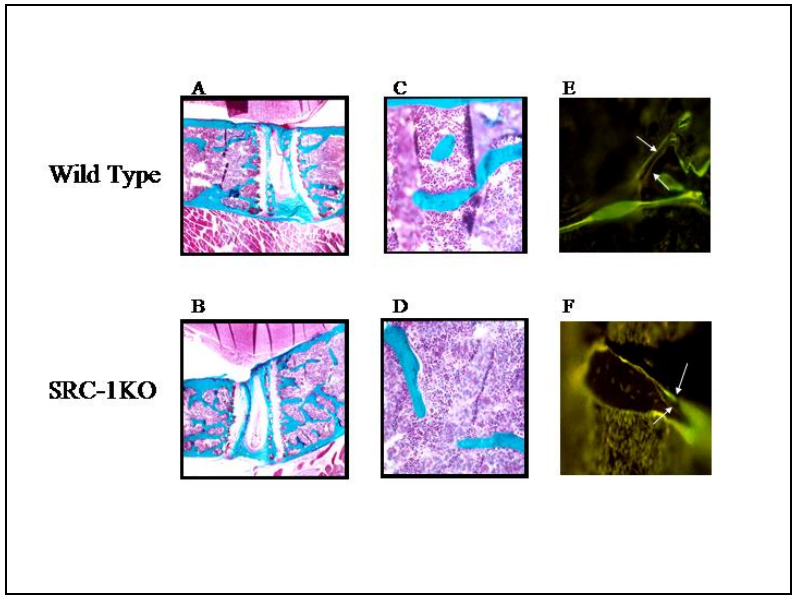

Figure 3.7. **A**, **B**: Goldner's Masson Trichrome stain of lumbar vertebrae at low power (intervertebral disc is at the center) (6 x) from WT (**A**) and SRC-1 KO (**B**) mice; **C**, **D**: Higher power view (25 x). Note absence of any abnormal osteoid accumulation in the SRC-1 KO mice (**D**) compared to the WT mice (**C**), consistent with the absence of any mineralization defects in these animals; **E**, **F**: Fluorescent microscopy showing incorporation of crisp double labels of tetracycline and calcein (arrows), consistent with normal mineralization in the SRC-1 KO mice, similar to the WT mice.

3.2.1 Effects of Ovariectomy and Estrogen Replacement on BMD in the Female SRC-1 KO Compared to the WT Mice

3.2.1.1 DXA and pQCT

To clearly define possible deficits in estrogen action in the female SRC-1 KO mice, I compared the effects of sham surgery, ovx with vehicle pellets, and ovx with E_2 replacement (at a dose of 10 μg/kg/day) on BMD in WT versus SRC-1 KO mice. The time of treatment was 60 days in this experiment, and BMD was measured at baseline and at the end of the experiment (see 2.13.2). Figure 3.8.A shows the percent changes in spine BMD in the three groups of WT and SRC-1 KO mice. As is evident, spine BMD decreased significantly following ovx in both the WT and SRC-1 KO mice. However, whereas E_2 treatment prevented this decrease in the WT mice, it was virtually ineffective in the SRC-1 KO mice. Similar findings were present at the femur, although here the deficit in E_2 action did not appear to be quite as severe as at the spine (Figure 3.8.B).

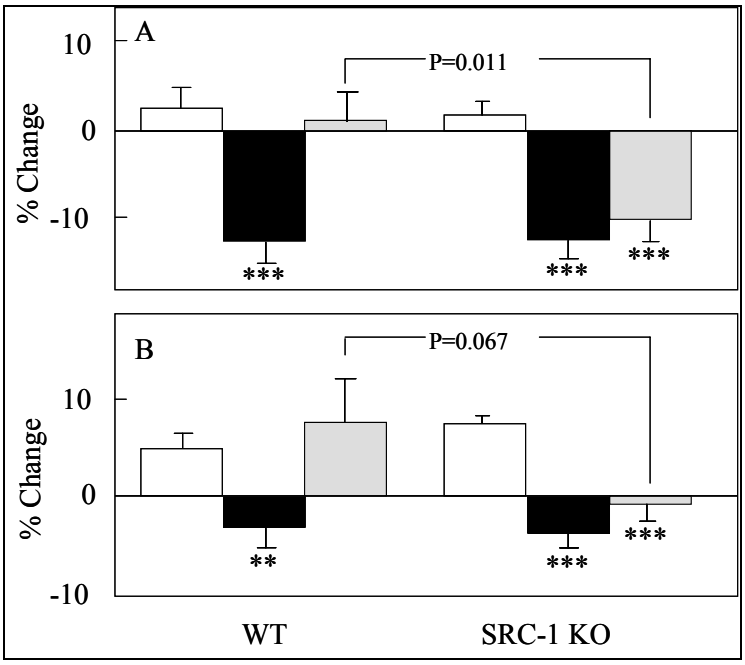

Figure 3.8. Percent changes in (**A**) lumbar spine and (**B**) femur BMD (both measured by DXA) in the WT and SRC-1 KO mice following sham surgery (open bars), ovx plus vehicle pellets (solid bars), or ovx and E_2 pellets (shaded bars, 10 μg/kg/day) for 60 days. The P-values for the main comparison (SRC-1 KO, ovx + E_2, versus WT, ovx + E_2) are as indicated. ANOVA P-values for within group comparisons: spine WT, P = 0.001 and SRC-1 KO, P < 0.001; femur WT, P = 0.03 and SRC-1 KO, P <0.001. **P < 0.01 and ***P < 0.001 for direct comparison with the respective sham group.

Since the spine contains predominantly cancellous bone, whereas the femur contains both cancellous and cortical bone, I further explored whether the deficit in estrogen action in the SRC-1 KO mice was present predominantly in cancellous bone. For this, I used the tibial BMD by pQCT, which can measure changes in cancellous and cortical bone combined, as well as separately in the two compartments. As shown in Figure 3.9.A combined cortical and cancellous (total) tibial BMD decreased similarly in the WT and SRC-1 KO mice, and E_2 prevented this decrease in both groups, although it appeared to be somewhat less effective in the SRC-1 KO as compared to the WT mice. However, as shown in Figure 3.9.B, similar to the spine DXA data, E_2 was entirely ineffective in the cancellous compartment of the tibia in the SRC-1 KO mice, whereas it not only maintained, but modestly increased cancellous tibial BMD in the WT mice. Moreover, as shown in Figure 3.9.C, estrogen effects on cortical BMD in the tibia were virtually identical in the WT and SRC-1 KO mice.

3.2.1.2 Micro-CT Analysis

The above data using DXA and pQCT strongly suggested that the SRC-1 KO mice had a clear defect in estrogen action in cancellous bone, but preserved responses to estrogen in cortical bone. To establish this more definitively, I performed detailed μCT analyses of the tibias (at the same site as used in the tibial pQCT measurements) using excised bones from the WT and KO mice (see 2.7). Figure 3.10 shows an example of these scans from WT and SRC-1 KO mice, ovx'd and treated with E_2, which are the key comparison groups. As is evident from the middle and right panels (and consistent with the pQCT data at this site), estrogen treatment of ovx'd WT versus SRC-1 KO mice resulted in markedly altered effects on cancellous bone, with much more cancellous bone present in the WT compared to the KO mice. By contrast, the amount of cortical bone present (seen best in the cross-sectional images in the right panels) was similar in the two groups following ovx and E_2 treatment.

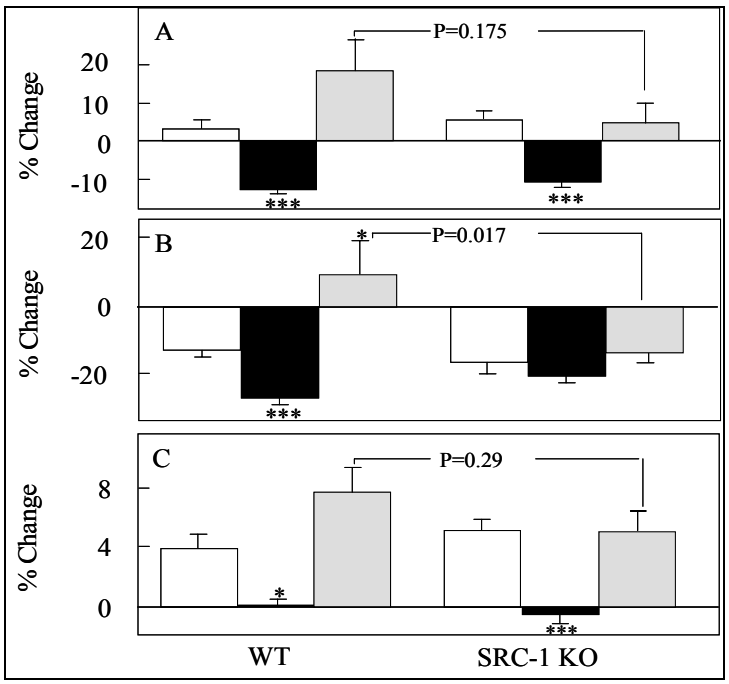

Figure 3.9. Percent changes in (**A**) tibial total volumetric (**B**) tibial cancellous and (**C**) tibial cortical BMD (all measured by pQCT) in the WT and SRC-1 KO mice following either sham surgery (open bars), ovx plus vehicle pellets (solid bars), or ovx and E_2 pellets (shaded bars, 10 μg/kg/day) for 60 days. The P-values for the main comparison (SRC-1 KO, ovx + E_2, versus WT, ovx + E_2) are as indicated. ANOVA P-values for within group comparisons: total tibia WT, P = 0.002 and SRC-1 KO, P = 0.003; cancellous WT, P < 0.001 and SRC-1 KO, P = 0.322; cortical WT and SRC-1 KO, both P = 0.002. *P < 0.05, **P < 0.01, and ***P < 0.001 for direct comparison with the respective sham group.

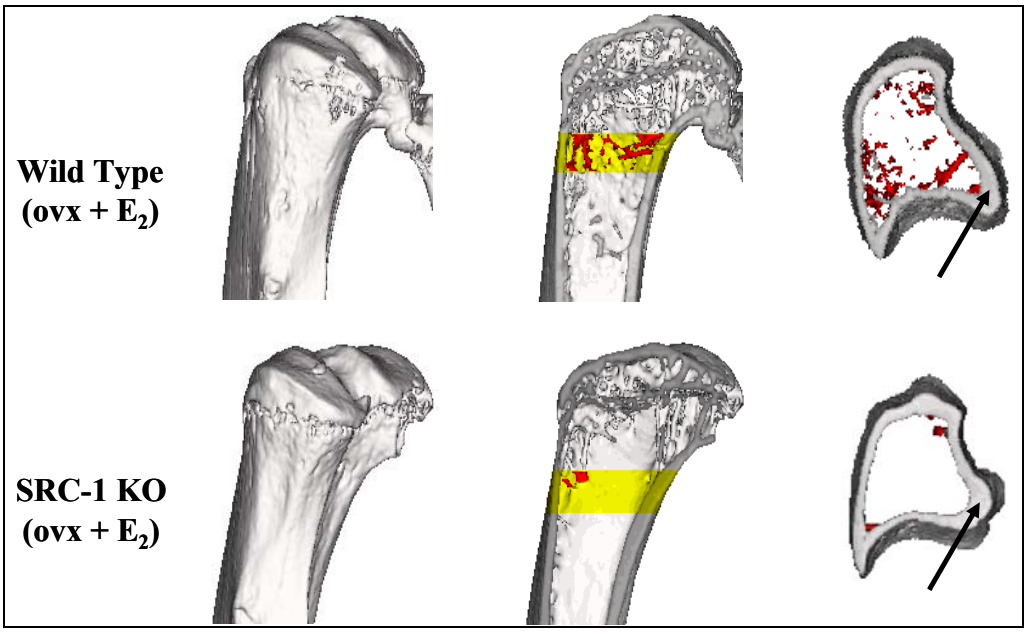

Figure 3.10. Examples of μCT analyses of tibias from WT (upper panels) and SRC-1 KO (lower panels) mice, ovx'd and treated with E_2. The yellow band in the middle panels identifies the region of interest using a saggital section, and the right panels show cross-sectional images through this region. Red indicates cancellous bone and arrows indicate cortical bone.

This was more rigorously quantified in Figure 3.11.A. As shown, cancellous bone volume (BV/TV) was significantly lower in the WT and SRC-1 KO mice following ovx as compared to the sham mice; however, whereas BV/TV was actually increased above levels in the sham mice in the WT, estrogen-treated mice, E_2 treatment at a dose of 10μg/kg/day failed to preserve BV/TV in the SRC-1 KO mice. By contrast, as shown in Figure 3.11.B, the pattern of changes in the ovx'd and ovx'd plus E_2-treated mice in cortical thickness was very similar in the WT and SRC-1 KO mice, consistent with a preservation of estrogen action in cortical bone in the KO mice.

3.2.1.3 Bone Histomorphometry

Table 3.4 shows the bone histomorphometry (see 2.10) data in the various groups. Consistent with the spine DXA measurements, BV/TV in cancellous bone in the spine was lower in both WT and SRC-1 KO mice following ovx. However, whereas estrogen treatment preserved cancellous BV/TV in the WT mice, it failed to do so in the KO mice. Similar results were seen with the other cancellous bone parameters (trabecular separation and trabecular number, Table 3.4). The bone formation rate was significantly higher in the ovx'd WT and KO mice as compared to the respective sham groups; however, while estrogen treatment of WT mice reduced bone formation rate to even below that in the sham animals, the bone formation rate in the estrogen-treated SRC-1 KO mice was similar to that in the ovx'd SRC-1 KO mice and clearly different from that in the WT estrogen-treated mice.

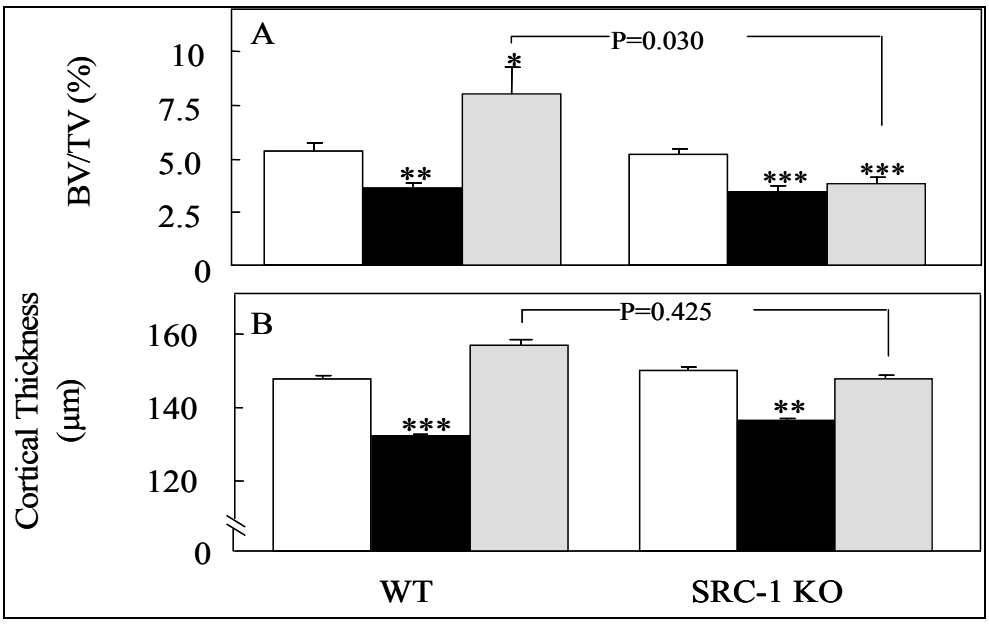

Figure 3.11. μCT analysis of tibias from WT and SRC-1 KO mice following sham surgery (open bars), ovx plus vehicle pellets (solid bars), or ovx and E_2 pellets (shaded bars, 10 μg/kg/day) for 60 days. (**A**) cancellous BV/TV and (**B**) cortical thickness. The P-values for the main comparison (SRC-1 KO, ovx + E_2, versus WT, ovx + E_2) are as indicated. ANOVA P-values for within group comparisons: BV/TV WT, P = 0.036 and SRC-1 KO, P < 0.001; cortical thickness WT, P = 0.038 and SRC-1 KO, P = 0.06. *P < 0.05, **P < 0.01, and ***P < 0.001 for direct comparison with the respective sham group.
BV/TV: Bone Volume/Measured Tissue Volume

Table 3.4. Bone histomorphometric parameters in the WT and SRC-1 KO mice following sham surgery, ovx with vehicle pellet replacement, or ovx with E_2 pellet replacement for 60 days. P-values for the main comparison (SRC-1 KO, ovx + E_2, versus WT, ovx + E_2) are as follows: $^{a}P < 0.05$, $^{b}P < 0.01$, $^{c}P < 0.001$. ANOVA P-values for within group comparisons are as indicated. *P < 0.05, **P < 0.01 and ***P < 0.001 for direct comparison with the respective sham group. BV/TV: Bone Volume/Measured Tissue Volume, BFR: Bone Formation Rate

	WT				**SRC-1 KO**			
	Sham	Ovx + Vehicle	Ovx + E_2	ANOVA	Sham	Ovx + Vehicle	Ovx + E_2	ANOVA
BV/TV (%)	25.5 ± 2.4	14.3 ± 0.8**	23.3 ± 2.8	0.01	22.4 ± 1.7	14.8 ± 1.6*	15.6 ± 1.1**, [a]	0.004
Trabecular separation (μm)	157 ± 16	249 ± 27*	155 ± 24	0.016	162 ± 5	257 ± 32*	246 ± 15**, [b]	0.01
Trabecular Number	4.9 ± 0.4	3.6 ± 0.3*	5.2 ± 0.4	0.015	4.8 ± 0.2	3.5 ± 0.4*	3.5 ± 0.2,[b]	0.004
BFR ($\mu m^3/\mu m^2/d$)	0.14 ± 0.04	0.26 ± 0.02**	0.07 ± 0.01**	< 0.001	0.10 ± 0.02	0.18 ± 0.04	0.20 ± 0.02*,[c]	0.04

3.2.1.4 Effects on Uterine Weights

As shown in Figure 3.12, the dose of E_2 used in this experiment was biologically meaningful, since it restored uterine weight in the ovx'd mice to near the level of the sham mice in the WT animals. Interestingly, while this dose of E_2 was clearly having at least partial effects on bone in the SRC-1 KO mice, particularly in cortical bone, it was totally ineffective at restoring uterine weight in the SRC-1 KO mice.

3.2.1.5 Elimination of the Defect in Estrogen Action on Bone in the SRC-1 KO Mice Using High Dose Estrogen

In order to establish that the defect in estrogen action in the SRC-1 KO mice was, in fact, due to estrogen resistance and that this could be overcome with a higher dose of E_2, the WT and SRC-1 KO mice were also treated with a high dose (40 μg/kg/day) of E_2 (see 2.13.2). As shown in Figure 3.13 (and in contrast to the findings with the lower dose of E_2 shown in Figure 3.8), a dose of 40 μg/kg/day of E_2 resulted in virtually identical changes in spine and femur BMD in the WT and SRC-1 KO mice. Thus, the defect in estrogen action present in the KO mice could be overcome using higher doses of E_2.

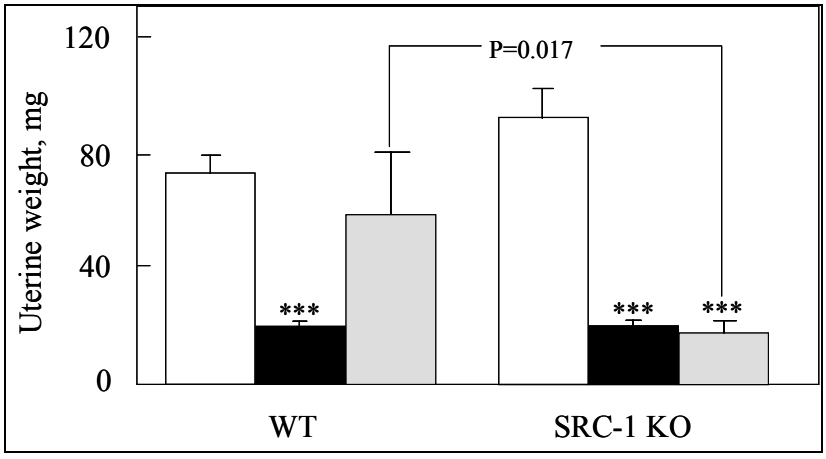

Figure 3.12. Uterine weights in the WT and SRC-1 KO mice following either sham surgery (open bars), ovx plus vehicle pellets (solid bars), or ovx and E_2 pellets (shaded bars, 10 μg/kg/day) for 60 days. The P-values for the main comparison (SRC-1 KO, ovx + E_2, versus WT, ovx + E_2) are as indicated. ANOVA P-values for within group comparisons: WT, P = 0.002 and SRC-1 KO, P < 0.001. ***P < 0.001 for direct comparison with the respective sham group.

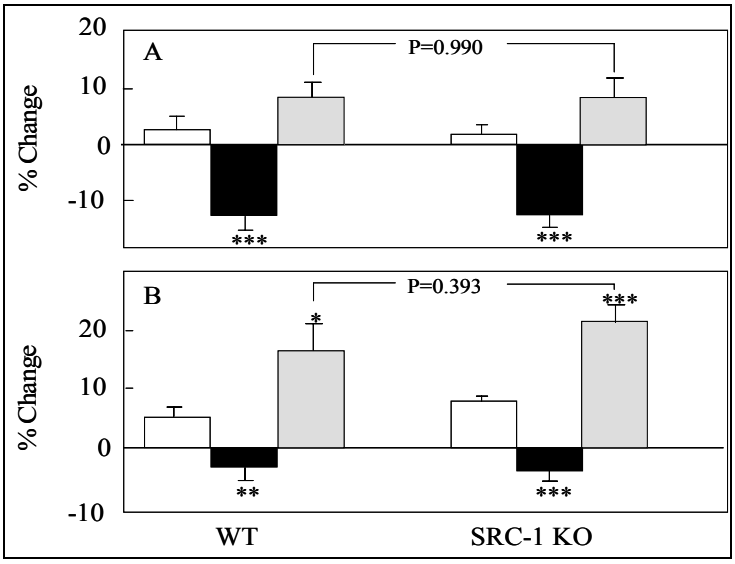

Figure 3.13. Percent changes in (**A**) lumbar spine and (**B**) femur BMD (both measured by DXA) in the WT and SRC-1 KO mice following sham surgery (open bars), ovx plus vehicle pellets (solid bars), or ovx and high dose E_2 pellets (shaded bars, 40 μg/kg/day) for 60 days. Note that the sham and ovx groups are the same as shown in Figure 3.8. The P-values for the main comparison (SRC-1 KO, ovx + E_2, versus WT, ovx + E_2) are as indicated. ANOVA P-values for within group comparisons: spine WT and KO, both $P < 0.001$; femur WT, $P = 0.003$ and SRC-1 KO, $P < 0.001$. *$P < 0.05$, **$P < 0.01$ and ***$P < 0.001$ for direct comparison with the respective sham group.

3.2.1.6 Comparison of Estrogen Receptor-α and Estrogen Receptor-β mRNA Expression Between Cancellous and Cortical Bone

The group of T.C. Spelsberg has recently reported that in osteoblastic cells, SRC-1 seems to preferentially enhance (at least *in vitro*) the transcriptional activity of co-expressed ER-α and -β or the ER-β homodimer to a much greater extent than of ER-α homodimer (Monroe et al., 2003). Since I had demonstrated what appeared to be a relatively selective defect in estrogen action in cancellous bone in the SRC-1 KO mice, I also compared the expression of ER-α and -β mRNAs in cancellous versus cortical bone by RT-PCR (see 2.3.2). Total RNA was extracted from either the lumbar vertebrae (a site rich in cancellous bone) or from the mid-shaft of the femur (which contains exclusively cortical bone). As shown in Figure 3.14, the expression of ER-α was similar in cancellous and cortical bone; by contrast, ER-β was only expressed in the cancellous bone of the lumbar spine, but not in the cortical bone of the femur shaft. In addition, there was no obvious difference in the expression of either ER-α or -β in bones from the WT versus the SRC-1 KO mice.

3.2.1.7 Expression of SRC-2 in Bones of SRC-1 KO Versus WT Mice

Since at least in some tissues (such as the brain and testis) expression of SRC-2 is upregulated in the SRC-1 KO mice and may partially compensate for loss of SRC-1 (Xu et al., 1998), also expression of SRC-2 in bones from WT and KO mice was examined using both conventional (Figure 3.15) (see 2.3.2) and real time RT-PCR (see 2.3.3). The SRC-2 mRNA was expressed in both the lumbar spine and femur shaft; however, there were no significant differences in the level of the SRC-2 mRNA in bones from the WT and SRC-1 KO mice (Figure 3.15). By real time RT-PCR, the copy number for SRC-2 (per 100.000 copies of GAPDH, n = 5 per group) was 1140 ± 188 (WT) versus 1440 ± 215 (SRC-1) in the spine (P = 0,324) and 2080 ± 206 versus 1720 ± 232 in the femur shaft (P = 0,279).

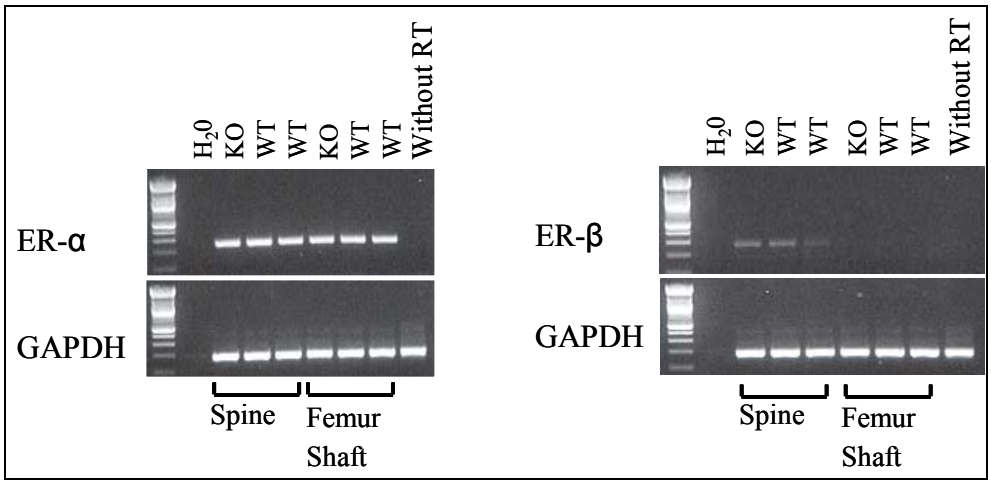

Figure 3.14. Expression of ER-α and -β mRNA, assessed by RT-PCR, in the lumbar spine (a site rich in cancellous bone) and the mid-shaft of the femur (which contains exclusively cortical bone). The expression of GAPDH mRNA indicated that the sample loading and amplification for each of the preparation was approximately the same. 40 PCR cycles were used.

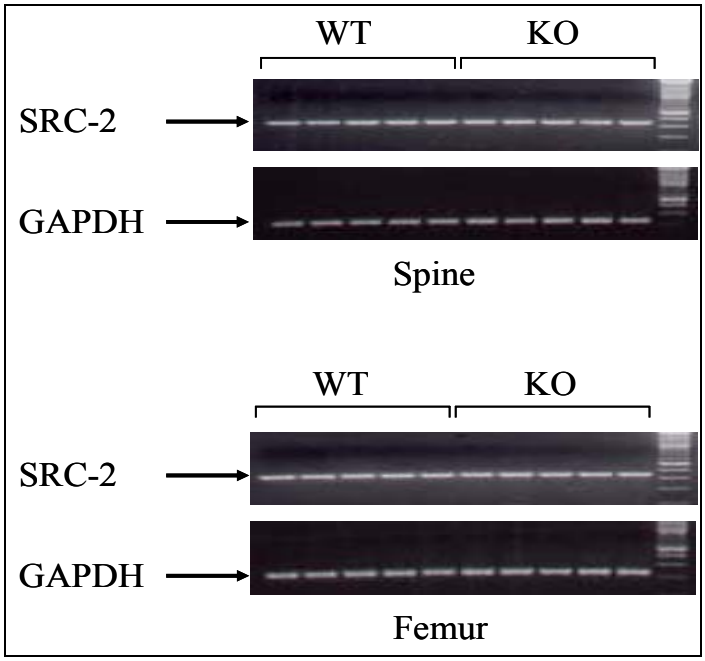

Figure 3.15. Expression of SRC-2 mRNA assessed by RT-PCR, in the lumbar spine and mid-shaft of the femur in the WT and SRC-1 KO mice. The expression of GAPDH mRNA indicated that the sample loading and amplification for each of the preparation was approximately the same. 40 PCR cycles were used.

3.2.2 Skeletal Phenotype of SRC-1 KO Male Mice Under Basal Conditions

Baseline measurements of the total, cancellous, and cortical volumetric tibial BMD, and the BMD of the spine, and the femur of the WT and SRC-1 KO male mice were not significantly different at 3 and 5 month of age (n = 9-10 animal per group) (Figure 3.16).

3.2.3 Effects of Orchidectomy and Estrogen Replacement on BMD in the Male SRC-1 KO Mice Compared to the WT Littermates

3.2.3.1 DXA and pQCT

To investigate if the regulation of estrogen action on bone is gender specific, I treated 3 month old male SRC-1 KO littermates of the female SRC-1 KO mice in parallel either with sham surgery, orchidectomy (orc) with vehicle, or orc with E_2 replacement (10 µg/kg/day, body weight of 0,025 kg) with slow release pellets for 60 days. The BMD was measured at baseline and at the end of the experiment (see 2.13.3). As shown in Figure 3.17., after orc the percent change of spine and femoral BMD which was determined by DXA decreased significantly in both the WT and SRC-1 KO mice. The dose of E_2 was efficient to maintain the BMD at the spine (predominantly cancellous bone) (Figure 3.17.A), and the femur

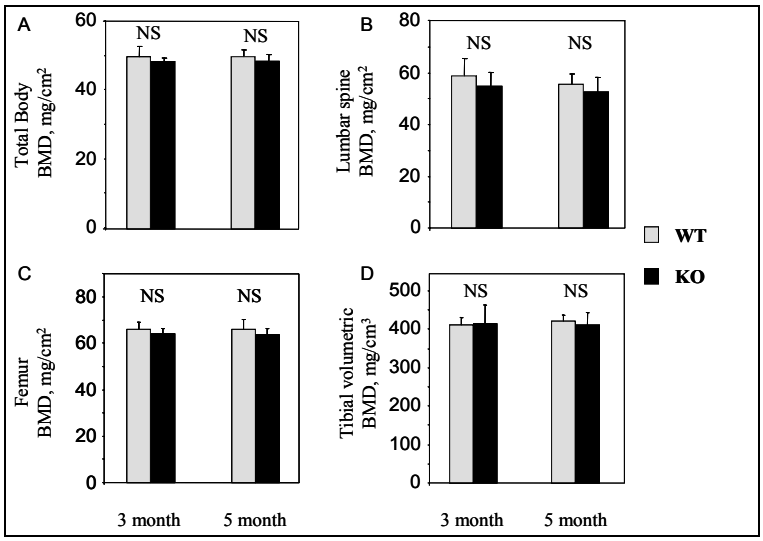

Figure 3.16. Graph .(**A**) Whole body BMD, (**B**) lumbar spine BMD, and (**C**) femur BMD (all measured by DXA) and (**D**) volumetric BMD at the proximal tibia (measured by pQCT) in WT and SRC-1 KO male mice at 3 and 5 months of age. n = 9-10 mice per group.

(cancellous and cortical bone) in the WT mice and, in contrast to the female SRC-1 KO mice, also in the male KO mice (Figure 3.17.B). There was no significant difference between the percent changes of the BMD in the WT versus the SRC-1 KO mice after the treatment. The treatment with estrogen after orc resulted in identical responses of the SRC-1 KO and WT mice in the spine and in the femur (P= 0,980; P= 0,667).

A significant decrease of total and cancellous volumetric tibial BMD (determined by pQCT) was observed after orc in the WT and the SRC-1 KO male mice, with a similar trend for cortical volumetric BMD (Table 3.5). Estrogen treatment in the WT and the SRC-1 KO mice was sufficient to maintain total and cortical volumetric tibial BMD at the level of the sham mice. However, the dose of E_2 used was not sufficient to maintain tibial cancellous volumetric BMD in either the WT or the SRC-1 KO male mice (Table 3.5). In contrast, in the female mice I observed that the dose of E_2 administrated to the WT maintained (even increased) cancellous bone density but in the SRC-1 KO mice the cancellous bone did not respond to the estrogen treatment.

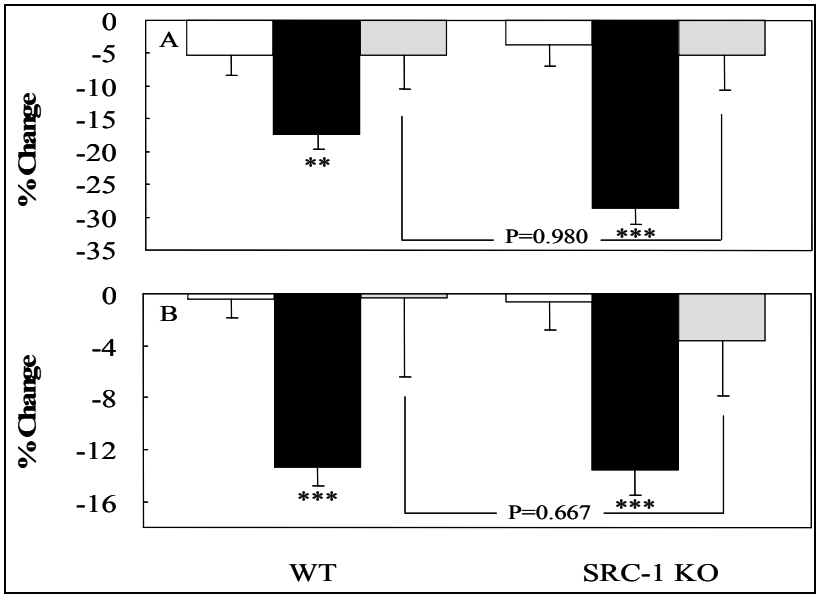

Figure 3.17. Percent changes in (**A**) lumbar spine and (**B**) femur BMD (both measured by DXA) in the WT and SRC-1 KO mice following sham surgery (open bars), orc plus vehicle pellets (solid bars), or orc and E_2 pellets (shaded bars, 10 μg/kg/day) for 60 days. The P-values for the main comparison (SRC-1 KO, orc + E_2, versus WT, orc + E_2) are as indicated. ANOVA P-values for within group comparisons: spine WT, P = 0.03 and SRC-1 KO, P < 0.001; femur WT, P = 0.01 and SRC-1 KO, P 0 0.003. **P < 0.01 and ***P < 0.001 for direct comparison with the respective sham group.

Table. 3.5. Percent Change of the volumetric BMD at the proximal tibial metaphysis, measured by pQCT (total vBMD, cancellous vBMD, and cortical vBMD) in the WT and SRC-1 KO male mice after either sham surgery, orc with vehicle pellet, or orc with E_2 pellet (10 μg/kg/day) replacement for 60 days. ANOVA P values for within group comparison are as indicated. *, $P < 0.05$; **, $P < 0.01$; ***, $P < 0.001$ for direct comparison with the respective sham group.

		Total vBMD (% change)	Cancellous vBMD (% change)	Cortical vBMD (% change)
WT	Sham	2.55 ± 2.24	-14.84 ± 2.01	2.20 ± 0.39
	Orc + Vehicle	-19.7 ± 5.03***	-39.71 ± 2.67***	-0.63 ± 0.89*
	Orc + E_2	3.65 ± 9.94	-24.2 ± 7.88	6.11 ± 2.41
ANOVA		P = 0.004	P = 0.001	P = 0.006
KO	Sham	-0.4 ± 2.17	-15.96 ± 2.39	1.61 ± 0.89
	Orc + Vehicle	-16.0 ± 1.95***	-34.59 ± 2.34***	0.58 ± 0.95
	Orc + E_2	-1.95 ± 6.2	-31.9 ± 3.17***	7.02 ± 1.66**
ANOVA		P = 0.002	P < 0.001	P = 0.002

3.2.4 Effects of Orchidectomy and Treatment with Testosterone and 5α-DHT on the Skeletal Phenotype of SRC-1 KO Male Mice and WT Littermates

3.2.4.1 DXA and pQCT

To define possible deficits in androgen action on bone in the male SRC-1 KO mice, I compared the effects of sham surgery, orc with vehicle pellets, orc with testosterone replacement (7 mg/kg/day), or orc with 5α-DHT (5,5 mg/kg/day) on bone in WT versus SRC-1 KO mice. The time of treatment was 60 days in this experiment, and BMD was measured at baseline and at the end of the experiment (see 2.13.4). As shown in Figure 3.18.A after orc the spine BMD (determined by DXA) was decreased significantly in the WT and SCR-1 KO mice. Unexpectedly, the treatment with a dose of 7 mg/kg/day testosterone was not sufficient to prevent the loss of bone at the spine in the orc'd WT mice. The treatment with testosterone resulted in the same loss of bone in both the WT and SRC-1 KO mice (P= 0,8). In contrast the dose of 5α-DHT was sufficient to maintain the spine BMD in the WT mice and even further increase the spine BMD in the SCR-1 KO mice compared to the sham operated mice (Figure 3.18.A).

Testosterone did not have any effect on the femur in the treated WT and SRC-1 KO mice (Figure 3.18.B). The treatment with 5α-DHT was not sufficient to prevent bone loss in the femur of the WT mice. However, in contrast, the dose of 5α-DHT prevented loss of bone at the femur in the SRC-1 KO mice in comparison with the sham mice (Figure 3.18.B). There was even a significant increase in BMD compared to the 5α-DHT-treated WT mice. The bone of the SRC-1 KO mice responded significantly better to the 5α-DHT treatment than the bones of the WT mice. The bone of the SRC-1 KO mice seems to be more sensitive to 5α-DHT than the bone of the WT mice.

Figure 3.19 shows that the percent change of total, cancellous, and cortical volumetric tibial BMD decreased significantly after orc in the WT and SRC-1 KO mice. The treatment with

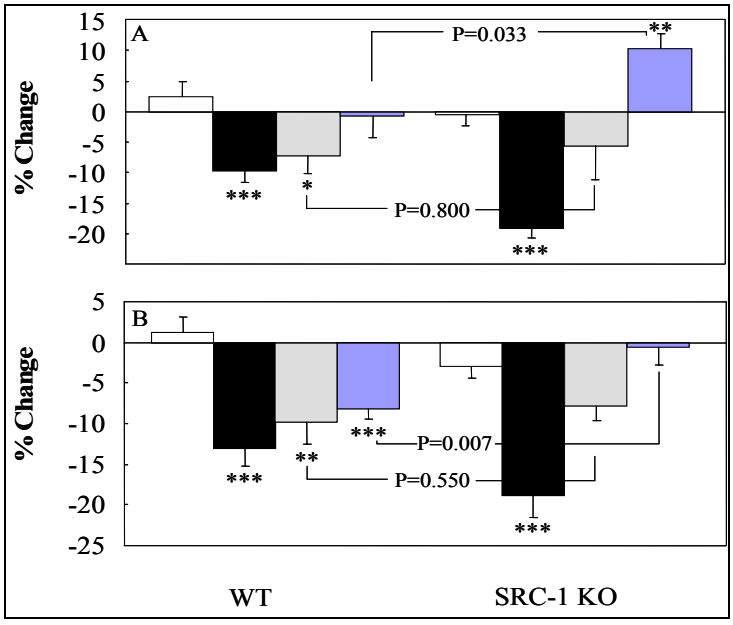

Figure 3.18. Percent changes in (**A**) lumbar spine and (**B**) femur BMD (both measured by DXA) in the WT and SRC-1 KO mice following either sham surgery (open bars), orc plus vehicle pellets (solid bars), orc and T pellets (light shaded bars, 7 mg/kg/d), or orc and 5α-DHT pellets (dark shaded bars, 5,5 mg/kg/d) for 60 days. The P-values for the main comparison (SRC-1 KO, orc + T, versus WT, orc + T, and SRC-1 KO, orc + 5α-DHT, versus WT, orc + 5α-DHT) are as indicated. ANOVA P-values for within group comparisons: spine WT, P = 0.01 and SRC-1 KO, P < 0.001; femur WT, P < 0.001 and SRC-1 KO, P <0.001. *P < 0.05, **P < 0.01 and ***P < 0.001 for direct comparison with the respective sham group.

testosterone did not have any effect on the total or cancellous volumetric BMD of the tibia in both the WT and SRC-1 KO mice.

The cortical volumetric BMD showed a partial response to the testosterone treatment in the SRC-1 KO mice compared to the treated WT mice (Figure 3.19.C).

The results from the percent change of the cancellous volumetric BMD in Figure 3.19.B show that the dose of 5α-DHT was sufficient to prevent the loss of cancellous bone in the WT mice. The percent change was even significantly lower in the treated mice than the sham operated mice. The 5α-DHT-treated SRC-1 KO mice were able to maintain BMD comparable to sham mice. The direct comparison between the WT and KO mice did not show a significant difference in the response to 5α-DHT (Figure 3.19.B).

The percent change of BMD at the femur suggested a better response of the cortical bone from the SRC-1 KO mice to the 5α-DHT treatment than the cortical bone of the WT mice. This notion could be confirmed with the cortical volumetric BMD measurements. Figure

3.19.C shows that the dose of 5α-DHT was not sufficient to maintain the cortical BMD in the WT mice. In contrast, volumetric BMD of the cortical bone was even higher in 5α-DHT treated SRC-1 KO mice than in the sham mice. The cortical bone of the SRC-1 KO mice responded significantly better to the 5α-DHT treatment than the WT mice.

The total volumetric BMD is a combination of the separate measurements of the cancellous and cortical bone in the metaphysis of the tibia. Because of the better response of the cortical bone from the SRC-1 KO mice, the percent change of the total BMD of the SRC-1 KO mice was similar to the sham mice (Figure 3.19.A), however, differences of the percent change of the total BMD between the 5α-DHT-treated WT and SRC-1 KO mice did not reach significance. In the WT mice the dose of 5α-DHT did not prevent the loss of total bone.

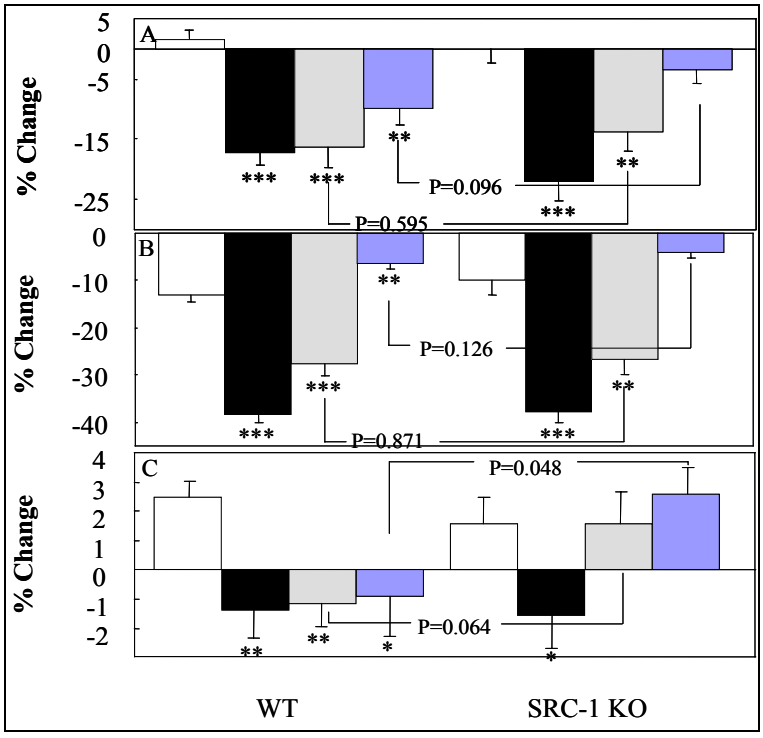

Figure 3.19. Percent changes in (**A**) tibial total (**B**) cancellous and (**C**) cortical volumetric BMD (all measured by pQCT) in the WT and SRC-1 KO mice following either sham surgery (open bars), orc plus vehicle pellets (solid bars), orc and T pellets (light shaded bars, 7 mg/kg/day), or orc and 5α-DHT pellets (dark shaded bars, 5,5 mg/kg/day) for 60 days. The P-values for the main comparison (SRC-1 KO, orc + T, versus WT, orc + T, and SRC-1 KO, orc + 5α-DHT, versus WT, orc + 5α-DHT) are as indicated. ANOVA P-values for within group comparisons: total tibia WT and SRC-1 KO, both $P < 0.001$; cancellous WT and SRC-1 KO, both $P < 0.001$; cortical WT and SRC-1 KO, both $P = 0.03$. *$P < 0.05$, **$P < 0.01$, and ***$P < 0.001$ for direct comparison with the respective sham group.

3.2.4.2 Effect of Testosterone and 5α-DHT Treatment on Seminal Vesicle Weight

The weight of the seminal vesicles from the WT and SRC-1 KO mice was significantly reduced after orc. Figure 3.20 shows that the dose of testosterone just lead to about 50% of the sham surgery values in the WT and the SRC-1 KO mice. In contrast, the treatment with 5α-DHT resulted in an increase of the seminal vesicles weight of about two fold compared to the sham mice. The seminal vesicles of the WT and the SRC-1 KO mice responded identically to the treatment with testosterone or 5α-DHT after orc.

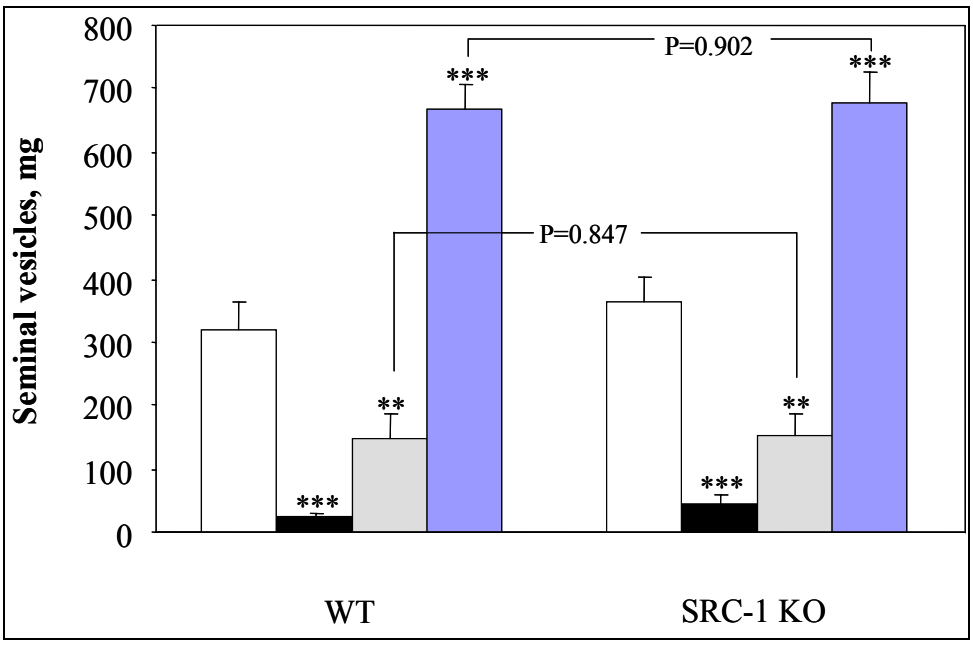

Figure 3.20. Seminal vesicle weights in the WT and SRC-1 KO mice following either sham surgery (open bars), orc plus vehicle pellets (solid bars), orc and T pellets (light shaded bars, 7 mg/kg/day), or orc and 5α-DHT pellet (dark shaded bars, 5,5 mg/kg/day) for 60 days. The P-values for the main comparison (SRC-1 KO, orc + T, versus WT, orc + T, and SRC-1 KO, orc + 5α-DHT, versus WT, orc + 5α-DHT) are as indicated. ANOVA P-values for within group comparisons: WT and SRC-1 KO, both $P < 0.001$. **$P < 0.01$, ***$P < 0.001$ for direct comparison with the respective sham group.

3.3 Aromatase

3.3.1 Expression of Aromatase in Human Cell Culture

The expression level of the enzyme aromatase was determined by conventional PCR (see 2.3.2) in different human cell lines. Therefore, total RNA was isolated from the cultured cell lines (see 2.2.1.1).

The enzyme aromatase was already expressed in undifferentiated hMS cells (see 2.1.). The expression increased clearly within the first three days of differentiation in the standard differentiation media. A further differentiation of the hMS cells for 7, 14, and 21 days to become osteoblasts did not result in an increased expression of the aromatase as compared with the differentiation after the first three days (Figure 3.21.A).

In the same cells the expression of the estrogen receptor-α (ER-α) was examined as well, because the action of E_2 is mediated by ER-α. The undifferentiated hMS cells already express ER-α (Figure 3.22). The lowest expression of ER-α was determined in the hMS differentiated for 21 days.

To test whether the expression of the aromatase is regulated by E_2, undifferentiated hMS cells were treated with vehicle, E_2 (10^{-8} M), IL-1β (10 ng/ml), or the estrogen antagonist ICI 182,780 (10^{-7} M) after the cells were cultured in steroid free medium (see 2.1). The treatment of the hMS cells with E_2 did not have any effect on the expression level of the aromatase. Only the treatment with ICI 182,780 decreased the expression slightly, the other treatments did not change the expression of the aromatase (Figure 3.23).

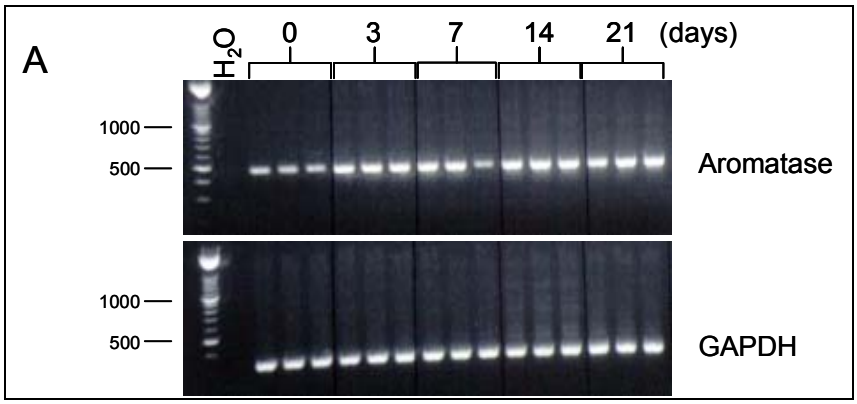

Figure 3.21. Time course change of mRNA expression of (A) aromatase in hMS cells during the differentiation into mature osteoblasts. hMS cells were cultured 0, 3, 7, 14, or 21 days in differentiation media. The expression was assessed by RT-PCR. The expression of GAPDH mRNA indicated that the sample loading and amplification for each of the preparation was approximately the same. 35 PCR cycles were used.

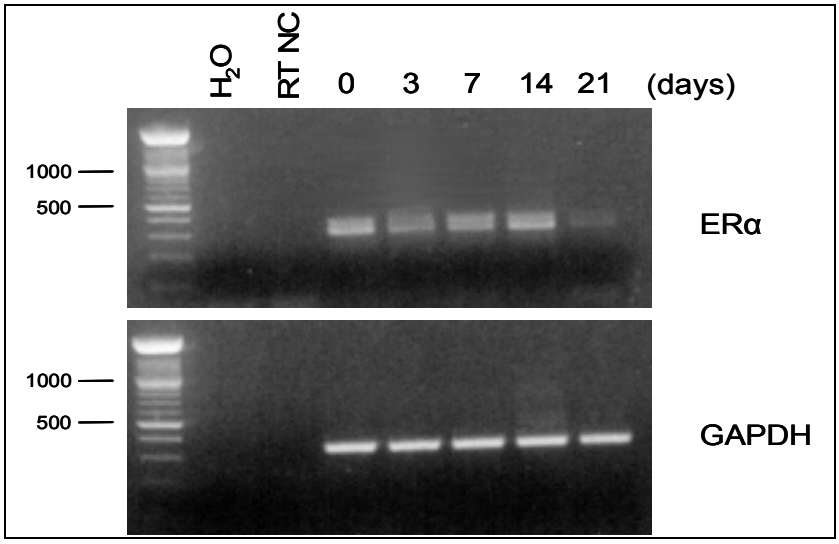

Figure 3.22. Time course of change of mRNA expression of ER-α in hMS cells during differentiation into mature osteoblasts. hMS cells were cultured up to 21 day in differentiation media. The mRNA expression was assessed by RT-PCR. The expression of GAPDH mRNA indicated that the sample loading and amplification for each of the preparation was approximately the same. 40 PCR cycles were used.
RT NC, Reverse Transcriptase negative control.

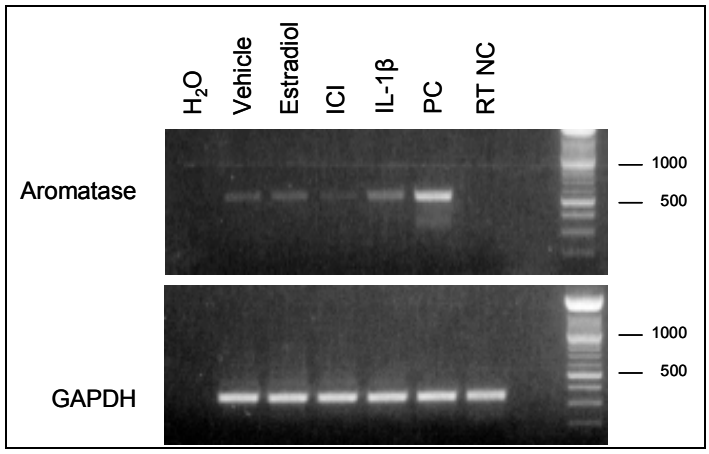

Figure 3.23. Expression of aromatase mRNA in undifferentiated hMS cells treated with vehicle, E_2, ICI, or IL-1β for 24 h was assessed by RT-PCR. The expression of GAPDH mRNA indicated that the sample loading and amplification for each of the preparation was approximately the same. 40 PCR cycles were used.
PC, positive control; RT NC, Reverse Transcriptase negative control.

The human osteoblastic osteosarcoma cell line SaOS2 was also examined for the expression of aromatase (see 2.1). In the SaOS2 cell line the aromatase expression was low, when the cells were maintained in standard growth medium. A very slight increase of aromatase expression was observed after the treatment with Dex and IL-1ß (Figure 3.24). The cells also expressed ER-α with and without preincubation of Dex and IL-1ß (data not shown). However, the treatment with different doses of E_2 (10^{-10}- 10^{-7} M) and preincubation with Dex and IL-1ß did not change the expression of the aromatase in the SaOS2 cells (Figure 3.25).

The conditionally immortalized, human osteoblastic FOB-ER9 cells which contain physiological concentrations of functional estrogen receptors were also examined for the expression of the enzyme aromatase (see 2.1). The FOB-ER9 cells did not show aromatase expression regardless of the presence or absence of E_2.

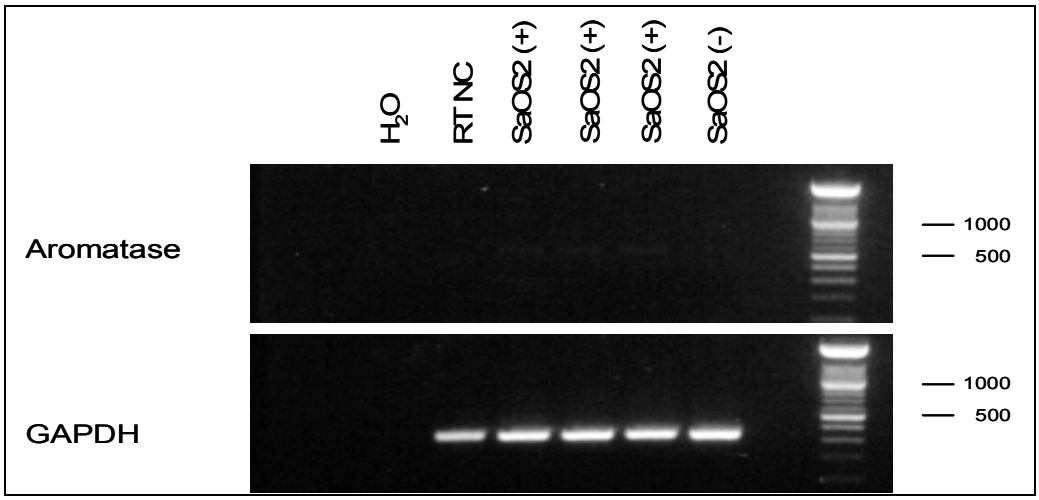

Figure 3.24. Expression of aromatase mRNA was assessed by RT-PCR in SaOS2 cells. The cells were maintained in growth media (SaOS2 (-)) or incubated with Dex for 72 h and IL-1β for the last 24 h (SaOS2 (+)). The expression of GAPDH mRNA indicated that the sample loading and amplification for each of the preparation was approximately the same. 35 PCR cycles were used.
RT NC, Reverse Transcriptase negative control.

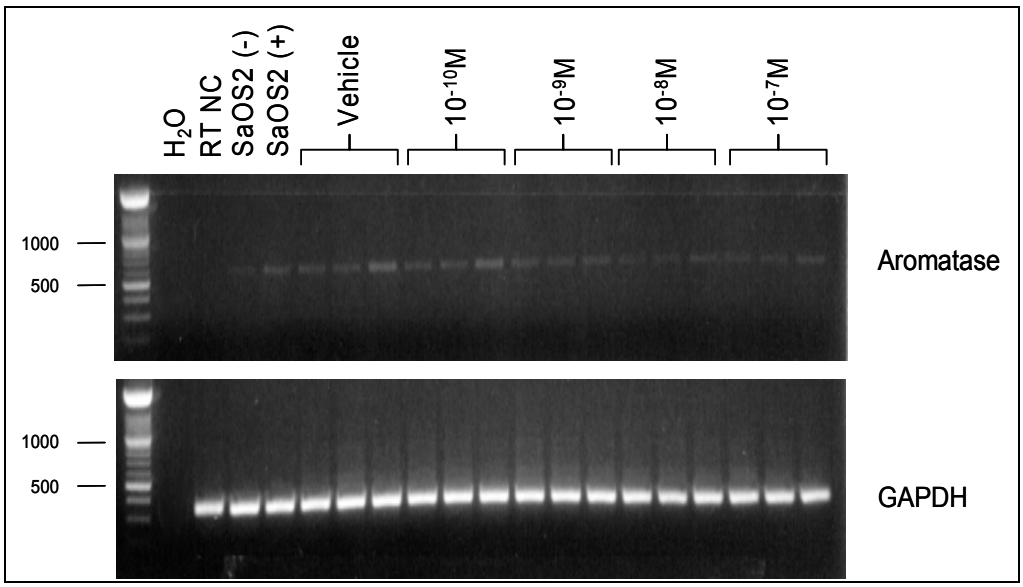

Figure 3.25. Determination of the aromatase expression in SaOS2 cells in response to different concentrations of E_2 (10^{-10}- 10^{-7} M) by RT-PCR. The cells were preincubated with Dex for 72 h and with IL-1β for the last 24 h. For comparison the expression of aromatase mRNA in cells without preincubation (SaOS2 (-)) was also determined. The expression of GAPDH mRNA indicated that the sample loading and amplification for each of the preparation was approximately the same. 35 PCR cycles were used.
RT NC, Reverse Transcriptase negative control.

3.3.2 Aromatase Expression and Activity in Rodent Cells and Bone

UMR cells are preosteoblastic, and ROS17/2.8 cells have a relatively mature osteoblast-like phenotype (see 2.1). RT-PCR analysis (see 2.3.2) of cDNA (see 2.2.1.1 and 2.2.2) from UMR and the ROS17/2.8 cells maintained in normal growth medium revealed the presence of aromatase and ER-α mRNA (Figure 3.26) in both cell lines.

Furthermore, it was tested whether the expression of the aromatase in ROS17/2.8 cells will change in the presence or the absence of E_2. After a treatment with E_2 (10^{-7} M), 4-hydroxyandrostenedione (aromatase inhibitor), or ICI 182,780 (estrogen antagonist) for 24 hours the expression of the aromatase did not change. Only the treatment with Dex together with IL-1β led to a slight decrease of the aromatase expression in ROS17/2.8 cells (Figure 3.27).

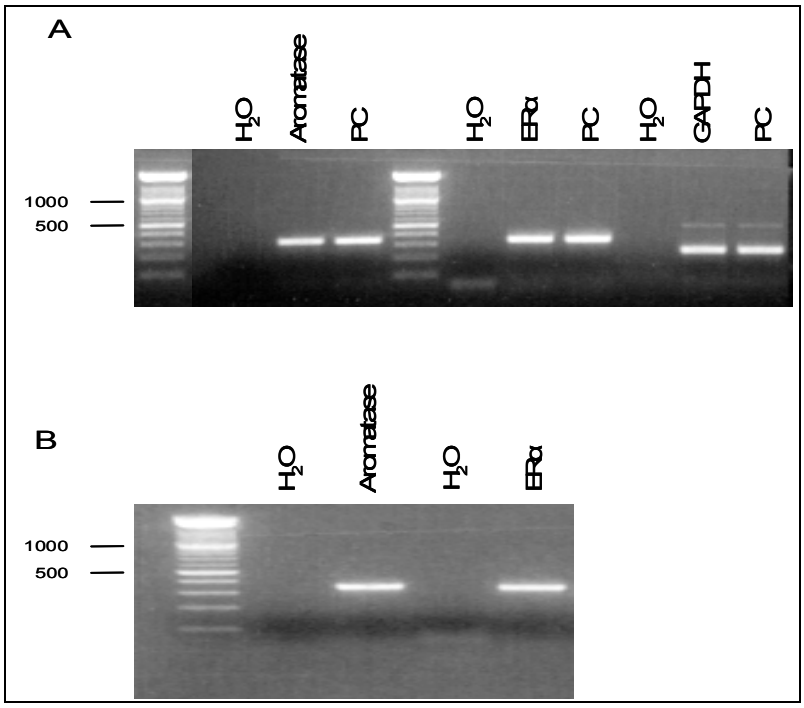

Figure 3.26. Expression of aromatase and ER-α mRNA in rat osteoblastic cells. Total RNA was extracted from (**A**) UMR cells and from (**B**) ROS17/2.8 cells. The expression of GAPDH mRNA indicated that the sample loading and amplification for each of the preparation was approximately the same. 40 PCR cycles were used. PC, positive control.

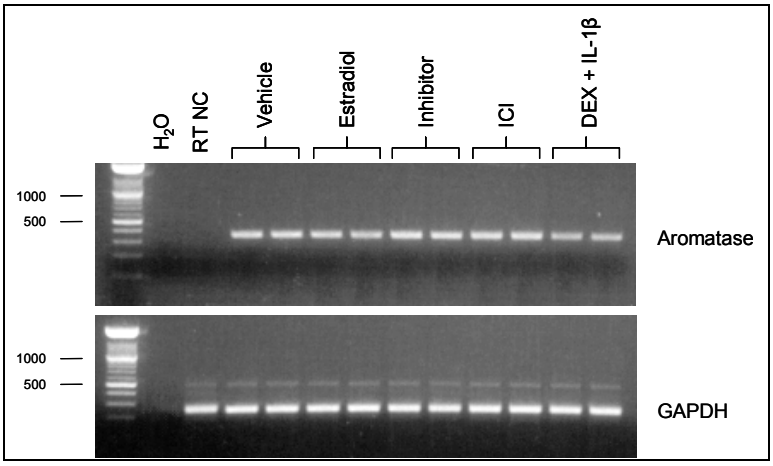

Figure 3.27. Ros17/2.8 cells were treated with vehicle, E_2, aromatase inhibitor (4-hydroxyandrostenedione), estrogen antagonist (ICI), or Dex plus IL-1β for 24 h. The expression of the aromatase mRNA was assessed by RT-PCR. The expression of GAPDH mRNA indicated that the sample loading and amplification for each of the preparation was approximately the same. 36 PCR cycles were used.
RT NC, Reverse Transcriptase negative control

Having established that the rodent cell lines (UMR and ROS17/2.8) express aromatase, it was of interest to determine whether long bones from rodents express aromatase and possess aromatase activity and whether the enzyme is regulated by estrogen.

Therefore mRNA from long bones of sham and ovariectomized (ovx'd) rats was analyzed (see 2.2.1.2, 2.2.2 and 2.3.2). All bone specimens from the ovx'd and sham operated rats (n=3) expressed aromatase but did not change in the two different conditions (Figure 3.28.A). Similar levels of aromatase mRNA between sham operated and ovx'd rats were observed using different numbers of RT-PCR cycles (Figure 3.28.B). The analysis of GAPDH mRNA expression indicated that the sample loading and amplification for each of the preparations was approximately the same.

Additionally, the aromatase expression in the long bones from 3 sham operated and 4 ovx'd mice was analyzed (see 2.2.1.2, 2.2.2 and 2.3.2). The expression of the aromatase did not show a clear difference between the two different conditions (Figure 3.29.A). Of note, ER-α mRNA was detectable in all bone samples (Figure 3.29.B).

To investigate whether the aromatase activity was different from the expression level the aromatase activity was determined following the protocol from Ackerman et al. (1981) (see 2.4). The aromatase activity in bone samples from sham operated and ovx'd mice (C57BL/6, 3 month) revealed similar values (sham: mean ± SEM, 0.61 ± 0.39 fmol/h/g bone; Ovx: 0.86 ± 0.50 fmol/h/g bone, n=3).

In an additional experiment 9 months old CFW mice were used. In these mice the aromatase activity was also clearly detectable (2.28 fmol/h/g bone). Moreover, the specific aromatase inhibitor, 4-hydroxyandrostenedione, markedly reduced aromatase activity in these mouse bone samples to 0.21 fmol/h/g bone, proving the specificity of the assay in assessing aromatase activity.

In the present study I analyzed the expression and possible regulation of aromatase in rodent bone, but neither aromatase activity nor its expression level was regulated by E_2. However, this study does indicate that human and rodent bone does express aromatase and the mice bones posse measurable aromatase activity.

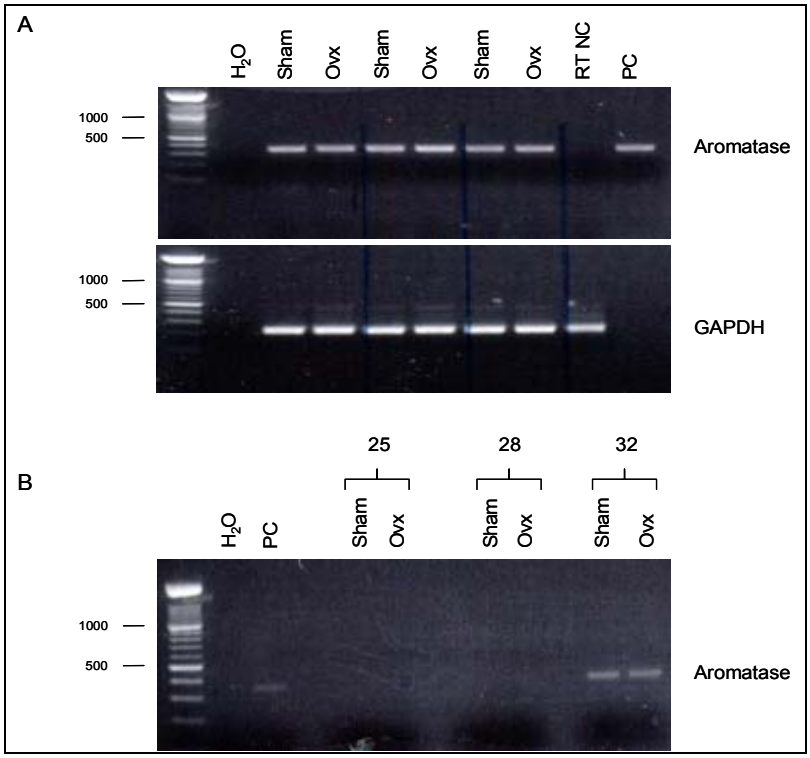

Figure 3.28. Total RNA was extracted from long bones of sham or ovx'd rats and the expression of aromatase mRNA was assessed by RT-PCR for (**A**) 34 cycles. (**B**) 25, 28, and 32 RT-PCR cycles were used to detect possible differences between the sham and ovx'd rats. The expression of GAPDH mRNA indicated that the sample loading and amplification for each of the preparation was approximately the same. PC, positive control.

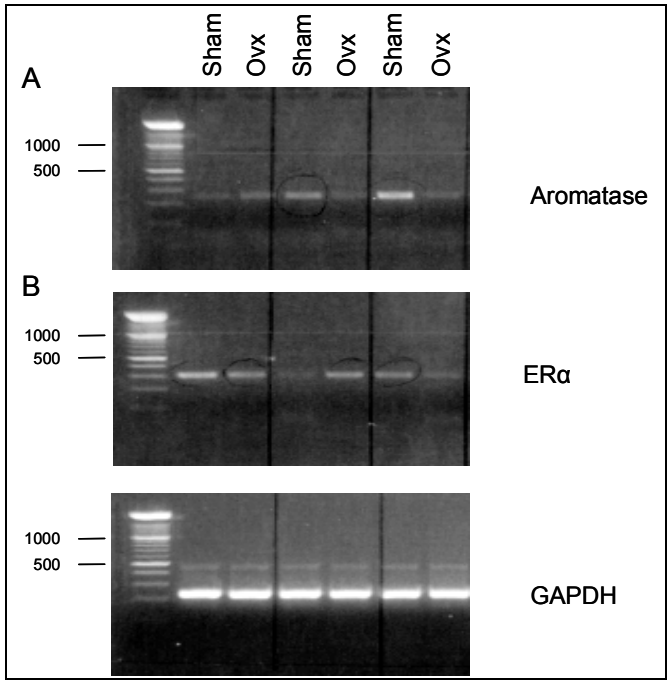

Figure 3.29. Total RNA was extracted from long bones of sham and ovx'd mice and the expression of (**A**) aromatase and (**B**) ER-α was assessed by RT-PCR. The expression of GAPDH mRNA indicated that the sample loading and amplification for each of the preparation was approximately the same. 34 PCR cycles were used.

4 Discussion

While estrogens and androgens are clearly critical for regulating bone remodeling in both females and males (Khosla et al., 2002; Riggs et al., 2002), our understanding of steroid hormone signaling pathways in bone are far from complete. In the presented work different aspects of estrogen and androgen action on bone were under investigation.

4.1 Dose Response of Estradiol on Bone Versus the Uterus in Ovariectomized Mice

In this study it was demonstrated that, in 6 month old C57BL/6 mice treated for 2 months, as little as 5 μg/kg/day of E_2 delivered using slow release pellets completely prevented loss of cortical and cancellous bone without a stimulatory effect on the uterus. Higher doses of E_2 further increased cortical and cancellous bone mass at various skeletal sites. In contrast to these findings, in 3 month old mice treated for 1 month, the 5 μg/kg/day dose resulted in uterine hypertrophy but was ineffective in preventing loss of cancellous bone and higher doses of E_2 were required to prevent bone loss. Collectively, these results (1) provide data on the dose response of estrogen, using E_2 pellets, on bone and the uterus; and (2) demonstrate that the relative effects of estrogen on these tissues depends on the particular experimental paradigm used. The findings in the younger mice are similar to recent results of Andersson et al. (Andersson et al., 2003), who also found that there was a dramatic uterine response to very low doses of E_2 in 2 month old mice, whereas both cancellous and cortical bone was less sensitive to the effects of estrogen in these mice.

In this study it was found that whereas the 6 month old mice had significant decreases in bone mass at the spine (which contains predominantly cancellous bone) following ovx, they did not lose cancellous bone (but did lose cortical bone) at the tibial metaphysis following ovx. Again, these findings were in contrast to the 3 month old mice, which lost cancellous bone at both the spine and tibial metaphysis following ovx (although the findings at the tibial

metaphysis did not achieve statistical significance). Of note, whereas spine BMD was similar in the 6 and 3 month old mice (57,3 ± 1,0 mg/cm^2 vs. 55,6 ± 2,0 mg/cm^2, P = 0,39), cancellous BMD at the tibial metaphysis was significantly lower in the 6 month as compared to the 3 month old mice (Tables 3.1. and 3.2., 172,8 ± 3,52 mg/cm^3 vs. 216.26 ± 8.14 mg/cm^3, P <0,001). This suggests that cancellous bone at the tibia may be progressively lost with aging in these mice, so that by 6 months of age, ovx does not result in further loss of cancellous bone at this site, whereas cortical bone mass is still reduced following ovx (Halloran et al., 2002) (Zhou et al., 2003).

Consistent with the here described findings in C57BL/6 mice, Gaumet et al. (Gaumet et al., 1998) found that whereas the skeletal response to estrogen was similar in young (6 month) versus old (12 month) rats, the uterus of the old rats was much less responsive to estrogen as compared to the young rats. It is also of interest that recent data indicate that very low doses of estrogen can prevent bone loss in elderly postmenopausal women without significant uterine stimulation (Cummings et al., 2003) (Utian et al., 1999). Collectively, the here discussed findings and those other findings in rats and in humans indicate that whereas the skeleton retains sensitivity to estrogen throughout life, the uterus may become progressively less sensitive to estrogen with aging. In light of the recent findings of the two studies from the Women's Health Initiative (Rossouw et al., 2002) (Anderson et al., 2004) demonstrating adverse effects of estrogen plus progesterone on cardiovascular events and the risk of breast cancer, and an increased risk of stroke, decreased risk of hip fracture, and no effect on coronary heart disease incidence in postmenopausal women with prior hysterectomy after the treatment with conjugated equine estrogen, these data provide a further impetus to examine the effects of low doses of estrogen in elderly women, which may result in skeletal protection without adverse sequellae in other tissues.

In this study it was found that the subcutaneous implantation of slow release pellets is the most convenient and efficacious way to deliver estrogen to mice. This avoids the handling and trauma associated with daily subcutaneous injections, as well as the possible peaks and valleys in serum E_2 levels associated with injections (Edwards et al., 1992; Sims et al., 1996). However, it is possible that bone versus the uterus may respond differently to a constant, low dose of estrogen as provided by subcutaneous pellets versus the peaks and valleys associated with daily injections. Indeed, previous studies have found that in mature rats subcutaneous injections of E_2 (10 µg/kg/48h) resulted in a distinct increase in uterine weight (21%) compared to sham rats at doses that were less effective on bone, whereas similar doses of E_2 (18µg/kg/d) given by subcutaneous pellets lead to an increase in cancellous bone area with no increase of the uterine weight above the weight of the sham rats (Gaumet et al., 1998) (Sibonga et al., 1998). Also of interest is the study from Erben et al. (Erben et al., 1998) in rats, where a dose of estrogen given by subcutaneous pellets (5.2 µg/kg/day) resulted in an increase in cancellous bone area with a concomitant decrease in uterine wet weight over the course of the treatment.

However, also the time of exposure (1 month versus 2 month) to E_2 may attenuate the response of the uteri. This is probably due to down regulation/desensitization of the ER in the uterus. The reports in the literature are very controversial regarding down- or up-regulation of estrogen receptors by estrogen in rodent uteri (Medlock et al., 1991) (Bergman et al., 1992) (Rosser et al., 1993).

In addition, the ratio between estrogen receptor alpha and beta and the homo- and heterodimerisation may also determine the downstream activities of estrogen in target tissues (Pace et al., 1997). Also, it is not clear whether the sensitivity of the skeletal or uteri response is altered by continuous or intermittent administration of estrogen.

More recently it was demonstrated that an active genomic steroid response mechanism coexists with a nongenomic steroid effect in reproductive and nonreproductive tissues. Kousteni et al. (Kousteni et al., 2002) demonstrated an antiapoptotic effect of sex steroids on bone cells with physiologic concentrations (10^{-11} - 10^{-10} M). They provided evidence that this is a nongenomic activation of a signaling pathway. The nongenomic effect of sex steroids on cells from reproductive and nonreproductive tissues is a rapid mechanism which is mediated via the classical estrogen receptors which are localized in the membrane. Data from other studies lead to the notion that a cross-talk between genomic responses to steroid hormones and cell surface receptor-mediated signal transduction pathways exists [for review see (Revelli et al., 1998)]. It is conceivable that different cell types in specific physiological situations use one or the other pathway to respond to sex steroids.

As previously demonstrated (Tobias et al., 1991) (Bain et al., 1993) (Samuels et al., 1999), also this study showed that a very high dose of E_2 (500 µg/kg/day) resulted in a dramatic increase in cancellous and cortical bone mass at the proximal tibia in the older mice. By contrast, the spine did not demonstrate this sclerotic response to high dose E_2. Thus, there are important differences between the axial and appendicular skeleton in terms of the response to high dose estrogen. The possible mechanism(s) for this are unclear, although it is of interest that studies with PTH have also shown different responses in axial versus appendicular sites. In rats treated with PTH, the relative BMD gain was highest at the distal femur and proximal tibia and lower at the lumbar vertebrae (Kishi et al., 1998). In mice, however, the PTH treatment augmented cancellous bones to a greater extend in the vertebral body than in the proximal tibia. In contrast, the same treatment added cortical bone in the tibia, a highly mechanically loaded site, but not in the cortex of the lumbar vertebrae, a less loaded site (Zhou et al., 1994). Moreover, in light of recent evidence that the skeletal response to mechanical loading may, at least in part, be mediated by ER-α (Lee et al., 2003),

it is possible that the differential sensitivity of axial versus appendicular sites to the sclerotic effect of high dose estrogen is related to weight bearing.

An aim of ongoing research is to find compounds that have selective effects on the different target tissues of estrogen. Two generations of these selective estrogen receptor modulators (SERMs) have already been generated. The most notable from the first generation is tamoxifen, and from the second generation is raloxifene. Tamoxifen possesses estrogen-like agonist activity on bone and simultaneously estrogen antagonist activity on the breast. An unwanted side effect of tamoxifen was its estrogen-like action on the endometrium (Cosman and Lindsay, 1999) (Jordan and Morrow, 1999). The National Surgical Adjuvant Breast and Bowel Project (NSABP) observed a 35% decrease of fractures of the hip, spine, and wrist and a 45% decrease in the incidence of breast cancer and a 2,5-fold increase in endometrial cancer with the treatment of tamoxifen (Fisher et al., 1998). However, not all trials evaluating the preventive benefit of tamoxifen have shown similar positive results (Powles et al., 1998) (Veronesi et al., 1998).

Raloxifene has estrogen-like effects on bone, lipids and the coagulation system, and estrogen antagonist actions on the breast and uterus. Raloxifene has been approved for prevention and/or treatment of post-menopausal osteoporosis. The Multiple Outcomes of Raloxifene Evaluation (MORE) study demonstrated an increase of bone density in femoral neck and spine and a reduced risk of vertebral fractures. Raloxifene is similar to placebo in its uterine effects (Ettinger et al., 1999). The mechanisms by which the same compound can exert estrogen agonist effects on one target tissue and antagonist effects on another still have to be clarified. It was demonstrated that the estrogen receptor undergoes different conformational changes during the ligand binding. Thus, the crystal structure of E_2 bound to the estrogen receptor differs from that of raloxifene bound to the same receptor (Brzozowski et al., 1997). Mechanisms include differing interactions with various domains of the estrogen receptor, and tissue-specific recruitment of steroid receptor co-activators and co-repressors may underlie

some of the tissue-specific effects (Shang and Brown, 2002). In light of the presented study it is important to test if also the SERMs show different responses at the different target tissues depending on the experimental conditions used.

In summary, the study provides data on the dose response of bone versus the uterus to E_2. In addition, the study shows that the relative effect of estrogen on these tissues depends on the particular experimental conditions used. The latter finding is of particular relevance in interpreting results of studies on new compounds (e.g. SERMs) with putative selective effects on bone versus reproductive tissues.

4.2 Function of Steroid Receptor Coactivator-1

SRC-1 was the first and one of the most important nuclear receptor coactivators to be characterized and cloned (Onate et al., 1995). Estrogen signaling via the estrogen response element (ERE) is clearly dependent on SRC-1 (Onate et al., 1995); however, there is evidence that alterations in SRC-1 levels also influence the regulation by the ER of genes such as *c-myc* and *IGF-I*, which lack a classical ERE (Shang and Brown, 2002). Whether estrogen signaling through nongenomic mechanisms also involves SRC-1 at some level is unclear at present, although it is of interest that Kousteni et al. (Kousteni et al., 2003) have demonstrated recently that estrogen regulation of the MAP kinase pathways eventually results in alterations in the activity of common transcription factors, such as Elk-1, CCAAT enhancer binding protein-β (C/EBPβ), cyclic adenosine monophosphate-response element binding protein (CREB), and c-Jun/c-Fos. Since it is possible (and perhaps even likely) that one or more of these transcription factors also interact with SRC-1, loss of SRC-1 would be expected to alter estrogen signaling not just through classical EREs, but also through one or more of these other pathways. Thus, a better understanding of the role of SRC-1 in mediating estrogen action on bone represents an important step towards further dissecting the overall mechanisms by which estrogen regulates bone metabolism.

The generation and characterization of SRC-1 KO mice by J. Xu and colleagues (Xu et al., 1998) provided the first *in vivo* evidence that loss of this coactivator could result in estrogen resistance in reproductive tissues. Using these mice in the here presented study, it was possible to characterize in detail the consequences of the loss of SRC-1 on estrogen and androgen action on bone of female and male mice.

4.2.1 Effects of Loss of SRC-1 on the Skeletal Response to Estrogen in Female Mice

Under basal conditions, SRC-1 KO mice represent a state of compensated estrogen resistance in a number of tissues: by maintaining a higher than normal E_2 level, they exhibit normal reproductive function. Yamada T. et al. also generated a SRC-1 knock out mouse line (SRC-1 -/-) however, they used for the generation of the SRC-1 -/- mouse line a Cre-loxP system (using a ubiquitous CMV promoter) (Yamada et al., 2004). In these SRC-1 -/- mice a stop-codon was created in the middle of the bHLH-PAS domain at exon 5, predicting a truncated product. Both mouse lines have a similar genetic background because they are intensively backcrossed into C57BL/6 mice. The SRC-1 KO mice appear to have a relatively normal skeletal phenotype and BMDs, at least in young adulthood (~3 months of age). Yamada T. also did not detect significant differences of bone density at 3 month of age between WT and SRC-1 -/- littermates of either sex under physiological conditions. Significant differences were only seen at 6 month of age (Yamada et al., 2004). It is speculated that with aging the compensatory elevation of sex hormone levels via a feedback mechanism becomes too weak to catch up with the decreased sensitivity to these hormones by the SRC-1 deficiency.

However, by ovx the SRC-1 KO mice and using a dose of E_2 (10µg/kg/day) that was clearly effective in preserving BMD in the WT mice, this study unequivocally demonstrated a profound defect in estrogen action on cancellous bone in the SRC-1 KO mice. Similar results were also seen from Yamada et al. (Yamada et al., 2004). Moreover, this defect could be overcome by using a 4-fold higher dose of estrogen, consistent with skeletal estrogen

resistance. In contrast to this marked deficit in estrogen action in cancellous bone, the effects of estrogen (even at the low dose) on cortical bone in the SRC-1 KO mice were relatively well preserved. This was established not only using cortical BMD measurements by pQCT (which has a voxel size of approximately 100 μm), but also by using what is generally considered the "gold standard" for such studies, μCT (which has a voxel size of approximately 20 μm). Interestingly, while the low dose of estrogen was effective in preserving cortical BMD and thickness in the SRC-1 KO mice, in addition to having no effect in cancellous bone, this dose of estrogen also failed to alter uterine weight in the ovx'd, SRC-1 KO mice, while maintaining it at sham levels in the WT, ovx'd mice.

Although a fairly high dose of E_2 (~ 4-fold over physiological replacement) was used to overcome the deficit in estrogen action in cancellous bone in the SRC-1 KO mice, it is possible that lower doses (i.e. 2-fold or less) might also have been effective. However, we wanted to establish, in principal, that the defect in estrogen action in the SRC-1 KO mice could be overcome, and further dose response studies are needed to establish the minimal dose of E_2 that is capable of overcoming the deficit in estrogen action in these mice.

There are several possible reasons why loss of SRC-1 results in a defect in estrogen action primarily in cancellous bone. Cancellous bone does have a higher rate of turnover than cortical bone, and estrogen deficiency clearly has a greater impact on cancellous as opposed to cortical bone in WT female mice or, for that matter, in women (Riggs et al., 2002). Thus, any defect in estrogen action (i.e. from loss of SRC-1) would be expected to perhaps be most evident in cancellous bone. While this may be part of the explanation for the predominant defect in estrogen action in cancellous bone in the SRC-1 KO mice, a second possibility that involves potential differential interactions of SRC-1 with ER-α versus ER-β in bone cells should also be considered.

In recent studies, it has been demonstrated that in osteoblastic cells, SRC-1 appears to preferentially enhance the transcriptional activity of either co-expressed ER-α and -β or ER-

β alone, without significant effects on the activity of ER-α alone (Monroe et al., 2003). By contrast, in non-osteoblastic (i.e. COS7) cells, this pattern is reversed, and SRC-1 preferentially enhances the activity of ER-α to a greater extent than that of ER-β or coexpressed ER-α and -β. The here presented findings also demonstrate that while the cancellous bone of the vertebrae contains both ER-α and -β, the cortical bone of the femur shaft contains almost exclusively ER-α. Consistent with these findings, Onoe Y. (Onoe et al., 1997) also found that the cancellous bone of the vertebrae and distal femoral metaphysis in rats expressed much higher levels of ER-β than the cortical bone of the femoral shaft. Moreover, Bord et al. (Bord et al., 2001) examined ER-α and -β expression by immunohistochemistry in neonatal human ribs and, demonstrated that cortical bone contained predominantly ER-α, whereas cancellous bone contained immunoreactivity for both ER-α and -β.

Collectively, the here described findings and the previous data indicate that cancellous bone contains both ER-α and -β [leading presumably to the formation of intracellular ER-α/β heterodimers (Pettersson et al., 1997)], whereas cortical bone primarily contains ER-α (resulting in the formation of ER-α homodimers). Thus, based on previous studies (Monroe et al., 2003), the activity of the ER-α/β heterodimers in cancellous bone would be predicted to be most affected by loss of SRC-1, potentially explaining the predominant deficit in estrogen action in cancellous bone of the SRC-1 KO mice. By contrast, the activity of the ER-α homodimers in cortical bone may not be significantly altered by SRC-1 deficiency, resulting in the relatively preserved responses to estrogen in cortical bone that were observed in the SRC-1 KO mice. Interestingly, it was also found that in contrast to SRC-1, SRC-2 does preferentially enhance the transcriptional activity of ER-α in osteoblastic cells to a greater extent than that of coexpressed ER-α and -β or ER-β alone (Monroe et al., 2003). This leads to the plausible prediction that estrogen effects on cortical bone would be more

impaired in the SRC-2 KO animals, with a relative preservation of estrogen action in cancellous bone in these mice, i.e. exactly the opposite of what was observed in the SRC-1 KO mice.

As noted earlier, the 10 μg/kg/day dose of E_2 preserved uterine weight in the WT mice, but failed to do so in the SRC-1 KO mice. Like cortical bone (Bord et al., 2001; Onoe et al., 1997), the uterus contains predominantly ER-α (Couse et al., 1997), and this finding may seem at odds with the hypothesis that estrogen action in cortical bone was preserved in the SRC-1 KO mice because the previous in vitro studies had suggested that SRC-1 did not significantly enhance the transcriptional activity of ER-α in osteoblastic cells (Monroe et al., 2003). However, in those studies, Monroe et al. also found that in a kidney cell line, SRC-1 did enhance the activity primarily of ER-α (Monroe et al., 2003). While endometrial cells were not studied, these data indicate that the specific interactions of SRC-1 with ER-α versus -β are likely tissue specific, perhaps explaining why estrogen action is impaired in the uterus but preserved in cortical bone in the SRC-1 KO mice, even though both tissues primarily contain ER-α.

The relatively selective loss of estrogen action which was observed in cancellous bone in the SRC-1 KO mice is consistent with other studies indicating that the cancellous and cortical compartments of bone are differentially regulated. Thus, in contrast to the greater effects of estrogen deficiency on cancellous as opposed to cortical bone (Riggs et al., 2002), chronic PTH exposure leads to greater losses of cortical bone, with relative preservation (or even an increase) in cancellous bone (Parisien et al., 1990). In addition, mice lacking plasminogen activator inhibitor 1 do not lose cancellous bone, but do lose cortical bone following ovx (Daci et al., 2000). Finally, IL-6 KO mice have relatively well preserved cancellous bone volumes, but do have significant deficits in cortical bone (Poli et al., 1994).

In summary, the here presented results establish that loss of SRC-1 leads to a predominant defect in estrogen action in cancellous bone, with a relative preservation of estrogen effects on cortical bone. However, the deficit in estrogen action in the SRC-1 KO mice can be overcome by using high doses of estrogen, consistent with estrogen resistance in bone. The differential expression of ER-α and -β in cancellous versus cortical bone and the specific interactions of these receptor isoforms with SRC-1 may, in part, explain why cancellous bone is more susceptible to loss of SRC-1 than cortical bone. In addition, these findings may also have significant implications for our understanding of the variability of skeletal responses to estrogen in humans, some of which may be due to alterations in the level or function of SRC-1 in bone.

4.2.2 Effects of Loss of SRC-1 on the Skeletal Response to Estrogen in Male Mice

SRC-1 KO male mice exhibit normal reproductive function and appear to have similar skeletal phenotype and BMDs like the WT littermates, at least in young adulthood (3-5 months of age) (Yamada et al., 2004). The examination of the function of SRC-1 in the male skeleton clearly showed the expected reduction of cancellous and cortical bone after orc at the different sites of the skeleton. In agreement with the well preserved estrogen action on cortical bone (femur and cortical volumetric BMD) of the SRC-1 KO female mice treated with E_2 there was no defect of estrogen action on the cortical bone of the SRC-1 male mice as well.

In contrast to the findings in the female SRC-1 KO mice, the orc of the male SRC-1 KO mice and treatment with E_2 delivered using slow release pellets (same pellets which were used in the female experiment; 10 µg/kg/day, body weight of 0,025 kg), did not show a defect of estrogen action on cancellous bone in the spine. The response of the WT and SRC-1 KO male mice to the E_2 treatment was similar. Also the cancellous volumetric BMD of the tibial metaphysis was not different between the WT and SRC-1 KO mice. The dose of E_2 was not sufficient to maintain the cancellous volumetric BMD in the metaphysis of the male SRC-1 KO mice, but it was not sufficient in the WT mice either. In the female SRC-1 KO mice it was suggested that the defect in response to physiological doses of E_2 resulted from the preferred interaction of SCR-1 with ER-β or coexpressed ER-α and -β, which are mainly expressed in cancellous bone. However, functional studies using sex steroid receptor inactivated mice (ERKO, BERKO) clearly show that ERKO male mice are totally unresponsive to E_2, even at high doses (Sims et al., 2003). This finding is consistent with previous results showing the lack of a bone phenotype in male BERKO mice, and the identical phenotypes of male ERKO and DERKO mice (Sims et al., 2002). It was unequivocally concluded that in male mice ER-α but not ER-β is mediating the estrogen

action on bone, and SRC-1 is not necessarily important to respond to E_2 and to maintain cancellous bone.

Another possible explanation for the different findings in the cancellous bone of the female versus the male SRC-1 KO mice may be, in part, a gender-related difference of SRC-1 steady state mRNA levels (Misiti et al., 1998). Significant gender- and area-specific differences in the expression of SRC-1 gene in the brain and pituitary under basal conditions and following acute stress were detected in rats by Northern blot analysis (Bousios et al., 2001).

The very similar second member of the SRC family, SRC-2, was overexpression twofold in the brain and testis of SRC-1 KO mice (Xu et al., 1998). Thus, an up-regulation of the SRC-2 may partially compensate for the loss of SRC-1 in the skeleton of the male mice, although, in the female SRC-1 KO mice, no significant difference in the level of the SRC-2 mRNA in bones from the WT and SRC-1 KO mice was detected.

Our data suggest that because the regulation of estrogen action on bone is gender specific with ER-α as the main effector in male bone and the preferred interaction of SRC-1 with ER-β, and a possible gender-related difference in the expression of the SRC-1 gene, the SRC-1 KO male mice have no defect in estrogen action on bone, in contrast to the SRC-1 KO female mice.

4.3 Effects of Loss of SRC-1 on the Skeletal Response to Testosterone or 5α-DHT in Male Mice

The effect of androgen can either be directly through the stimulation of androgen receptors (ARs) or indirectly through aromatization of androgens into estrogens and, thereafter, through stimulation of ERs. However, the androgen 5α-DHT can not be aromatized to estrogen; thus, the effect of 5α-DHT is mediated through ARs.

As shown in this study 5α-DHT was able to maintain cancellous BMD in the spine and in the proximal metaphysis of the tibia in the WT male mice. The activation of the AR through 5α-DHT regulates the amount of cancellous bone in male mice. Recently, Vandenput et al. (Vandenput et al., 2002) demonstrated a better response of cancellous BMD compared to cortical thickness in WT rats after the treatment with 5α-DHT. In contrast, no effect on cortical bone in WT mice was seen after the administration of 5α-DHT. The cortical bone of the double knock-out mouse line ER-$\alpha^{-/-}\beta^{-/-}$ also did not respond to 5α-DHT, which leads to the presumption that the AR is not mediating the effect of 5α-DHT in cortical bone (Moverare et al., 2003). This is in agreement with the findings that the conversion of androgens into estrogens is required for normal body growth in male rats, indicating that indirect effects of androgen, mediated by estrogens are also important (Vanderschueren et al., 1997).

The data of the SRC-1 KO male mice that the loss of SRC-1 has not impaired the effect of the administrated 5α-DHT in bone, and that 5α-DHT is even more effective in the bones of the SRC-1 KO mice especially in cortical bone was unexpected. These data suggest that in cortical bone of WT mice SRC-1 functions as an inhibitor. It can be speculated that in the presence of SRC-1 cortical bone is less protected against bone loss during the administration with 5α-DHT. Contrary is the report from Yamada et al. (Yamada et al., 2004); they found that the restoration of the bone volumes in the SRC-1 -/- mice were limited to approximately one half due to insensitivity to 5α-DHT in the male mice.

SRC-1 interacts with ARs *in vitro*; however, this interaction is different from that with ER. Mediating the action of estrogen, SRC-1 interacts with the AF2 domain of the ER. In contrast, at the AR it seemed that the N-terminal AF1 activation domain was most critical to activate transcription and that AF1 contributes all the activity of the receptor (Jenster et al., 1991; Rundlett et al., 1990; Simental et al., 1991; Zhou et al., 1994). These differences may differentially influence ligand-dependent activation of ERs and ARs such that SRC-1 interaction with ERs is essential for estrogen action, but its interaction with ARs is not essential for androgen action; SRC-1 even inhibits the interaction of the AR with the ligand. In addition, SRC-1 has been reported to either increase or decrease AR activity *in vitro* (Ikonen et al., 1997; Takeshita et al., 1996). The presented data suggest that SRC-1 has an inhibitory effect on mediating androgen action on cortical bone in male mice, and that the loss of SRC-1 leads to the abolition of the repressing action.

In addition, other androgen receptor coactivators, for example ARA70, which is specific for androgen receptors and SRC-2, have been reported to interact and activate the androgen receptor and to mediate AR-mediated transactivation (Yeh and Chang, 1996). Thus, it might be possible that these coactivators and other coactivators for androgen receptors are able to not only compensate for the loss of SRC-1 but also to be expressed and active more efficiently.

Recent studies presented a positive effect of testosterone on bones in rats and mice (Vandenput et al., 2001; Vanderschueren et al., 2000). The concentrations of administrated testosterone in these studies were in the same range or even lower than the dose of testosterone used in the here presented study. However, the weight of the seminal vesicles of the WT male mice in this study was just restored to about 50 % of the weight from the sham operated mice after the treatment with 7 mg/kg/day of testosterone which is in contrast to other studies that determined a nearly 100 % restoration of the seminal vesicles after orc and testosterone treatment. So far it is not clear why the 7 mg/kg/day of testosterone did not

restore the weight of the seminal vesicles in the WT mice and also did not prevent any loss of bone at the different sites of the skeleton. One presumption is that the pellet did not have the expected dose of testosterone right from the beginning. Because of the good experience with the slow release pellets in former experiments, there is not doubt on the general reliability of the pellets. Because of the uncertainty whether the expected concentration of testosterone was administrated, no conclusions were drawn out of this part of the experiment.

4.4 Expression and Regulation of Aromatase *in vitro* and *in vivo*

Previous studies *in vivo* have assessed the impact of circulating rather than local estrogens on bone cell activity. However, more recent reports indicate that human osteoblast cells express the enzyme aromatase and therefore are able to generate estrogens from androgens locally (Nawata et al., 1995) (Sasano et al., 1997; Schweikert et al., 1995). In this work, the differentiation of the hMS cells reveals that undifferentiated marrow stromal cells express aromatase and that there is a clear increase at the beginning of differentiation. The expression of the aromatase did not further change during the remaining time of differentiation. These data are supported by a previous study using SV-HFO (immortalized human fetal osteoblast) cells, which indicated that at the beginning of the differentiation the expression of aromatase increases, but there is no further increase during the remaining time of differentiation (Janssen et al., 1999). However, the determination of the aromatase activity exhibits a significant decrease of activity by day 10 of culture (Janssen et al., 1999). Post-translational modifications, protein stability, or cofactor variations may be responsible for the described changes in aromatase activity. Estrogen synthesis by osteoblasts may be partly dependent on osteoblast cell differentiation. Probably the endogenous E_2 synthesis is more important during the early proliferation phase of osteoblast development than during a more differentiated mineralizing phase. Previous studies suggested that aromatase mRNA is undetectable in normal bone or bone marrow, but expression is induced under pathological conditions such as a fracture (Lea et al., 1997).

It was of interest that treatment of ROS17/2.8 cells with Dex and IL-1β decreased the aromatase expression. This is in agreement with the study from Eyre et al. (Eyre et al., 1998). They likewise reported a decrease of E_1 and E_2 production after the treatment with Dex. In contrast, in human osteoblast cell lines a treatment with Dex increased the aromatase expression and activity, as demonstrated in this study in the osteosarcoma cell line SaOS2

and by other investigators (Tanaka et al., 1993) (Nawata et al., 1995) (Shozu et al., 2000). Why this and other studies see an opposite response to the treatment with Dex in human and rodent bone cell lines is not clear yet. These observations show that there is a difference in the regulation of bone mass in humans and rodents.

In this study, the expression of aromatase and ER in different human (hMS, SaOS2) and rodent (ROS17/2.8, UMR) bone cell lines was demonstrated, which opens the chance to elucidate the regulation of the aromatase in osteoblasts. Yue et al. (Yue et al., 2001) demonstrated that the aromatase activity in breast tumors correlated inversely with tissue E_2 concentration. Using long term estrogen deprivated MCF-7 cells they found a 4-6 fold higher aromatase activity compared to wild-type MCF-7 cells. The re-exposition to estrogen containing medium decreased the activity significantly. A recent report demonstrated that estrogen might serve as a negative factor for the regulation of aromatase activity in mammary glands of nonhuman primates. Aromatase activity was increased significantly in the mammary glands after ovariectomy of the nonhuman primates and was reduced to the level in the intact animals by subsequent treatment with E_2 benzoate (Nakamura et al., 1999). In contrast, neither the aromatase expression nor activity of the different human and rodent bone cell lines, including SaOS2, hMS or ROS 17/2.8, nor the long bones of sham and ovariectomized mice and rats were regulated by E_2. Down regulation of aromatase by estrogen seems to be restricted to certain tissues because no effect was seen in human placental microsomes (Long et al., 1998) and in the here presented data with bone cell lines and bone tissue.

5 Summary

1. Estrogen is known to have important effects on both reproductive and non-reproductive tissues. In this study it was demonstrated that an E_2 dose of as little as 5μg/kg/d completely prevented loss of cancellous bone (at the lumbar spine and tibial metaphysis), and it had no stimulatory effects on the uterus in 6 month old C57BL/6 mice. By contrast, when 3 month old C56BL/6 mice were administered the same doses of E_2 and studied after 1 month; the 5 μg/kg/d dose resulted in uterine hypertrophy, but was not able to prevent loss of cancellous bone. These results, thus, a) provide data on the dose response for E_2 effects on mouse bone; and b) indicate that the relative effects of E_2 on bone versus the uterus are highly dependent on the particular experimental conditions used. This issue needs to be considered in evaluating agents with potential "selective" effects on bone versus reproductive tissues.

2. Steroid receptor coactivator (SRC)-1 is an important nuclear receptor coactivator that enhances estrogen action in a number of tissues. The presented study has established that SRC-1 KO female and male mice have a comparable skeletal phenotype to their WT littermates at 3 and 5 months of age. The treatment of ovariectomized SRC-1 KO female mice with a physiological concentration of E_2 led to a predominant defect in estrogen action in cancellous bone, with a relative preservation of estrogen effects on cortical bone. However, the deficit in estrogen action in the female SRC-1 KO mice was overcome by using a higher dose of E_2, consistent with estrogen resistance in bone. The differential expression of the interacting nuclear receptors, ER-α and -β, in cancellous versus cortical bone and the specific interactions of these receptor isoforms with SRC-1 may, in part, explain why cancellous bone is more susceptible to loss of SRC-1 than cortical bone.

3. In contrast, the SRC-1 male mice lack the defect in estrogen action on bone. These findings are consistent with a gender-related difference that in male mice ER-α but not ER-β is mediating the estrogen action on bone.

The treatment of SRC-1 KO male mice with 5α-DHT resulted in a significant better response of the cortical bone from the KO male mice compared to the WT mice. The findings lead to the suggestion that in male WT mice SRC-1 might inhibit the action of 5α-DHT on bone.

4. Peripheral tissues including bone are dependent on circulating active sex steroids, but also synthesize estrogen from circulating C19 precursor locally. The conversion of the precursors to estrogen is mediated by aromatase. In this work it has been shown that human and rodent osteoblastic cells at different stages of differentiation express aromatase. Furthermore, the expression and activity has been demonstrated in bone tissues of mice and rats. Although a regulation of the aromatase by E_2 was reported by other investigators in certain tissues, such as breast tissue and mammary glands, I did not find a change of aromatase expression and activity in the various bone cell lines and bone tissue under estrogen deficiency and estrogen exposure.

6 Zusammenfassung

1. Östrogene haben einen wesentlichen Einfluß auf reproduktive und nichtreproduktive Gewebe. In der vorliegenden Studie konnten wir zeigen, daß die niedrigste verwendete Östradiolkonzentration von 5 µg/kg/Tag den Verlust von spongialem Knochen (in den Lendenwirbeln und der tibialen Metaphyse) verhinderte und keinen anregenden Einfluß auf das Uterusgewebe in 6 Monate alten C57BL/6 Mäusen hatte. Im Gegensatz dazu kam es bei 3 Monate alten Mäusen des gleichen Stammes nach einer einmonatigen Behandlung mit den gleichen Östradiolkonzentrationen bereits bei 5 µg/kg/Tag zu einer Hypertrophie des Uterus, ohne jedoch den Verlust von spongialem Knochen zu verhindern. Die Ergebnisse dieser Studie liefern a) Daten über die Östradiol-Konzentrationsabhängigkeit der Knochen von Mäusen, und b) weisen darauf hin, daß die Effekte von Östrogenen am Knochen gegenüber dem Uterus stark abhängig sind von den jeweilig gewählten experimentellen Bedingungen. Dieser Aspekt muß bei der Beurteilung von möglichen Knochen- oder Uterus-selektiv-wirkenden Mitteln beachtet werden.

2. Der Steroidrezeptor Coaktivator (SRC)-1 ist ein wichtiger Zellkernrezeptor-Coaktivator, der in verschiedenen Geweben den Einfluß von Östrogenen verstärkt. In der vorliegenden Studie wurde gezeigt, daß weibliche und männliche SRC-1 KO Mäuse im Alter von 3 und 5 Monaten einen ähnlichen skeletalen Phänotypen besitzen wie die WT Mäuse. Die Behandlung von weiblichen SRC-1 KO Mäusen mit einer physiologischen Östradiolkonzentration führt zu einem Defekt der Östrogenwirkung in spongialem aber nicht in kortikalem Knochen. Dieses Defizit der Östrogenwirkung in den weiblichen SRC-1 KO Mäusen kann durch die Behandlung mit einer höheren Östradiolkonzentration aufgehoben werden. Die unterschiedliche Expression der mit SRC-1 interagierenden Zellkernrezeptoren, ER-α and -β, in spongialem und kortikalem Knochen und die bevorzugte Interaktion der ER-α/β heterodimere und ER-β homodimere mit SRC-1 in Knochenzellen könnte eine mögliche

Erklärung liefern, warum spongialer Knochen anfälliger ist gegenüber dem Verlust von SRC-1 als der kortikale Knochen.

3. Im Gegensatz dazu weisen die männlichen SRC-1 KO Mäusen keinen Verlust der Östradiolwirkung am Knochen auf. Diese Ergebnisse stimmen mit dem geschlechter-bedingten Unterschied der Rolle des ER-β im Knochen von männlichen gegenüber weiblichen Mäusen überein.

Die Behandlung männlicher SRC-1 KO Mäuse mit 5α-DHT führte zu einer signifikant höheren Knochendichte im kortikalen Knochen der KO Mäuse im Vergleich zu den WT Mäusen. Dieses Ergebnis läßt darauf schließen, daß in WT Mäusen SRC-1 möglicherweise hemmend wirkt auf die Bindung von 5α-DHT an den SRC-1-Rezeptor Komplex und dadurch das Androgen nicht dem Verlust von Knochenmasse entgegenwirken kann.

4. Periphere Gewebe, wie der Knochen, sind abhängig von zirkulierenden Steroidhormonen, aber auch von der lokalen Östrogensynthese aus 19 C-Atom Androgenen. Diese Androgene werden durch Aromatisierung in Östrogene umgewandelt, und dieser Schritt wird von dem Enzym Aromatase katalysiert. In der vorliegenden Arbeit wurde gezeigt, daß menschliche Osteoblastenzelllinien und Osteoblastenzelllinien von Nagetieren, die sich in verschiedenen Differenzierungsstufen befinden, das Enzym Aromatase exprimieren. Des weiteren konnten wir die Expression und die Aktivität in Knochengeweben von Mäusen und Raten nachweisen. Obwohl für einige Gewebe, wie Brust und Milchdrüse, berichtet wurde, daß die Aromatase von Östrogenen reguliert wird, konnte in den untersuchten Zelllinien und Knochengeweben keine Änderung der Expression oder Aktivität unter Östrogendefizienz oder –behandlung beobachtet werden.

7 Abbreviations

1,25 $(OH)_2D_3$	1α,25 dihydroxyvitamin D_3
3-D	three dimensional
A	adenine
AD	activation domain
AF-1	activation function 1
AF-2	activation function 2
AMV	avian myeloblastosis virus
AR	androgen receptor
AscP	ascorbic phosphate
βGP	β-glycerolphosphate
BERKO	ER- β knock-out
BFR	bone formation rate
bHLH	basic helix loop helix
BMC	bone mineral content
BMD	bone mineral density
bp	base pairs
BS	bone surface
BV/TV	bone volume/measured tissue volume (%)
C	cytosine
Cbfa 1	core-binding factor alpha-1 (transcription factor)
CBP/p300	transcription factor
cDNA	complementary DNA
Ci	Curie

cm	centimeter
cm^2	square centimeter
cm^3	cubic centimeter
CO_2	carbon dioxide
CSS	charcoal stripped serum
CV	coefficient of variation
DERKO	ER- α/β double knock-out
Dex	dexamethasone
5α-DHT	5α-dihydroxytestosterone
dNTPs	2'- desoxyribonucleotid-5'-triphosphates
DXA	dual energy X-ray absorptiometry
E	estrogen
E_1	estrone
E_2	estradiol
E_3	estriol
ERKO	ER- α knock-out
ER-α	estrogen receptor-α
ER-β	estrogen receptor-β
EtOH	ethanol
g	gram
g	gravity unit
G	guanine
h	hour
HAT	histone acetyl transferase
HCl	hydroxychloride
HI-FBS	heat inactivated fetal bovine serum

kb	kilo bases
KCl	potassium chloride
KO	knock-out
L	leucine
l	liter
µ	micro: x 10^{-6}
µm	micrometer
M	molar
MCS-F	macrophage colony-stimulating factor
mg	milligram
MgCl	magnesium chloride
min	minute
ml	milliliter
mm	millimeter
mM	millimolar
mRNA	messenger ribonucleic acid
n	nano: x 10^{-9}
n	number of animals per treatment group
N_2	nitrogen
NADPH	nicotinamide-adenine dinucleotide phosphate, reduced
nm	nanometer (Wavelength)
NR box	nuclear receptor box
ºC	Celsius
OPG	Osteoprotegerin
PAS	Pas/Arnt/Sims
PBS	phosphate buffered saline

PEG	polyethylenglycol
pmol	picomol
pQCT	peripheral quantitative computer tomography
PTH	parathyroid hormone
RANK	receptor for activation of nuclear factor kappa B
RANKL	receptor for activation of nuclear factor kappa B ligand
RID	receptor interaction domain
RNA	ribonucleic acid
rpm	rounds per minute
SCR-1	steroid receptor coactivator 1
SCR-2	steroid receptor coactivator 2
SCR-3	steroid receptor coactivator 3
sec	second
SEM	standard error
SERMs	selective estrogen receptor modulators
T	thymine
Tb.N	trabecular number(mm^{-1})
Tb.Sp	trabecular separation (µm)
TbTh	trabecular thickness (µm)
TRAP	tartrate resistance acid phosphatase
UV	ultra violet light
WT	wild type
X	any other amino acid

8 References

Abu, E. O., Horner, A., Kusec, V., Triffitt, J. T., and Compston, J. E. (1997). The localization of androgen receptors in human bone. *J Clin Endocrinol Metab* **82**, 3493-7.

Ackerman, G. E., Smith, M. E., Mendelson, C. R., MacDonald, P. C., and Simpson, E. R. (1981). Aromatization of androstenedione by human adipose tissue stromal cells in monolayer culture. *J Clin Endocrinol Metab* **53**, 412-7.

Akhtar, M., Calder, M. R., Corina, D. L., and Wright, J. N. (1982). Mechanistic studies on C-19 demethylation in oestrogen biosynthesis. *Biochem J* **201**, 569-80.

Albright, F., Smith, P. H., and Richardson, A. M. (1941). Postmenopausal osteoporosis. *JAMA* **116**, 2465-2474.

Alen, P., Claessens, F., Verhoeven, G., Rombauts, W., and Peeters, B. (1999). The androgen receptor amino-terminal domain plays a key role in p160 coactivator-stimulated gene transcription. *Mol Cell Biol* **19**, 6085-97.

Anderson, G. L., Limacher, M., Assaf, A. R., Bassford, T., Beresford, S. A., Black, H., Bonds, D., Brunner, R., Brzyski, R., Chlebowski, R., Curb, D., Gass, M., Hays, J., Heiss, G., Hendrix, S., Howard, B. V., Hsia, J., Hubbell, A., Jackson, K. C., Johnson, K. C., Judd, H., Kotchen, J. M., Kuller, L., LaCroix, A. Z., Lane, D., Langer, R. D., Lasser, N., Lewis, C. E., Manson, J., Margolis, K., Ockene, J., O'Sullivan, M. L., Phillips, L., Prentice, R. L., Ritenbaugh, C., Robbins, J., Rossouw, J. E., Sarto, G., Stefanick, M. L., Van Horn, L., Wactawski-Wende, J., Wallace, R., Wassertheil-Smoller, S., and Committee, W. s. H. I. S. (2004). Effects of conjugated equine estrogen in postmenopausal women with hysterectomy: the Women's Health Initiative randomized controlled trial. *Jama* **291**, 1701-12.

Andersson, N., Egecioglu, E., and Ohlsson, C. (2003). Tissue specific differences in response to estrogenic stimulation in ovariectomized mice. *J Bone Miner Res* **18**, S178.

Bain, S. D., Bailey, M. C., Celino, D. L., Lantry, M. M., and Edwards, M. W. (1993). High-dose estrogen inhibits bone resorption and stimulates bone formation in the ovariectomized mouse. *J Bone Miner Res* **8**, 435-42.

Baron, R., Chakraborty, M., Chatterjee, D., Horne, W., Lomri, A., and Ravesloot, J.-H. (1993). Biology of the osteoclast. *In* "Physiology and pharmacology of bone." (G. R. Mundy and T. J. Martin, eds.), pp. 111-147. Springer-Verlag, New York.

Beamer, W. G., Donahue, L. R., Rosen, C. J., and Baylink, D. J. (1996). Genetic variability in adult bone density among inbred strains of mice. *Bone* **18**, 397-403.

Bergman, M. D., Schachter, B. S., Karelus, K., Combatsiaris, E. P., Garcia, T., and Nelson, J. F. (1992). Up-regulation of the uterine estrogen receptor and its messenger ribonucleic acid during the mouse estrous cycle: the role of estradiol. *Endocrinology* **130**, 1923-30.

Bevan, C. L., Hoare, S., Claessens, F., Heery, D. M., and Parker, M. G. (1999). The AF1 and AF2 domains of the androgen receptor interact with distinct regions of SRC1. *Mol Cell Biol* **19**, 8383-92.

Bikle, D. D., Halloran, B. P., McGalliard-Cone, C., and Morey-Holton, E. (1990). Different responses of trabecular and cortical bone to 1,25(OH)2D3 infusion. *Am J Physiol* **259**, E715-22.

Bilezikian, J. P. (1998). Estrogens and postmenopausal osteoporosis: was Albright right after all? *J Bone Miner Res* **13**, 774-6.

Bord, S., Horner, A., Beavan, S., and Compston, J. (2001). Estrogen receptors alpha and beta are differentially expressed in developing human bone. *J Clin Endocrinol Metab* **86**, 2309-14.

Bousios, S., Karandrea, D., Kittas, C., and Kitraki, E. (2001). Effects of gender and stress on the regulation of steroid receptor coactivator-1 expression in the rat brain and pituitary. *J Steroid Biochem Mol Biol* **78**, 401-7.

Brzozowski, A. M., Pike, A. C., Dauter, Z., Hubbard, R. E., Bonn, T., Engstrom, O., Ohman, L., Greene, G. L., Gustafsson, J. A., and Carlquist, M. (1997). Molecular basis of agonism and antagonism in the oestrogen receptor. *Nature* **389**, 753-8.

Bucay, N., Sarosi, I., Dunstan, C. R., Morony, S., Tarpley, J., Capparelli, C., Scully, S., Tan, H. L., Xu, W., Lacey, D. L., Boyle, W. J., and Simonet, W. S. (1998). osteoprotegerin-deficient mice develop early onset osteoporosis and arterial calcification. *Genes Dev* **12**, 1260-8.

Carani, C., Qin, K., Simoni, M., Faustini-Fustini, M., Serpente, S., Boyd, J., Korach, K. S., and Simpson, E. R. (1997). Effect of testosterone and estradiol in a man with aromatase deficiency. *N Engl J Med* **337**, 91-5.

Castagnetta, L. A., Lo Casto, M., Granata, O. M., Polito, L., Calabro, M., Lo Bue, A., Bellavia, V., and Carruba, G. (1996). Estrogen content and metabolism in human breast tumor tissues and cells. *Ann N Y Acad Sci* **784**, 314-24.

Cole, P. A., and Robinson, C. H. (1990). Mechanism and inhibition of cytochrome P-450 aromatase. *J Med Chem* **33**, 2933-42.

Colvard, D. S., Eriksen, E. F., Keeting, P. E., Wilson, E. M., Lubahn, D. B., French, F. S., Riggs, B. L., and Spelsberg, T. C. (1989). Identification of androgen receptors in normal human osteoblast-like cells. *Proc Natl Acad Sci U S A* **86**, 854-7.

Cosman, F., and Lindsay, R. (1999). Selective estrogen receptor modulators: clinical spectrum. *Endocr Rev* **20**, 418-34.

Couse, J. F., Lindzey, J., Grandien, K., Gustafsson, J. A., and Korach, K. S. (1997). Tissue distribution and quantitative analysis of estrogen receptor-alpha (ERalpha) and estrogen receptor-beta (ERbeta) messenger ribonucleic acid in the wild-type and ERalpha-knockout mouse. *Endocrinology* **138**, 4613-21.

Cowley, S. M., Hoare, S., Mosselman, S., and Parker, M. G. (1997). Estrogen receptors alpha and beta form heterodimers on DNA. *J Biol Chem* **272**, 19858-62.

Cummings, S. R., Yankov, V., Ensrud, K. E., Ettinger, B., Wallace , R., Johnson, K., Macer, J., Vittinghoff, E., and Grady, D. (2003). Ultralow estradiol increases BMD and decreases bone turnover in older women, particularly those with undetectable estradiol: the ULTRA trial. *J Bone Miner Res* **18**, S53.

Daci, E., Verstuyf, A., Moermans, K., Bouillon, R., and Carmeliet, G. (2000). Mice lacking the plasminogen activator inhibitor 1 are protected from trabecular bone loss induced by estrogen deficiency. *J Bone Miner Res* **15**, 1510-6.

Denger, S., Reid, G., Kos, M., Flouriot, G., Parsch, D., Brand, H., Korach, K. S., Sonntag-Buck, V., and Gannon, F. (2001). ERalpha gene expression in human primary osteoblasts: evidence for the expression of two receptor proteins. *Mol Endocrinol* **15**, 2064-77.

Ducy, P., Desbois, C., Boyce, B., Pinero, G., Story, B., Dunstan, C., Smith, E., Bonadio, J., Goldstein, S., Gundberg, C., Bradley, A., and Karsenty, G. (1996). Increased bone formation in osteocalcin-deficient mice. *Nature* **382**, 448-52.

Ducy, P., Zhang, R., Geoffroy, V., Ridall, A. L., and Karsenty, G. (1997). Osf2/Cbfa1: a transcriptional activator of osteoblast differentiation. *Cell* **89**, 747-54.

Edwards, M. W., Bain, S. D., Bailey, M. C., Lantry, M. M., and Howard, G. A. (1992). 17 beta estradiol stimulation of endosteal bone formation in the ovariectomized mouse: an animal model for the evaluation of bone-targeted estrogens. *Bone* **13**, 29-34.

Erben, R. G., Harti, G., and Graf, H. (1998). Ovariectomy does not alter CD4+/CD8+ ratio in peripheral blood T-lymphocytes in the rat. *Horm Metab Res* **30**, 50-4.

Eriksen, E. F., Axelrod, D. W., and Melsen, F. (1994). "Bone histomorphometry," Raven Press, New York.

Ettinger, B., Black, D. M., Mitlak, B. H., Knickerbocker, R. K., Nickelsen, T., Genant, H. K., Christiansen, C., Delmas, P. D., Zanchetta, J. R., Stakkestad, J., Gluer, C. C., Krueger, K., Cohen, F. J., Eckert, S., Ensrud, K. E., Avioli, L. V., Lips, P., and Cummings, S. R. (1999). Reduction of vertebral fracture risk in postmenopausal women with osteoporosis treated with raloxifene: results from a 3-year randomized clinical trial. Multiple Outcomes of Raloxifene Evaluation (MORE) Investigators. *Jama* **282**, 637-45.

Eyre, L. J., Bland, R., Bujalska, I. J., Sheppard, M. C., Stewart, P. M., and Hewison, M. (1998). Characterization of aromatase and 17 beta-hydroxysteroid dehydrogenase expression in rat osteoblastic cells. *J Bone Miner Res* **13**, 996-1004.

Falahati-Nini, A., Riggs, B. L., Atkinson, E. J., O'Fallon, W. M., Eastell, R., and Khosla, S. (2000). Relative contributions of testosterone and estrogen in regulating bone resorption and formation in normal elderly men. *J Clin Invest* **106**, 1553-60.

Feng, W., Ribeiro, R. C., Wagner, R. L., Nguyen, H., Apriletti, J. W., Fletterick, R. J., Baxter, J. D., Kushner, P. J., and West, B. L. (1998). Hormone-dependent coactivator binding to a hydrophobic cleft on nuclear receptors. *Science* **280**, 1747-9.

Fisher, B., Costantino, J. P., Wickerham, D. L., Redmond, C. K., Kavanah, M., Cronin, W. M., Vogel, V., Robidoux, A., Dimitrov, N., Atkins, J., Daly, M., Wieand, S., Tan-Chiu, E., Ford, L., and Wolmark, N. (1998). Tamoxifen for prevention of breast cancer: report of the National Surgical Adjuvant Breast and Bowel Project P-1 Study. *J Natl Cancer Inst* **90**, 1371-88.

Gaumet, N., Braillon, P., Seibel, M. J., Pointillart, A., Coxam, V., and Davicco, M. J. (1998). Influence of aging on cortical and trabecular bone response to estradiol treatment in ovariectomized rats. *Gerontology* **44**, 132-9.

Gill, R. K., and Bell, N. H. (2000). Steroid receptor co-activator-1 mediates 1,25-dihydroxyvitamin D(3)-stimulated alkaline phosphatase in human osteosarcoma cells. *Calcif Tissue Int* **66**, 370-4.

Gori, F., Thomas, T., Hicok, K. C., Spelsberg, T. C., and Riggs, B. L. (1999). Differentiation of human marrow stromal precursor cells: bone morphogenetic protein-2 increases OSF2/CBFA1, enhances osteoblast commitment, and inhibits late adipocyte maturation. *J Bone Miner Res* **14**, 1522-35.

Grumbach, M. M., and Auchus, R. J. (1999). Estrogen: consequences and implications of human mutations in synthesis and action. *J Clin Endocrinol Metab* **84**, 4677-94.

Halloran, B. P., Ferguson, V. L., Simske, S. J., Burghardt, A., Venton, L. L., and Majumdar, S. (2002). Changes in bone structure and mass with advancing age in the male C57BL/6J mouse. *J Bone Miner Res* **17**, 1044-50.

Harada, N., Yamada, K., Saito, K., Kibe, N., Dohmae, S., and Takagi, Y. (1990). Structural characterization of the human estrogen synthetase (aromatase) gene. *Biochem Biophys Res Commun* **166**, 365-72.

Herdick, M., and Carlberg, C. (2000). Agonist-triggered modulation of the activated and silent state of the vitamin D(3) receptor by interaction with co-repressors and co-activators. *J Mol Biol* **304**, 793-801.

Hong, H., Kohli, K., Trivedi, A., Johnson, D. L., and Stallcup, M. R. (1996). GRIP1, a novel mouse protein that serves as a transcriptional coactivator in yeast for the hormone binding domains of steroid receptors. *Proc Natl Acad Sci U S A* **93**, 4948-52.

Hounsfield, G. N. (1973). Computerized transverse axial scanning (tomography). 1. Description of system. *Br J Radiol* **46**, 1016-22.

Hounsfield, G. N. (1976). Picture quality of computed tomography. *Am J Roentgenol* **127**, 3-9.

Ikonen, T., Palvimo, J. J., and Janne, O. A. (1997). Interaction between the amino- and carboxyl-terminal regions of the rat androgen receptor modulates transcriptional activity and is influenced by nuclear receptor coactivators. *J Biol Chem* **272**, 29821-8.

Jakob, F., Siggelkow, H., Homann, D., Kohrle, J., Adamski, J., and Schutze, N. (1997). Local estradiol metabolism in osteoblast- and osteoclast-like cells. *J Steroid Biochem Mol Biol* **61**, 167-74.

Janssen, J. M., Bland, R., Hewison, M., Coughtrie, M. W., Sharp, S., Arts, J., Pols, H. A., and van Leeuwen, J. P. (1999). Estradiol formation by human osteoblasts via multiple pathways: relation with osteoblast function. *J Cell Biochem* **75**, 528-37.

Jenster, G., van der Korput, H. A., van Vroonhoven, C., van der Kwast, T. H., Trapman, J., and Brinkmann, A. O. (1991). Domains of the human androgen receptor involved in steroid binding, transcriptional activation, and subcellular localization. *Mol Endocrinol* **5**, 1396-404.

Jordan, V. C., and Morrow, M. (1999). Tamoxifen, raloxifene, and the prevention of breast cancer. *Endocr Rev* **20**, 253-78.

Jorgensen, S. M., Demirkaya, O., and Ritman, E. L. (1998). Three-dimensional imaging of vasculature and parenchyma in intact rodent organs with X-ray micro-CT. *Am J Physiol* **275**, H1103-14.

Kameda, T., Mano, H., Yuasa, T., Mori, Y., Miyazawa, K., Shiokawa, M., Nakamaru, Y., Hiroi, E., Hiura, K., Kameda, A., Yang, N. N., Hakeda, Y., and Kumegawa, M. (1997). Estrogen inhibits bone resorption by directly inducing apoptosis of the bone-resorbing osteoclasts. *J Exp Med* **186**, 489-95.

Karsenty, G. (1999). The genetic transformation of bone biology. *Genes Dev* **13**, 3037-51.

Ke, H. Z., Chidsey-Frink, K. L., Qi, H., Crawford, D. T., Simmons, H. A., Brown, T. A., Petersen, D. N., Allen, M. R., McNeish, J. D., and Thompson, D. D. (2001). The role of estrogen receptor- (ER-) in the early age-related bone gain and later age-related bone loss. *J Bone Miner Res* **16**, 160.

Khosla, S., Atkinson, E. J., Melton, L. J., 3rd, and Riggs, B. L. (1997). Effects of age and estrogen status on serum parathyroid hormone levels and biochemical markers of bone turnover in women: a population-based study. *J Clin Endocrinol Metab* **82**, 1522-7.

Khosla, S., Melton, L. J., 3rd, Atkinson, E. J., O'Fallon, W. M., Klee, G. G., and Riggs, B. L. (1998). Relationship of serum sex steroid levels and bone turnover markers with bone mineral density in men and women: a key role for bioavailable estrogen. *J Clin Endocrinol Metab* **83**, 2266-74.

Khosla, S., Melton, L. J., 3rd, and Riggs, B. L. (2002). Clinical review 144: Estrogen and the male skeleton. *J Clin Endocrinol Metab* **87**, 1443-50.

Kishi, T., Hagino, H., Kishimoto, H., and Nagashima, H. (1998). Bone responses at various skeletal sites to human parathyroid hormone in ovariectomized rats: effects of long-term administration, withdrawal, and readministration. *Bone* **22**, 515-22.

Klein, R. F., Mitchell, S. R., Phillips, T. J., Belknap, J. K., and Orwoll, E. S. (1998). Quantitative trait loci affecting peak bone mineral density in mice. *J Bone Miner Res* **13**, 1648-56.

Kong, Y. Y., Feige, U., Sarosi, I., Bolon, B., Tafuri, A., Morony, S., Capparelli, C., Li, J., Elliott, R., McCabe, S., Wong, T., Campagnuolo, G., Moran, E., Bogoch, E. R., Van, G., Nguyen, L. T., Ohashi, P. S., Lacey, D. L., Fish, E., Boyle, W. J., and Penninger, J. M. (1999). Activated T cells regulate bone loss and joint destruction in adjuvant arthritis through osteoprotegerin ligand. *Nature* **402**, 304-9.

Kousteni, S., Chen, J. R., Bellido, T., Han, L., Ali, A. A., O'Brien, C. A., Plotkin, L., Fu, Q., Mancino, A. T., Wen, Y., Vertino, A. M., Powers, C. C., Stewart, S. A., Ebert, R., Parfitt, A. M., Weinstein, R. S., Jilka, R. L., and Manolagas, S. C. (2002). Reversal of bone loss in mice by nongenotropic signaling of sex steroids. *Science* **298**, 843-6.

Kousteni, S., Han, L., Chen, J. R., Almeida, M., Plotkin, L. I., Bellido, T., and Manolagas, S. C. (2003). Kinase-mediated regulation of common transcription factors accounts for the bone-protective effects of sex steroids. *J Clin Invest* **111**, 1651-64.

Kuiper, G. G., Carlsson, B., Grandien, K., Enmark, E., Haggblad, J., Nilsson, S., and Gustafsson, J. A. (1997). Comparison of the ligand binding specificity and transcript tissue distribution of estrogen receptors alpha and beta. *Endocrinology* **138**, 863-70.

Kuiper, G. G., Enmark, E., Pelto-Huikko, M., Nilsson, S., and Gustafsson, J. A. (1996). Cloning of a novel receptor expressed in rat prostate and ovary. *Proc Natl Acad Sci U S A* **93**, 5925-30.

Labrie, F., Belanger, A., Cusan, L., and Candas, B. (1997a). Physiological changes in dehydroepiandrosterone are not reflected by serum levels of active androgens and estrogens but of their metabolites: intracrinology. *J Clin Endocrinol Metab* **82**, 2403-9.

Labrie, F., Belanger, A., Cusan, L., Gomez, J. L., and Candas, B. (1997b). Marked decline in serum concentrations of adrenal C19 sex steroid precursors and conjugated androgen metabolites during aging. *J Clin Endocrinol Metab* **82**, 2396-402.

Labrie, F., Belanger, A., Luu-The, V., Labrie, C., Simard, J., Cusan, L., Gomez, J. L., and Candas, B. (1998). DHEA and the intracrine formation of androgens and estrogens in peripheral target tissues: its role during aging. *Steroids* **63**, 322-8.

Lacey, D. L., Timms, E., Tan, H. L., Kelley, M. J., Dunstan, C. R., Burgess, T., Elliott, R., Colombero, A., Elliott, G., Scully, S., Hsu, H., Sullivan, J., Hawkins, N., Davy, E., Capparelli, C., Eli, A., Qian, Y. X., Kaufman, S., Sarosi, I., Shalhoub, V., Senaldi, G., Guo, J., Delaney, J., and Boyle, W. J. (1998). Osteoprotegerin ligand is a cytokine that regulates osteoclast differentiation and activation. *Cell* **93**, 165-76.

Lea, C. K., Ebrahim, H., Tennant, S., and Flanagan, A. M. (1997). Aromatase cytochrome P450 transcripts are detected in fractured human bone but not in normal skeletal tissue. *Bone* **21**, 433-40.

Lee, K., Jessop, H., Suswillo, R., Zaman, G., and Lanyon, L. (2003). Endocrinology: bone adaptation requires oestrogen receptor-alpha. *Nature* **424**, 389.

Li, H., Gomes, P. J., and Chen, J. D. (1997). RAC3, a steroid/nuclear receptor-associated coactivator that is related to SRC-1 and TIF2. *Proc Natl Acad Sci U S A* **94**, 8479-84.

Lindberg, M. K., Moverare, S., Skrtic, S., Gao, H., Dahlman-Wright, K., Gustafsson, J. A., and Ohlsson, C. (2003). Estrogen receptor (ER)-beta reduces ERalpha-regulated gene transcription, supporting a "ying yang" relationship between ERalpha and ERbeta in mice. *Mol Endocrinol* **17**, 203-8.

Lindsay, R., Hart, D. M., Aitken, J. M., MacDonald, E. B., Anderson, J. B., and Clarke, A. C. (1976). Long-term prevention of postmenopausal osteoporosis by oestrogen. Evidence for an increased bone mass after delayed onset of oestrogen treatment. *Lancet* **1**, 1038-41.

Lindsay, R., Hart, D. M., MacLean, A., Clark, A. C., Kraszewski, A., and Garwood, J. (1978). Bone response to termination of oestrogen treatment. *Lancet* **1**, 1325-7.

Long, B. J., Tilghman, S. L., Yue, W., Thiantanawat, A., Grigoryev, D. N., and Brodie, A. M. (1998). The steroidal antiestrogen ICI 182,780 is an inhibitor of cellular aromatase activity. *J Steroid Biochem Mol Biol* **67**, 293-304.

Mahendroo, M. S., Mendelson, C. R., and Simpson, E. R. (1993). Tissue-specific and hormonally controlled alternative promoters regulate aromatase cytochrome P450 gene expression in human adipose tissue. *J Biol Chem* **268**, 19463-70.

Mangelsdorf, D. J., and Evans, R. M. (1995). The RXR heterodimers and orphan receptors. *Cell* **83**, 841-50.

Manolagas, S. C. (2000). Birth and death of bone cells: basic regulatory mechanisms and implications for the pathogenesis and treatment of osteoporosis. *Endocr Rev* **21**, 115-37.

Manolagas, S. C., and Kousteni, S. (2001). Perspective: nonreproductive sites of action of reproductive hormones. *Endocrinology* **142**, 2200-4.

Marcus, R., Leary, D., Schneider, D. L., Shane, E., Favus, M., and Quigley, C. A. (2000). The contribution of testosterone to skeletal development and maintenance: lessons from the androgen insensitivity syndrome. *J Clin Endocrinol Metab* **85**, 1032-7.

McKenna, N. J., Lanz, R. B., and O'Malley, B. W. (1999). Nuclear receptor coregulators: cellular and molecular biology. *Endocr Rev* **20**, 321-44.

Means, G. D., Kilgore, M. W., Mahendroo, M. S., Mendelson, C. R., and Simpson, E. R. (1991). Tissue-specific promoters regulate aromatase cytochrome P450 gene expression in human ovary and fetal tissues. *Mol Endocrinol* **5**, 2005-13.

Means, G. D., Mahendroo, M. S., Corbin, C. J., Mathis, J. M., Powell, F. E., Mendelson, C. R., and Simpson, E. R. (1989). Structural analysis of the gene encoding human aromatase cytochrome P-450, the enzyme responsible for estrogen biosynthesis. *J Biol Chem* **264**, 19385-91.

Medlock, K. L., Lyttle, C. R., Kelepouris, N., Newman, E. D., and Sheehan, D. M. (1991). Estradiol down-regulation of the rat uterine estrogen receptor. *Proc Soc Exp Biol Med* **196**, 293-300.

Misiti, S., Schomburg, L., Yen, P. M., and Chin, W. W. (1998). Expression and hormonal regulation of coactivator and corepressor genes. *Endocrinology* **139**, 2493-500.

Mizuno, Y., Hosoi, T., Inoue, S., Ikegami, A., Kaneki, M., Akedo, Y., Nakamura, T., Ouchi, Y., Chang, C., and Orimo, H. (1994). Immunocytochemical identification of androgen receptor in mouse osteoclast-like multinucleated cells. *Calcif Tissue Int* **54**, 325-6.

Modder, U. I., Sanyal, A., Kearns, A. E., Sibonga, J. D., Nishihara, E., Xu, J., O'Malley, B. W., Ritman, E. L., Riggs, B. L., Spelsberg, T. C., and Khosla, S. (2004). Effects of loss of steroid receptor coactivator-1 on the skeletal response to estrogen in mice. *Endocrinology* **145**, 913-21.

Monroe, D. G., Johnsen, S. A., Subramaniam, M., Getz, B. J., Khosla, S., Riggs, B. L., and Spelsberg, T. C. (2003). Mutual antagonism of estrogen receptors alpha and beta and their preferred interactions with steroid receptor coactivators in human osteoblastic cell lines. *J Endocrinol* **176**, 349-57.

Morishima, A., Grumbach, M. M., Simpson, E. R., Fisher, C., and Qin, K. (1995). Aromatase deficiency in male and female siblings caused by a novel mutation and the physiological role of estrogens. *J Clin Endocrinol Metab* **80**, 3689-98.

Moverare, S., Venken, K., Eriksson, A. L., Andersson, N., Skrtic, S., Wergedal, J., Mohan, S., Salmon, P., Bouillon, R., Gustafsson, J. A., Vanderschueren, D., and Ohlsson, C. (2003). Differential effects on bone of estrogen receptor alpha and androgen receptor activation in orchidectomized adult male mice. *Proc Natl Acad Sci U S A* **100**, 13573-8.

Mullis, P. E., Yoshimura, N., Kuhlmann, B., Lippuner, K., Jaeger, P., and Harada, H. (1997). Aromatase deficiency in a female who is compound heterozygote for two new point mutations in the P450arom gene: impact of estrogens on hypergonadotropic hypogonadism, multicystic ovaries, and bone densitometry in childhood. *J Clin Endocrinol Metab* **82**, 1739-45.

Mundy, G. R. (1999). What can we learn from bone biology for the treatment for osteoporosis? *Osteoporos Int* **9 Suppl 2**, S40-7.

Nakamura, J., Lu, Q., Aberdeen, G., Albrecht, E., and Brodie, A. (1999). The effect of estrogen on aromatase and vascular endothelial growth factor messenger ribonucleic acid in the normal nonhuman primate mammary gland. *J Clin Endocrinol Metab* **84**, 1432-7.

Nawata, H., Tanaka, S., Takayanagi, R., Sakai, Y., Yanase, T., Ikuyama, S., and Haji, M. (1995). Aromatase in bone cell: association with osteoporosis in postmenopausal women. *J Steroid Biochem Mol Biol* **53**, 165-74.

Onate, S. A., Tsai, S. Y., Tsai, M. J., and O'Malley, B. W. (1995). Sequence and characterization of a coactivator for the steroid hormone receptor superfamily. *Science* **270**, 1354-7.

Onoe, Y., Miyaura, C., Ohta, H., Nozawa, S., and Suda, T. (1997). Expression of estrogen receptor beta in rat bone. *Endocrinology* **138**, 4509-12.

Orwoll, E. S. (1996). "Androgens.," Academic Press, San Diego, CA.

Orwoll, E. S., and Klein, R. F. (1995). Osteoporosis in men. *Endocr Rev* **16**, 87-116.

Pace, P., Taylor, J., Suntharalingam, S., Coombes, R. C., and Ali, S. (1997). Human estrogen receptor beta binds DNA in a manner similar to and dimerizes with estrogen receptor alpha. *J Biol Chem* **272**, 25832-8.

Paech, K., Webb, P., Kuiper, G. G., Nilsson, S., Gustafsson, J., Kushner, P. J., and Scanlan, T. S. (1997). Differential ligand activation of estrogen receptors ERalpha and ERbeta at AP1 sites. *Science* **277**, 1508-10.

Parfitt, A. M., Drezner, M. K., Glorieux, F. H., Kanis, J. A., Malluche, H., Meunier, P. J., Ott, S. M., and Recker, R. R. (1987). Bone histomorphometry: standardization of nomenclature, symbols, and units. Report of the ASBMR Histomorphometry Nomenclature Committee. *J Bone Miner Res* **2**, 595-610.

Parisien, M., Silverberg, S. J., Shane, E., Dempster, D. W., and Bilezikian, J. P. (1990). Bone disease in primary hyperparathyroidism. *Endocrinol Metab Clin North Am* **19**, 19-34.

Partridge, N. C., Alcorn, D., Michelangeli, V. P., Kemp, B. E., Ryan, G. B., and Martin, T. J. (1981). Functional properties of hormonally responsive cultured normal and malignant rat osteoblastic cells. *Endocrinology* **108**, 213-9.

Pasqualini, J. R., Chetrite, G., Blacker, C., Feinstein, M. C., Delalonde, L., Talbi, M., and Maloche, C. (1996). Concentrations of estrone, estradiol, and estrone sulfate and evaluation of sulfatase and aromatase activities in pre- and postmenopausal breast cancer patients. *J Clin Endocrinol Metab* **81**, 1460-4.

Pettersson, K., Grandien, K., Kuiper, G. G., and Gustafsson, J. A. (1997). Mouse estrogen receptor beta forms estrogen response element-binding heterodimers with estrogen receptor alpha. *Mol Endocrinol* **11**, 1486-96.

Pham, T. A., Hwung, Y. P., Santiso-Mere, D., McDonnell, D. P., and O'Malley, B. W. (1992). Ligand-dependent and -independent function of the transactivation regions of the human estrogen receptor in yeast. *Mol Endocrinol* **6**, 1043-50.

Poli, V., Balena, R., Fattori, E., Markatos, A., Yamamoto, M., Tanaka, H., Ciliberto, G., Rodan, G. A., and Costantini, F. (1994). Interleukin-6 deficient mice are protected from bone loss caused by estrogen depletion. *Embo J* **13**, 1189-96.

Powles, T., Eeles, R., Ashley, S., Easton, D., Chang, J., Dowsett, M., Tidy, A., Viggers, J., and Davey, J. (1998). Interim analysis of the incidence of breast cancer in the Royal Marsden Hospital tamoxifen randomised chemoprevention trial. *Lancet* **352**, 98-101.

Purohit, A., Flanagan, A. M., and Reed, M. J. (1992). Estrogen synthesis by osteoblast cell lines. *Endocrinology* **131**, 2027-9.

Qiu, Y., Pereira, F. A., DeMayo, F. J., Lydon, J. P., Tsai, S. Y., and Tsai, M. J. (1997). Null mutation of mCOUP-TFI results in defects in morphogenesis of the glossopharyngeal ganglion, axonal projection, and arborization. *Genes Dev* **11**, 1925-37.

Razandi, M., Pedram, A., and Levin, E. R. (2000). Plasma membrane estrogen receptors signal to antiapoptosis in breast cancer. *Mol Endocrinol* **14**, 1434-47.

Revelli, A., Massobrio, M., and Tesarik, J. (1998). Nongenomic actions of steroid hormones in reproductive tissues. *Endocr Rev* **19**, 3-17.

Riggs, B. L., Khosla, S., and Melton, L. J., 3rd (2002). Sex steroids and the construction and conservation of the adult skeleton. *Endocr Rev* **23**, 279-302.

Rochira, V., Faustini-Fustini, M., Balestrieri, A., and Carani, C. (2000). Estrogen replacement therapy in a man with congenital aromatase deficiency: effects of different doses of

transdermal estradiol on bone mineral density and hormonal parameters. *J Clin Endocrinol Metab* **85**, 1841-5.

Rosser, M., Chorich, L., Howard, E., Zamorano, P., and Mahesh, V. B. (1993). Changes in rat uterine estrogen receptor messenger ribonucleic acid levels during estrogen- and progesterone-induced estrogen receptor depletion and subsequent replenishment. *Biol Reprod* **48**, 89-98.

Rossouw, J. E., Anderson, G. L., Prentice, R. L., LaCroix, A. Z., Kooperberg, C., Stefanick, M. L., Jackson, R. D., Beresford, S. A., Howard, B. V., Johnson, K. C., Kotchen, J. M., and Ockene, J. (2002). Risks and benefits of estrogen plus progestin in healthy postmenopausal women: principal results From the Women's Health Initiative randomized controlled trial. *Jama* **288**, 321-33.

Rundlett, S. E., Wu, X. P., and Miesfeld, R. L. (1990). Functional characterizations of the androgen receptor confirm that the molecular basis of androgen action is transcriptional regulation. *Mol Endocrinol* **4**, 708-14.

Samuels, A., Perry, M. J., and Tobias, J. H. (1999). High-dose estrogen induces de novo medullary bone formation in female mice. *J Bone Miner Res* **14**, 178-86.

Sasano, H., Uzuki, M., Sawai, T., Nagura, H., Matsunaga, G., Kashimoto, O., and Harada, N. (1997). Aromatase in human bone tissue. *J Bone Miner Res* **12**, 1416-23.

Schweikert, H. U., Wolf, L., and Romalo, G. (1995). Oestrogen formation from androstenedione in human bone. *Clin Endocrinol (Oxf)* **43**, 37-42.

Shang, Y., and Brown, M. (2002). Molecular determinants for the tissue specificity of SERMs. *Science* **295**, 2465-8.

Shozu, M., Zhao, Y., and Simpson, E. R. (2000). TGF-beta1 stimulates expression of the aromatase (CYP19) gene in human osteoblast-like cells and THP-1 cells. *Mol Cell Endocrinol* **160**, 123-33.

Sibonga, J. D., Bell, N. H., and Turner, R. T. (1998). Evidence that ibuprofen antagonizes selective actions of estrogen and tamoxifen on rat bone. *J Bone Miner Res* **13**, 863-70.

Simental, J. A., Sar, M., Lane, M. V., French, F. S., and Wilson, E. M. (1991). Transcriptional activation and nuclear targeting signals of the human androgen receptor. *J Biol Chem* **266**, 510-8.

Simonet, W. S., Lacey, D. L., Dunstan, C. R., Kelley, M., Chang, M. S., Luthy, R., Nguyen, H. Q., Wooden, S., Bennett, L., Boone, T., Shimamoto, G., DeRose, M., Elliott, R., Colombero, A., Tan, H. L., Trail, G., Sullivan, J., Davy, E., Bucay, N., Renshaw-Gegg, L., Hughes, T. M., Hill, D., Pattison, W., Campbell, P., Boyle, W. J., and et al. (1997). Osteoprotegerin: a novel secreted protein involved in the regulation of bone density. *Cell* **89**, 309-19.

Simpson, E., Rubin, G., Clyne, C., Robertson, K., O'Donnell, L., Jones, M., and Davis, S. (2000). The role of local estrogen biosynthesis in males and females. *Trends Endocrinol Metab* **11**, 184-8.

Simpson, E. R., Clyne, C., Rubin, G., Boon, W. C., Robertson, K., Britt, K., Speed, C., and Jones, M. (2002). Aromatase--a brief overview. *Annu Rev Physiol* **64**, 93-127.

Sims, N. A., Clement-Lacroix, P., Minet, D., Fraslon-Vanhulle, C., Gaillard-Kelly, M., Resche-Rigon, M., and Baron, R. (2003). A functional androgen receptor is not sufficient to allow estradiol to protect bone after gonadectomy in estradiol receptor-deficient mice. *J Clin Invest* **111**, 1319-27.

Sims, N. A., Dupont, S., Krust, A., Clement-Lacroix, P., Minet, D., Resche-Rigon, M., Gaillard-Kelly, M., and Baron, R. (2002). Deletion of estrogen receptors reveals a regulatory role for estrogen receptors-beta in bone remodeling in females but not in males. *Bone* **30**, 18-25.

Sims, N. A., Morris, H. A., Moore, R. J., and Durbridge, T. C. (1996). Estradiol treatment transiently increases trabecular bone volume in ovariectomized rats. *Bone* **19**, 455-61.

Smith, E. P., Boyd, J., Frank, G. R., Takahashi, H., Cohen, R. M., Specker, B., Williams, T. C., Lubahn, D. B., and Korach, K. S. (1994). Estrogen resistance caused by a mutation in the estrogen-receptor gene in a man. *N Engl J Med* **331**, 1056-61.

Takeshita, A., Yen, P. M., Misiti, S., Cardona, G. R., Liu, Y., and Chin, W. W. (1996). Molecular cloning and properties of a full-length putative thyroid hormone receptor coactivator. *Endocrinology* **137**, 3594-7.

Tanaka, S., Haji, M., Nishi, Y., Yanase, T., Takayanagi, R., and Nawata, H. (1993). Aromatase activity in human osteoblast-like osteosarcoma cell. *Calcif Tissue Int* **52**, 107-9.

Tasset, D., Tora, L., Fromental, C., Scheer, E., and Chambon, P. (1990). Distinct classes of transcriptional activating domains function by different mechanisms. *Cell* **62**, 1177-87.

Tobias, J. H., Chow, J., Colston, K. W., and Chambers, T. J. (1991). High concentrations of 17 beta-estradiol stimulate trabecular bone formation in adult female rats. *Endocrinology* **128**, 408-12.

Toda, K., Terashima, M., Kawamoto, T., Sumimoto, H., Yokoyama, Y., Kuribayashi, I., Mitsuuchi, Y., Maeda, T., Yamamoto, Y., Sagara, Y., and et al. (1990). Structural and functional characterization of human aromatase P-450 gene. *Eur J Biochem* **193**, 559-65.

Tora, L., White, J., Brou, C., Tasset, D., Webster, N., Scheer, E., and Chambon, P. (1989). The human estrogen receptor has two independent nonacidic transcriptional activation functions. *Cell* **59**, 477-87.

Torchia, J., Rose, D. W., Inostroza, J., Kamei, Y., Westin, S., Glass, C. K., and Rosenfeld, M. G. (1997). The transcriptional co-activator p/CIP binds CBP and mediates nuclear-receptor function. *Nature* **387**, 677-84.

Turner, R. T., Riggs, B. L., and Spelsberg, T. C. (1994). Skeletal effects of estrogen. *Endocr Rev* **15**, 275-300.

Tzukerman, M. T., Esty, A., Santiso-Mere, D., Danielian, P., Parker, M. G., Stein, R. B., Pike, J. W., and McDonnell, D. P. (1994). Human estrogen receptor transactivational capacity is determined by both cellular and promoter context and mediated by two functionally distinct intramolecular regions. *Mol Endocrinol* **8**, 21-30.

Udagawa, N., Takahashi, N., Akatsu, T., Tanaka, H., Sasaki, T., Nishihara, T., Koga, T., Martin, T. J., and Suda, T. (1990). Origin of osteoclasts: mature monocytes and macrophages are capable of differentiating into osteoclasts under a suitable microenvironment prepared by bone marrow-derived stromal cells. *Proc Natl Acad Sci U S A* **87**, 7260-4.

Utian, W. H., Burry, K. A., Archer, D. F., Gallagher, J. C., Boyett, R. L., Guy, M. P., Tachon, G. J., Chadha-Boreham, H. K., and Bouvet, A. A. (1999). Efficacy and safety of low, standard, and high dosages of an estradiol transdermal system (Esclim) compared with placebo on vasomotor symptoms in highly symptomatic menopausal patients. The Esclim Study Group. *Am J Obstet Gynecol* **181**, 71-9.

Vandenput, L., Boonen, S., Van Herck, E., Swinnen, J. V., Bouillon, R., and Vanderschueren, D. (2002). Evidence from the aged orchidectomized male rat model that 17beta-estradiol is a more effective bone-sparing and anabolic agent than 5alpha-dihydrotestosterone. *J Bone Miner Res* **17**, 2080-6.

Vandenput, L., Ederveen, A. G., Erben, R. G., Stahr, K., Swinnen, J. V., Van Herck, E., Verstuyf, A., Boonen, S., Bouillon, R., and Vanderschueren, D. (2001). Testosterone prevents orchidectomy-induced bone loss in estrogen receptor-alpha knockout mice. *Biochem Biophys Res Commun* **285**, 70-6.

Vanderschueren, D., Van Herck, E., Geusens, P., Suiker, A., Visser, W., Chung, K., and Bouillon, R. (1994). Androgen resistance and deficiency have different effects on the growing skeleton of the rat. *Calcif Tissue Int* **55**, 198-203.

Vanderschueren, D., van Herck, E., Nijs, J., Ederveen, A. G., De Coster, R., and Bouillon, R. (1997). Aromatase inhibition impairs skeletal modeling and decreases bone mineral density in growing male rats. *Endocrinology* **138**, 2301-7.

Vanderschueren, D., Van Herck, E., Suiker, A. M., Visser, W. J., Schot, L. P., and Bouillon, R. (1992). Bone and mineral metabolism in aged male rats: short and long term effects of androgen deficiency. *Endocrinology* **130**, 2906-16.

Vanderschueren, D., Van Herck, E., Suiker, A. M., Visser, W. J., Schot, L. P., Chung, K., Lucas, R. S., Einhorn, T. A., and Bouillon, R. (1993). Bone and mineral metabolism in the androgen-resistant (testicular feminized) male rat. *J Bone Miner Res* **8**, 801-9.

Vanderschueren, D., Vandenput, L., Boonen, S., Van Herck, E., Swinnen, J. V., and Bouillon, R. (2000). An aged rat model of partial androgen deficiency: prevention of both loss of bone and lean body mass by low-dose androgen replacement. *Endocrinology* **141**, 1642-7.

Veronesi, U., Maisonneuve, P., Costa, A., Sacchini, V., Maltoni, C., Robertson, C., Rotmensz, N., and Boyle, P. (1998). Prevention of breast cancer with tamoxifen: preliminary findings from the Italian randomised trial among hysterectomised women. Italian Tamoxifen Prevention Study. *Lancet* **352**, 93-7.

Wakley, G. K., Schutte, H. D., Jr., Hannon, K. S., and Turner, R. T. (1991). Androgen treatment prevents loss of cancellous bone in the orchidectomized rat. *J Bone Miner Res* **6**, 325-30.

Webster, N. J., Green, S., Jin, J. R., and Chambon, P. (1988). The hormone-binding domains of the estrogen and glucocorticoid receptors contain an inducible transcription activation function. *Cell* **54**, 199-207.

Williams, D. C., and Frolik, C. A. (1991). Physiological and pharmacological regulation of biological calcification. *Int Rev Cytol* **126**, 195-292.

Windahl, S. H., Hollberg, K., Vidal, O., Gustafsson, J. A., Ohlsson, C., and Andersson, G. (2001). Female estrogen receptor beta-/- mice are partially protected against age-related trabecular bone loss. *J Bone Miner Res* **16**, 1388-98.

Xu, J., Qiu, Y., DeMayo, F. J., Tsai, S. Y., Tsai, M. J., and O'Malley, B. W. (1998). Partial hormone resistance in mice with disruption of the steroid receptor coactivator-1 (SRC-1) gene. *Science* **279**, 1922-5.

Yamada, T., Kawano, H., Sekine, K., Kato, S., and Kawaguchi, H. (2004). Steroid receptor coactivator/1 (SRC-1) contributes to the maintenance of bone volume by sex hormones in both males and females. *Journal of Bone and Mineral Research* **18**, S19.

Yeh, S., and Chang, C. (1996). Cloning and characterization of a specific coactivator, ARA70, for the androgen receptor in human prostate cells. *Proc Natl Acad Sci U S A* **93**, 5517-21.

Yue, W., Berstein, L. M., Wang, J. P., Clark, G. M., Hamilton, C. J., Demers, L. M., and Santen, R. J. (2001). The potential role of estrogen in aromatase regulation in the breast. *J Steroid Biochem Mol Biol* **79**, 157-64.

Zhou, H., Iida-Klein, A., Lu, S. S., Ducayen-Knowles, M., Levine, L. R., Dempster, D. W., and Lindsay, R. (2003). Anabolic action of parathyroid hormone on cortical and cancellous bone differs between axial and appendicular skeletal sites in mice. *Bone* **32**, 513-20.

Zhou, Z. X., Sar, M., Simental, J. A., Lane, M. V., and Wilson, E. M. (1994). A ligand-dependent bipartite nuclear targeting signal in the human androgen receptor. Requirement for the DNA-binding domain and modulation by NH2-terminal and carboxyl-terminal sequences. *J Biol Chem* **269**, 13115-23.

9 Lebenslauf

Angaben zur Person

Name:	Ulrike Mödder
Adresse:	Gertrudenhof 50129 Bergheim
Telefon:	02183-320
E-mail:	moedder@aol.com

Geburtsdatum:	11.April 1976
Geburtsort:	Bedburg (Nordrhein-Westfalen)
Familienstand:	verheiratet (03.09.2004)
Nationalität:	deutsch

Schulischer Werdegang

1982 - 1986	Odilia-Weidenfeld Grundschule (Hüchelhoven)
1986 – 1992	Albert-Einstein-Realschule (Oberaußem)
1992 – 1995	Erftgymnasium (Bergheim-Erft)
13.06.1995	Allgemeine Hochschulreife

Akademische Ausbildung

WS 95/95 – SS 97	Studium der Biologie an der Universität zu Köln
10/1997	Vordiplom
11/1999	Diplomprüfung im Hauptfach Botanik und in den Nebenfächern Genetik und Biochemie
11/1999 – 11/2000	Diplomarbeit bei Herrn Prof Dr. U.I. Flügge, Botanisches Institut der Universität zu Köln Thema; „Einführung einer gerichteten Punktmutation in das Genom von *Arabidopsis thaliana* Suspensionskulturzellen mittels chimaeren RNA/DNA Oligonukleotiden“
11/2000 – 08/2001	Wissenschaftliche Mitarbeiterin im Botanischen Institut der Universität zu Köln in der Arbeitsgruppe von Herrn Prof. Dr. U.I. Flügge
09/2001 -. 08/2003	Special Project Associate in der Endokrinologischen Abteilung der Mayo Clinic, Rochester, USA Durchführung der praktischen Arbeiten zur Erstellung meiner Promotion Gruppenleiter: Herr Prof. Dr. S. Khosla
09/2003 – gegenwärtig	Promotionsstudentin der Philipps-Universität Marburg Doktorandin von Herrn Prof. Dr. R. Arnold

Bibliographie

-Präsentationen-

29.04.2003	Endocrine Research Seminar, Mayo Clinic, Rochester, USA **Co-regulator Proteins and Estrogen Receptor Function: Results with SRC-1 Knockout Mice**
20.09.2003	ASBMR 25th Annual Meeting, Minneapolis, USA **Steroid Receptor Coactivator (SRC)-1 Knockout Mice Have an Impaired Response to Estrogen in Cancellous but not in Cortical Bone**

-Forschungspreis-

American Society of Bone and Mineral Research Young Investigator Award 2003
Verliehen am 22. September 2003 in Minneapolis, USA

-Veröffentlichungen-

Mödder UI, Sanyal A, Kearns AE, Sibonga JD, Xu J, O'Malley BW, Ritman EL, Riggs BL, Spelsberg TC, and Khosla S

Effects of Loss of Steroid Receptor Coactivator-1 on the Skeletal Response to Estrogen in Mice
Endocrinology. 2004 Feb; 145(2): 913-21

Mödder UI, Riggs BL, Spelsberg TC, Fraser DG, Atkinson EJ, Arnold R, and Khosla S

Dose Response of Estrogen on Bone Versus the Uterus in Ovariectomized Mice
European Journal of Endocrinology (akzeptiert zur Publikation am 30.06.2004)

-Abstracts-

Mödder UI, Riggs BL, and Khosla S

Demonstration of Aromatase Activity in Rodent Bone
JBMR, Vol. 17, Suppl 1, September 2002: S436-437

Mödder UI, Riggs BL, Kearns AE, Sanyal A, Sibonga JD, Xu J, O'Malley BW, Spelsberg TC, and Khosla S

Steroid Receptor Coactivator (SRC)-1 Knockout Mice Have an Impaired Response to Estrogen in Cancellous but not in Cortical Bone
JBMR, Vol. 18, Suppl 2, September 2003: S9

Mödder UI, Riggs BL, Spelsberg TC, Fraser DG, Atkinson EJ, and Khosla S

Dose Response of Estradiol in Bond and the Uterus in Mice: Evidence that Bone is More Sensitive to Estrogen than Reproductive Tissue
JBMR, Vol. 18, Suppl 2, September 2003: S368

Mödder UI, Sanyal A, Xu J, O'Malley BW, Spelsberg TC, Riggs BL, and Khosla S

The Skeletal Response to Estrogen is Impaired in Female but not in Male Steroid Receptor Coactivator-1 Knock Out Mice
(eingesendet zum ASBMR Meeting 2004, Seattle)

Verzeichnis der akademischen Lehrer

Meine akademischen Lehrer waren:

Herr Prof. Dr. R. Arnold (Philipps-Universität Marburg)

Herr Prof Dr. S. Khosla (Mayo Clinic, Rochester, USA)

Herr Prof Dr. BL. Riggs (Mayo Clinic, Rochester, USA)

Herr Prof. Dr. TC Spelsberg (Mayo Clinic, Rochester, USA)

Danksagung

Herrn Prof. Dr. med. R. Arnold danke ich für die Möglichkeit, unter seiner hervorragenden Leitung an der Philipps-Universität Marburg zu promovieren. So konnte ich die großartige Gelegenheit wahrnehmen, meine praktische Arbeit an der Mayo Clinic durchzuführen.

Herrn Prof. Dr. med. S. Khosla danke ich für die Überlassung dieses interessanten Themas und für seine hervorragende Betreuung. Ich danke ihm dafür, Dinge kritisch zu betrachten, jedoch immer das Beste daran zu sehen.

Herrn Prof. Dr. med. BL Riggs danke ich, daß er seine langjährige Erfahrungen mit mir und den anderen in der Arbeitsgruppe geteilt hat und immer zu konstruktiven Diskussionen bereit war.

Herrn Prof. Dr. B. O'Malley danke ich für die Bereitstellung der SRC-1 KO Mäuse, um eine eigene Zucht aufbauen zu können.

Frau Dr. J. Sibonga danke ich für die Möglichkeit, ihr Histomorphometrie-Labor nutzen zu dürfen und eine ausführliche Einführung in dieses Thema bekommen zu haben.

Herrn Dr. D. Fraser danke für die unerschöpfliche Hilfe in der Aufzucht, genotypischen Bestimmung der SRC-1 KO Mäuse und allen anderen „Mausangelegenheiten".

Herrn Priv. Doz. Dr. L. Hofbauer danke ich für seine Hilfestellung bezüglich organisatorischer Fragen.

Jesse, Dave, Kelly, Jim, Arunik, Guitty, Farhan, Cheryl, Donna, Pat, Mimi, Peter, Edward, Jaleel, Theresa, dem Pflegepersonal der Mausabteilung danke ich für die überaus liebevolle Aufnahme in die Arbeitsgruppe(n), unerschöpfliche Bereitschaft, mit Hand anzulegen, wenn meine zwei nicht reichten und einfach für die Tatsache, daß sie alle meinen Aufenthalt an der Mayo Clinic zu einem unvergesslichen Erlebnis gemacht haben.

Meinem Mann Mario danke ich für seine nie endende Unterstützung.

...ganz besonders danken möchte ich meinen Eltern und meinen Geschwistern, die mich immer bedingungslos unterstützt und mir die Möglichkeit eröffnet haben, all die Dinge zu tun, die ich mir vorgenommen habe.

Ehrenwörtliche Erklärung

Ich erkläre ehrenwörtlich, dass ich die dem Fachbereich Medizin der Philipps-Universität Marburg zur Promotionsprüfung eingereichte Arbeit mit dem Titel "Function of Estrogen on Bone and the Characterization of the Skeletal Phenotype of Steroid Receptor Coactivator (SRC)-1 KO Mice" in der endokrinologischen Abteilung der Mayo Clinic Rochester (USA) unter der Leitung von Herrn Prof. Dr. S. Khosla, der Unterstützung von Herrn Prof. Dr R. Arnold (Philipps-Universität Marburg) und mit denen im Material- und Methodenteil erwähnten Hilfen und Hilfsmitteln durchgeführt habe.

Ich habe die vorliegende Doktorarbeit selbst schriftlich verfasst. Die in dieser Doktorarbeit verwendeten Textpassagen aus meiner bereits veröffentlichten Publikation (Endocrinology 145(2): 913) und einer weiteren akzeptierten Publikation sind von mir unter Berücksichtigung von Korrekturvorschlägen meines Mentors Prof. Dr. Khosla und die der Mitautoren geschrieben worden.

Die Abbildungen in dieser Doktorarbeit wurden zum überwiegenden Teil von mir selbst mit dem Program PowerPoint erstellt. Die Abbildungen, die bereits in der Publikation (Endocrinology 145(2): 913) abgebildet wurden, sind in Zusammenarbeit mit Herrn Peterson erstellt worden.

Ich habe bisher an keinem in- und ausländischen Medizinischen Fachbereich ein Gesuch um Zulassung zur Promotion eingereicht noch die vorliegende oder eine andere Arbeit als Dissertation vorgelegt.

Die vorliegende Arbeit wurde in Teilen in dem Publikationsorgan Endocrinology veröffentlicht. Ein weiterer Teil dieser Arbeit wurde von dem Publikationsorgan European Journal of Endocrinology zur Publikation akzeptiert.

Beiliegend zu dieser Arbeit befinden sich die schriftlichen Bestätigungen aller Mitautoren, dass die Arbeit, die den Publikationen zugrunde liegt, im wesentlichen von mir stammt.

Marburg, den 20. September 2004